MAGNETICALLY ANCHORED "REDUCED TROCAR" LAPAROSCOPY: EVOLUTION OF SURGICAL ROBOTICS

by

RICHARD ANTONE BERGS

Presented to the Faculty of the Graduate School of

The University of Texas at Arlington in Partial Fulfillment

of the Requirements

for the Degree of

MASTER OF SCIENCE IN BIOMEDICAL ENGINEERING

THE UNIVERSITY OF TEXAS AT ARLINGTON

May 2006

ACKNOWLEDGEMENTS

> A human being is a part of the whole, called by us "Universe," a part limited in time and space. He experiences himself, his thoughts and feelings as something separated from the rest a kind of optical delusion of his consciousness. This delusion is a kind of prison for us, restricting us to our personal desires and to affection for a few persons nearest to us. Our task must be to free ourselves from this prison by widening our circle of compassion to embrace all living creatures and the whole of nature in its beauty. Nobody is able to achieve this completely, but the striving for such achievement is in itself a part of the liberation and a foundation for inner security.
>
> Albert Einstein, *Mathematical Circles Adieu*

I have been fortunate enough in my life to meet many people from different walks of life. While I would be kidding myself if I was to state that every interaction was good, each was beneficial, although the benefits may be hard to see and understand. There have been, however, people that I have met that without their support, I would not be where I am today.

I met Dennis “Keith” Jones when I first started at the Automation & Robotics Research Institute (ARRI). At that time he was the institute’s machinist, but more than that, he was one of the most practical engineers that I have ever met, even though, he

did not officially hold an engineering degree. Much of the MAS project was developed by working with Mr. Jones to determine how to design the structures in such a way as to be manufactured using the institute's equipment. There were constraints on the size and materials of the project from the medical requirements, but also, from the manufacturing requirements. Without his expertise in machining, some of the tools may be drastically different. For this, I thank you.

I met Dr. Cadeddu during one of the very first meetings regarding the Trans-abdominal Magnetic Anchoring System (TMAS), which is the precursor to the Magnetic Anchoring System (MAS) about four years ago. At that time, all there was of the tooling was a dream. I was brought onto the project as the sole student to determine whether or not magnets would be capable of accomplishing this task. Over the years of working with him on this project, I have gained a new understanding of the medical community and the dedication that it takes. Many see the doctor, few get to know them. I thank you for believing in a simple college student being able to make a dream a reality.

When I first started at ARRI, my supervisor was Peter Tanguy. Shortly after being assigned the TMAS project, he accepted employment elsewhere and I was transferred to Dr. Fernandez. We had never worked together, nor really been formally introduced before Peter left, but, we came to an understanding of our collected talents. When the MAS project truly started, I was given the freedom to work at my own pace, as well as choose the priorities in the project. I believe, and this may or may not be true, without this freedom, much of what was developed would not have happened. He

joked once that all he had to do was pay the bills, and luckily for the project he did. He was there when help was needed, but also had enough trust to believe my word, even though sometimes the reasoning was not clear. For taking a chance that I may know what I am doing, I thank you.

I first met Dr. Eberhart when he was working with Peter and a friend of mine on a trainer for laparoscopic surgery. When I was chosen as the student for the TMAS, it was the first time that we were introduced. I was finishing my undergraduate degree at the time and was trying to decide whether or not to continue for graduate studies. Dr. Eberhart asked me to consider it, and at the very least, take the introduction class offered by the University of Texas at Arlington's Biomedical Engineering department to see what was available. I became a biomedical engineering graduate student the semester following the introduction class. While personal difficulties have slowed my progress, I do not regret the decision. For opening my eyes to a field and possibilities that I may not have ever known, I thank you.

To truly acknowledge everyone that has affected my life and this project in one way or another would take many, many pages. Before I conclude, I do want to thank my family, from my sister to my great-grandfather, who wanted his grandchildren and great grandchildren to go to college. While the preparations he made may have eroded with time, I was started on this path due to his forethought.

My grandparents were very helpful in being supportive as well as allowing access to their vehicle(s) to transport the equipment from the lab at ARRI to the animal lab.

My father and mother, who would allow me to bounce ideas off of them, even though they may have not had an idea of what I was talking about. Many of the concepts that the tools are build off came from these discussions.

And finally, my sister, for her enthusiasm that kept me going through the trials and tribulations of the project, and graduate school itself. She does not understand how many of the tools function, or what they do, but she appreciates the “toys” that I have created and allowed her to play with.

November 11, 2005

ABSTRACT

MAGNETICALLY ANCHORED "REDUCED TROCAR"

LAPAROSCOPY: EVOLUTION OF SURGICAL

ROBOTICS

Publication No. _____

Richard Antone Bergs, MS

The University of Texas at Arlington, 2006

Supervising Professor: Dr. Robert Eberhart

Laparoscopic surgery has become increasingly popular over the last few years due to its benefits; lower morbidity, less perceived pain, better cosmesis results, and less hospital time. For the surgeon however, there are fundamental issues that can make a laparoscopic procedure more difficult than a simple open surgery; loss of tactile feel, limited working envelope, high demand for hand-eye coordination, and one trocar-port required for each tool. A revolutionary concept of using magnetics to support tooling across the abdominal wall was conceived by Dr. Jeffrey Cadeddu and his colleagues at the University of Texas Southwestern Medical Center (UTSW). A set of tooling was the developed permitting examination of the feasibility of mobile surgical tools that do not require separate ports spanning the abdominal wall: a sling organ retractor, a paddle

organ retractor, a camera, and a pneumatically actuated robotic arm configured to operate as a hook cautery. Each tool offers increased degrees of freedom and flexibility, all enter through the same trocar-port, all are positioned where needed inside the abdominal cavity via manipulation of the external magnetic anchor. The anchoring system and tools, collectively referred to as the Magnetic Anchoring System (MAS) have been tested in various porcine surgical procedures at the UTSW animal lab, and on several occasions they have been proven capable of two-trocar-port nephrectomy, something not possible with conventional laparoscopic equipment. The development of the magnetic anchor platform, the cited tools and the evaluation of the system and its components are the topics of this thesis.

TABLE OF CONTENTS

LIST OF ILLUSTRATIONS

LIST OF TABLES

CHAPTER 1

INTRODUCTION

Between 1993 and 2004, more than 20 million minimally invasive surgeries were performed, with another 1.8 million being performed each year. Minimally invasive surgery is so successful, that close to 90% of cholecystectomy surgeries are now accomplished this way. Minimally invasive surgery has proven effective for colectomy, appendectomy, ventral hernia repair, hysterectomy, surgery for acid reflux, as well as gastric bypass, just to name a few. The technique of minimally invasive surgery has multiple advantages for the patient, such as:

- Reduced trauma to the body
- Less anesthesia
- Less blood loss and need for transfusions
- Less post-operative pain and discomfort
- Less risk of infection
- Shorter hospital stay
- Faster recovery and return to daily activities
- Less scarring and improved comesis

1.1 Fundamental Concepts of Laparoscopic Surgery

Laparoscopic surgery is viewed as a fairly recent addition to surgical techniques, but, its early developments can be traced back as far as 1585.

“Conventional” laparoscopic surgery was first attempted in 1901 by Georg Kelling, who used a cystoscope to view the abdominal cavity of a dog after it was inflated with air. His testing was aimed toward stopping of intra-abdominal bleeding, but the concept of being able to insuflate the abdomen can be traced back to his studies. In 1911, Bertram Bernheim of John Hopkins Hospital introduced laparoscopic surgery to the United States. While World War I and II slowed progress, development continued and continues today, but the technique remains virtually the same.

In most procedures, small incisions, approximately the size of a dime, are made in the abdominal wall to allow for the insertion of trocar ports, which are the thin tubes that are used to allow for insertion and extraction of tools (Figure 1).

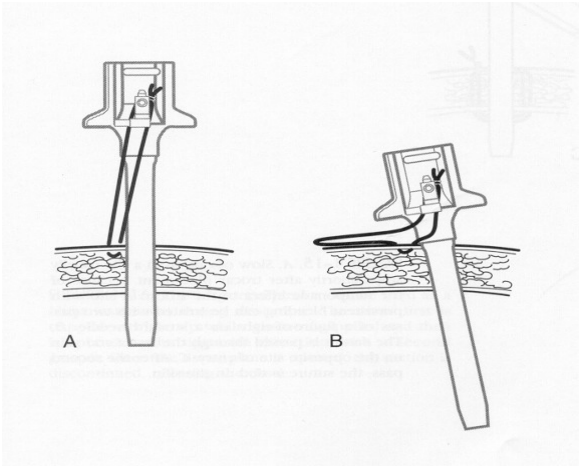

Figure 1. Trocar port introduction. As shown, the trocar port spans the thickness of the abdominal wall to allow for tool introduction and extraction, while minimizing gas loss.

The abdominal cavity is normally pressurized with carbon dioxide to around 15-16 mmHg to create a working space between the internal organs and the peritoneum. The first tool introduced into and the last to be extracted from the abdominal cavity is

the endoscope with its built in light source. The endoscope sends video images to a monitor that is used by surgeon and the medical staff to watch the introduction of other tools, to make sure that additional tooling is properly introduced, without unnecessary damage to biological structures. In most surgeries, there are a minimum of 3 tools that are required, an endoscope, a grasper and a cutting tool that is a scissor tool or an electro-cautery (Figure 2).

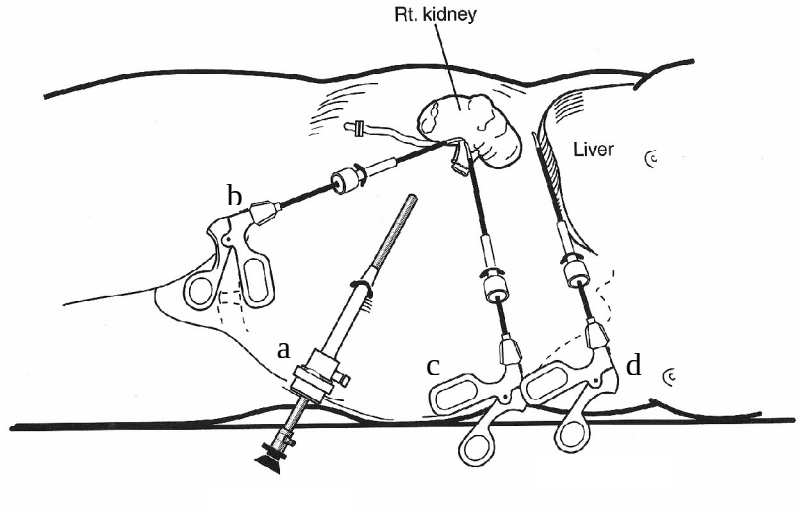

Figure 2. Conventional minimally invasive surgery layout. As shown in the figure, there is an endoscopic camera (a), a graspers (b), a cutting instrument (c) and a retractor (d). Notice that each tool requires its own trocar port.

For every tool that is needed for the surgery, an additional trocar port is required. Also, if access to a specific location is not possible from the current port, either a new port must be inserted, or the tool in one of the other ports must be removed, and reinstalled. There is always the risk of puncturing vital organs or blood vessels during the insertion of the trocar ports. The repositioning of the tools or the insertion of another trocar port results in a delay in the progress of the surgery, adding a longer time

under anesthesia for the patient, and delay for the surgeon. Because of the way the tools are designed, there is a loss of tactile feel of the tissues for the surgeon, due to the long distance from tool head to handle as well as limited degrees of freedom at the tool head, and limited working volumes for the tools.

Because of these concerns, and the desire to develop less invasive procedures, two other technologies have recently been developed, needle-oscopy and tele-robotic surgery. These will be briefly described.

1.2 Needle-oscopy

Needle-oscopy is a relatively new concept in which "probes" the size of hypodermic needles are passed directly through the abdominal wall, while the tool head is passed through a conventional trocar port and connected to the probe in situ. Using this technology, fewer trocar ports are required because once the tool head is connected to the probe, the trocar port is free for use to introduce another tool head, or a conventional tool. This is a step in the right direction, since the patient receives fewer incisions, the surgeon gains a larger working volume since the tool and trocar port can be in different locations. Tactile sensation and tool control are improved due to the shorter distance from the surgeon's hand to the tool tip. However, due to the constraints placed on the probes and tool heads, this technology is insufficient for important applications such as retractors, due to the probe's small cross section, as well as highly active tools such as a graspers because of the inability to actuate the tool head.

1.3 Tele-Robotic Surgery

Intuitive Surgical's daVinci Surgical System (Figure 3) is based on delivering more degrees of freedom, up to 7, at the tool head. Since the tools are manipulated by the robot, the operating room requires less staff, but this comes at the price of a longer setup time as well as a significant learning curve for the surgeon. The vision system allows for high resolution 3-d imaging, as well as panoramic views of the surgical area, something not possible with conventional vision tools. The motion of the surgeon's hands can be scaled and tremor can be filtered out: these advances allow procedures that were originally thought to be too delicate for minimally invasive techniques to be accomplished. Also, the surgery can be accomplished with the surgeon sitting at a console, instead of standing, which leads to less fatigue.

Figure 3. The daVinci surgical system. The surgeon sits at a console away from the surgical table and controls the motions of the robot.

The daVinci system has been shown to offer many benefits relevant to minimally invasive surgical techniques, but the tools require the same number of incisions as conventional minimally invasive surgery. While a full medical staff is not needed for the surgery, they must nevertheless be prepped and on stand-by since if there is a malfunction with the robot, it must be removed and the surgery finished by conventional means. If an area cannot be reached with the current insertion location, the tools must be removed and reinserted, just as if they were conventional minimally invasive surgical tooling.

1.4 A Shift in Conventional Thinking

To allow for true freedom of motion for the surgeon, reduction of surgical staff, as well as fewer incisions needed to perform the surgery, a shift in thinking needs to occur. Up until this point in the development of minimally invasive surgical tooling, the design and development has centered on a rigid structure being passed through its own trocar port, and manipulated through the trocar port. The needle-oscopy approach limits the need for a trocar required for each tool, but tool strength and capabilities are limited. While the daVinci surgical system shows that more degrees of freedom and steadier tools can be employed, which is both beneficial for the patient and surgeon, the costs associated with the setup time, the learning curve and need for standby surgical staff cannot be neglected.

Drs. Baker and Cadeddu devised a clever and simple solution to some of these problems that has the capability to revolutionize minimally invasive surgery: develop

surgical tools that can be supported inside the abdominal cavity without puncturing the abdominal wall by using an external magnetic source and an internal target. A similar concept of using magnetic guidance for catheters in interventional radiology has been studied since the early 1950s. In this concept, the magnet is used for assisting navigation rather than anchoring the catheter. In the Cadeddu-Baker approach, the magnet stabilizes and positions the laparoscopic tool. Furthermore, conventional tooling is broken down to its core functions, passing the entire tool through a trocar port and move to the required area, all the while being magnetically coupled by the external source and the base of the tool. This concept has many potential advantages, namely:

- Multiple tools can be introduced through just one trocar port. The patient has the advantage of fewer incisions and potentially less post operative pain. The surgeon is not limited to only the work volume surrounding the single trocar.
- Since fewer trocar ports are required, there is less chance of vital organs and blood vessels being damaged during insertion of the trocar port.
- The tools can be positioned anywhere they are needed without the need to remove other tooling. The potential benefit for the patient is that there is less time under anesthesia, while for the surgeon there is potentially less frustration.
- Less medical staff is required since the tools would be held and positioned by the magnets, not residents or nurses. While the patient may not see a direct benefit, the facility sees a reduction in cost for staffing.

While this concept had the possibility to revolutionize minimally invasive surgery, key questions and concerns had to be addressed, with the highest priority one of whether the magnets were capable of accomplishing this task.

1.5 Magnetic Coupling Viability

The concepts raised in the previous section depend on developing sufficient magnetic force to anchor the tool. In most common applications, magnets are either in direct contact with what they are going to be used with, or the force capacity is not required, as the magnetic field interacts with copper wires. The earliest magnets that were strong enough to be viable for most applications were aluminum-nickel-cobalt (AlNiCo) which were introduced in the 1920s. In the 1950s, they were replaced with ferrite-based magnets, which are the foundation of most magnets used today. Currently, samarium-cobalt (Sm_2Co_{12}) and neodymium-iron-boron (NdFeB) permanent magnets, commonly referred to as “rare-earth” magnets, are the most powerful commercial available magnets.

The question remains whether or not the rare-earth magnets are capable of generating the required force necessary to support tooling capable of surgical applications. Early testing showed that the attraction force between a magnet and a ferromagnetic material degrades as a decaying exponential as a function of distance. Because of this high degree of degradation, testing and analysis has centered around NdFeB magnets due to their high magnetic strength, and has proven to be capable of

generating sufficient attraction force to support tools for specific applications. These findings are discussed in greater detail in Chapter 4, Section 2.

1.6 Magnetically Anchored Surgical Tooling System

The Magnetically Anchored Surgical Tooling System (MAS) developed in this thesis exploits the concept of modularizing the functions of conventional laparoscopic tooling so that the essential mechanisms could be mounted on an internal platform coupled to an external magnet. The development originally centered around an organ retractor.

An organ retractor is a tool that is relatively static once it is positioned, nevertheless it consumes a trocar port for the length of the surgery. Over the course of the development, the equipment increased to include an internal camera, being able to view the surgical area from different angles, which can be very beneficial. Development then continued to include a pneumatically powered robotic arm capable of mimicking a hook cauterizer. Notice in the diagram below (Figure 4), conventional surgery requires four incisions, four separate chances for infection, four chances of severe injury, while MAS only requires one incision, one chance for infection, one chance of severe injury.

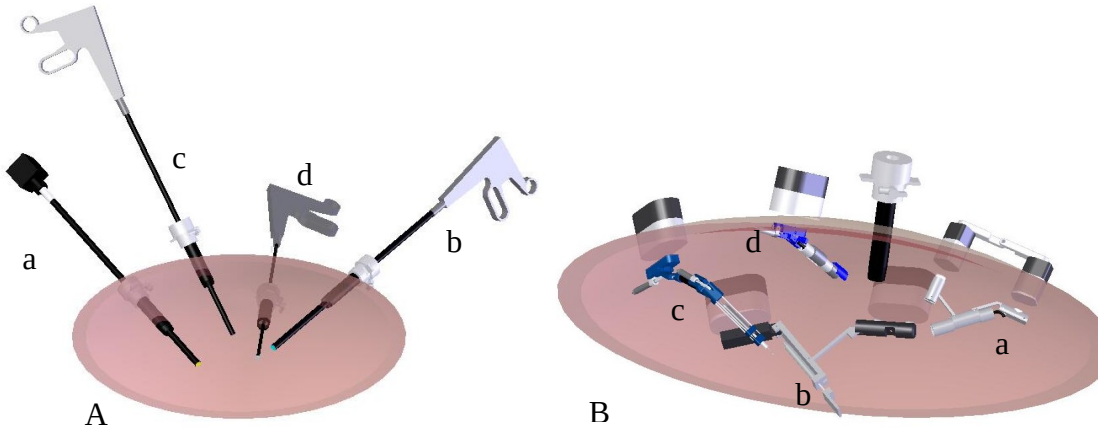

Figure 4. Comparison of conventional and MAS approach. In this figure, the same 4 tools are shown in both the conventional and MAS approach: camera (a), retractor (b), cauterizer (c) and an additional tool (d). In the conventional configuration (A), each of the four tools requires its own trocar. In the MAS configuration (B), showing a subdermal view of the same four tools, each can be introduced and extracted by using the same trocar port.

1.7 Magnetic Anchoring System Rationale

While the development of the MAS system was originally centered around the possibility of magnetic coupling and magnetic manipulation of equipment inside the body, the question of what to do with such a technology was raised. While conventional laparoscopic surgery is more appealing for the patient because of the aforementioned advantages, one could see that offering the additional advantage of being able to accomplish the same surgical procedure by reducing the number of the incisions would offer further benefits. Once the magnets reached satisfactory performance levels, the question of which tools to attempt was raised. As stated previously, most surgical procedures require three tools, a camera, a grasper and cutting tool. These three tools were looked into as the primary candidates for the MAS system.

The camera was chosen to receive most of the development time because of having one of the greatest impacts to the surgical procedures. A camera that is not limited to a trocar port offers the ability to have multiple views of the same area and the ability to move about the abdominal cavity at will, without having to remove or reposition other tooling. The development the camera tool eliminates one of the three mandatory trocar ports.

A grasper tool was considered for development, but due to the actuation and strength requirements, it was deemed too challenging for a first generation tool. After all, the magnetic components as well as the tool associated with them were to be tested.

A cutting tool was chosen to be developed because, while it did require high degrees of motion, the motions are simpler than that of the grasper. The loads on the tool tip are less than that of the grasper because the tissue is being cut rather than being moved. An electro-cautery was chosen since the cutting action does not require moving blades but rather an electrical connection, simplifying the design. The development of the cutting tool eliminates one of the three mandatory trocar ports.

The organ retractors were chosen for development because unlike the previous examples, during conventional laparoscopic procedures, once positioned, the tool is rarely repositioned. The development of a magnetically supported retractor means that the benefits of reduced trocar surgery could be utilized in multiple sugeries, not just the relatively simple ones.

Using the MAS system, multiple two-trocar port nephrectomies have been successfully completed in porcine models. Two trocar surgery is not possible with

conventional laparoscopic tools, especially nephrectomies, since the aforementioned necessary tools are required.

It should be noted, while two trocars were inserted into the porcine model, only one of the ports was actively used. The other port was used for taking video and pictures of the tooling at work. The mini-camera tool (MAS camera), was used as the surgical camera, not the conventional camera. The conventional camera, and hence second trocar port, was used only for documentation purposes due to difficulties connecting the MAS camera to the recording components available in the operating room. The surgeries that were accomplished could easily be accomplished with a single trocar port.

CHAPTER 2

MAS BACKGROUND AND PROTOTYPE TOOLS

Over the course of the work on MAS, multiple tools were developed to accomplish specific tasks. While the specifics of the tools are described in detail in Chapter 4, a description of the operation is required to fully understand the problems that were raised and addressed over the development process.

The tools developed, unless the tool was intended as a proof of concept, were designed with the constraint that the tool must pass through a conventional 15 millimeter trocar port without causing damage to the port. While 15 millimeters is rather large compared with conventional equipment, this decision was made to make the design and fabrication of the equipment easier since the goal was to test the validity of the concept, not the ability to fabricate small components.

It should be noted that all tools were designed with conventional machining practices in mind, e.g., all tooling was manufactured with 3 axis machining processes and a lathe. Because the tools had to be made conventionally, the designs were constrained by this requirement as well as the size constraints of the trocar port. The implementation of rapid prototyping would allow for more flexibility in design, but has limited availability.

2.1 Electromagnets

The electromagnet prototype was originally conceived as a simple magnetic source that could be varied depending upon the needs of the surgery or tool. The electromagnet was connected to a variable power supply, which in-turn, varies the magnetic strength (Figure 5). Specifics of the prototype's construction are given in Chapter 3 Section 1 and Chapter 4 Section 1.1.

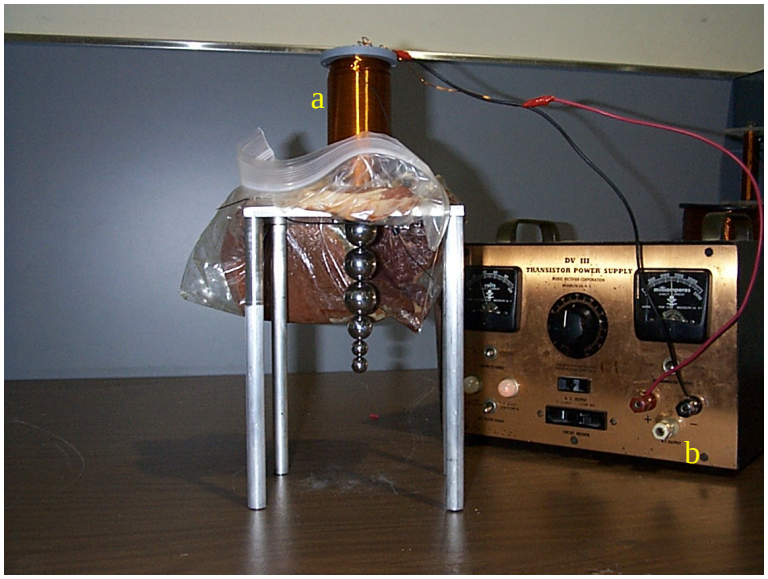

Figure 5. Electromagnet prototype. The electromagnet prototype (a) was powered by a variable power supply (b).

A larger, more powerful magnet was designed and outsourced for construction. Much like the prototype, it was powered by a variable power supply (Figure 6). A detailed discussion of the electromagnet revision b is available in Chapter 4 Section 1.2.

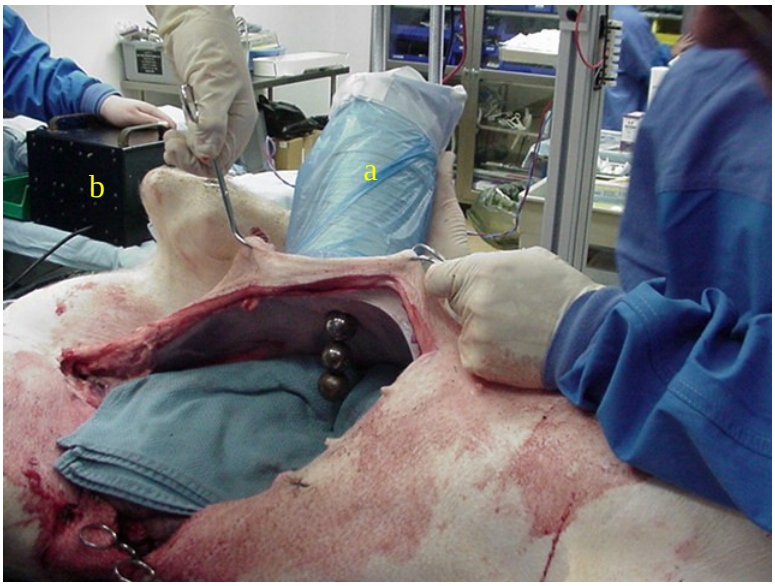

Figure 6. Electromagnet second prototype. As with the prototype, the second generation electromagnet (a) was powered by a variable power supply (b).

2.2 Permanent Magnet Test Structure

Since the magnet would need to function at different angles, a lock mechanism was devised to work at any given angle. The locking of the magnets was accomplished by moving a thumb-screw to different locations in the aluminum housing and tightening the screw. This simple adjustment allowed for large changes in the coupling force (Figure 7). Details on the permanent magnet test structure are available in Chapter 3 Section 2, and the information gathered can be found in Chapter 4 Section 2.1.

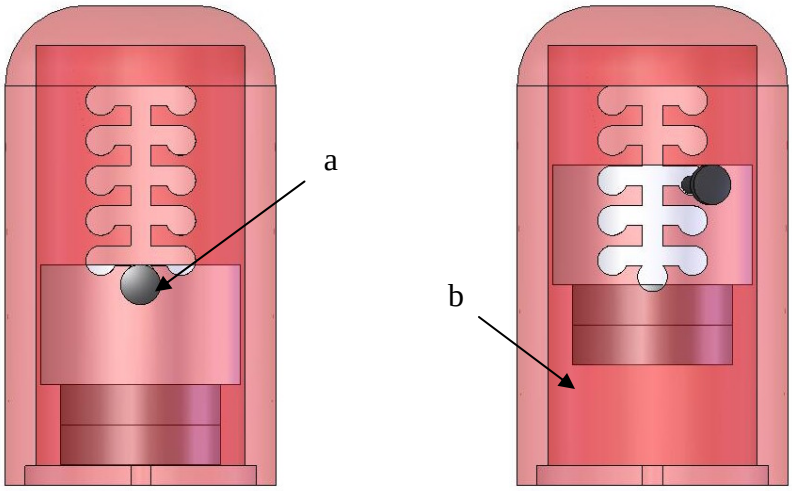

Figure 7. Permanent magnet test structure. By changing the location of the thumb screw (a) the magnet stack can be raised or lowered in the aluminum structure (b). The aluminum structure has been made transparent to allow the viewing of the change in magnet position.

2.3 Permanent Magnet Enclosures

To protect the magnets from the surgical area, as well as the surgical area from the magnets, a set of enclosures were developed to house the magnets. Type 1 has a single stack of magnets in the external as well as the internal enclosure and is shown in Figure 8. Type 2 has a dual stack of magnets in the external as well as the internal enclosure and is shown in Figure 9. Type 3 not only has a dual stack of magnets, but also a channel for the anchoring needle to pass through the external as well as the internal enclosure and is shown in Figure 10. Details on the Type 1, Type 2 and Type 3 are available in Chapter 3 Section 3, and in Chapter 4 Sections 3.1 ,3.2 and 3.3, respectively.

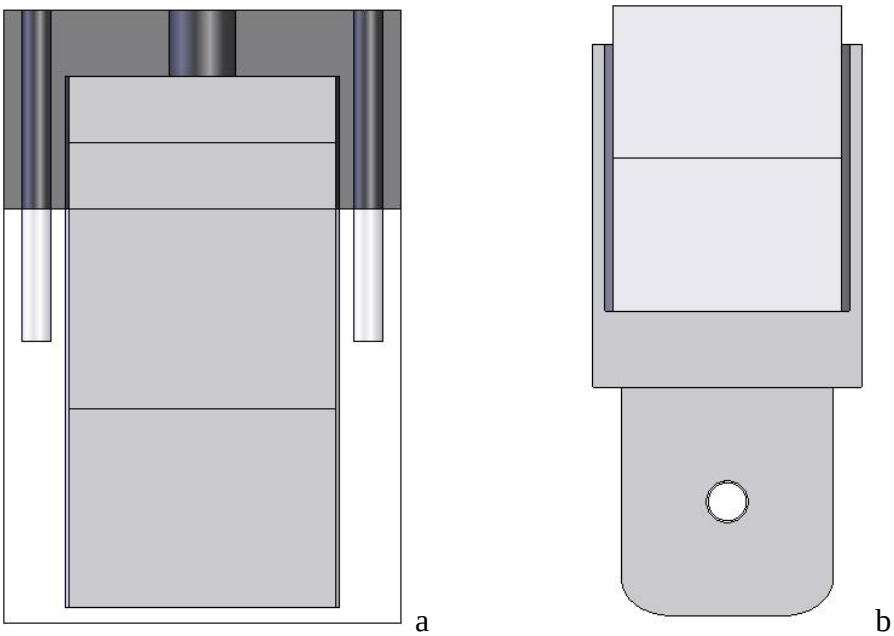

a b

Figure 8. Type 1 enclosures, external (a) and internal (b).

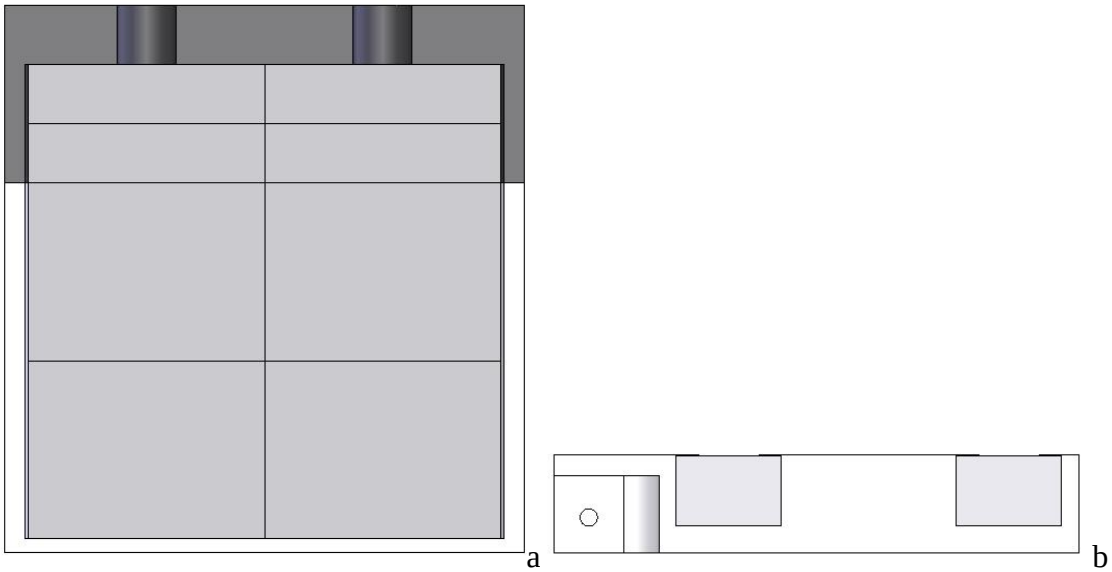

a b

Figure 9. Type 2 enclosures, external (a) and internal (b)

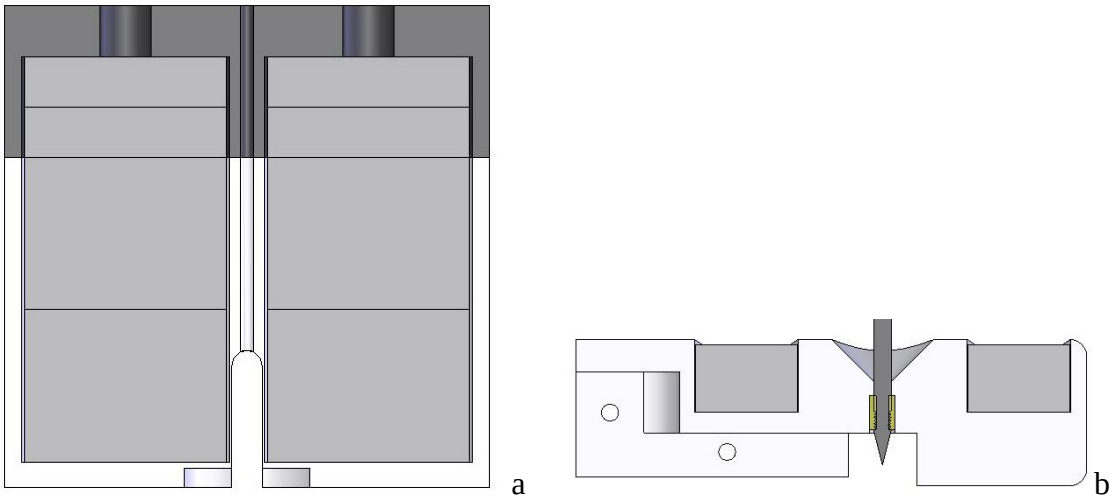

Figure 10. Type 3 enclosures, external (a) and internal (b).

2.4 Sling Retractor

The sling retractor prototype (Figure 11) was the first of the tools to be developed and is discussed in detail in Chapter 3 Section 4 and in Chapter 4 Section 4.1.

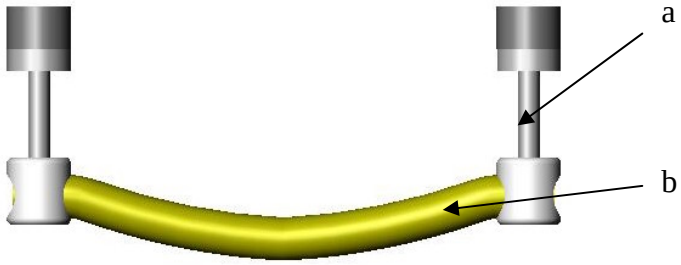

Figure 11. Sling retractor prototype. The anchors (a) support a medium between them (b) to support the tissue.

The second generation of the sling retractor (Figure 12) proved capable during a surgical test and developed ceased while more challenging tools were developed. The tool is discussed in detail in Chapter 3 Section 5 and in Chapter 4 Section 4.2.

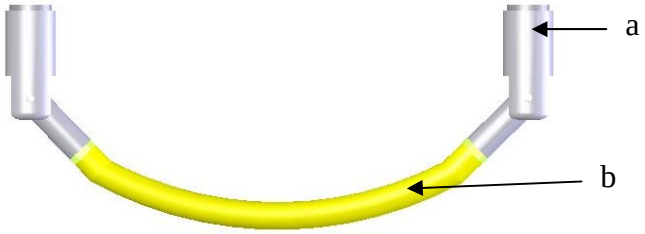

Figure 12. Sling retractor revision b. The anchors (a) support a medium between them (b) to support the tissue.

2.5 Paddle Retractor

The paddle retractor prototype (Figure 13) was the next tool to go into development. The height and angle of the paddle are adjusted by moving the anchors closer or further apart (Figure 13). The paddle retractor prototype is discussed in detail in Chapter 3 Section 6 and Chapter 4 Section 5.1.

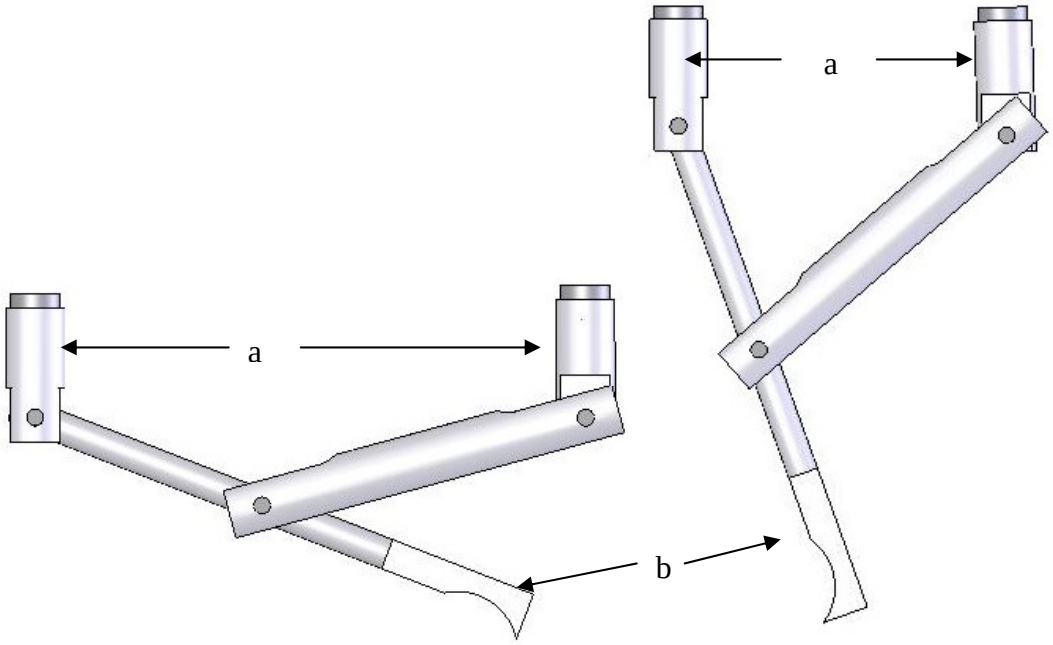

Figure 13. Paddle retractor prototype. As the anchors (a) are moved closer and farther apart, the height and angle of the paddle (b) is changed.

The second generation paddle retractor (Figure 14) was the first to incorporate the Type 2 anchors. The paddle retractor revision b is discussed in detail in Chapter 3 Section 7 and Chapter 4 Section 5.2.

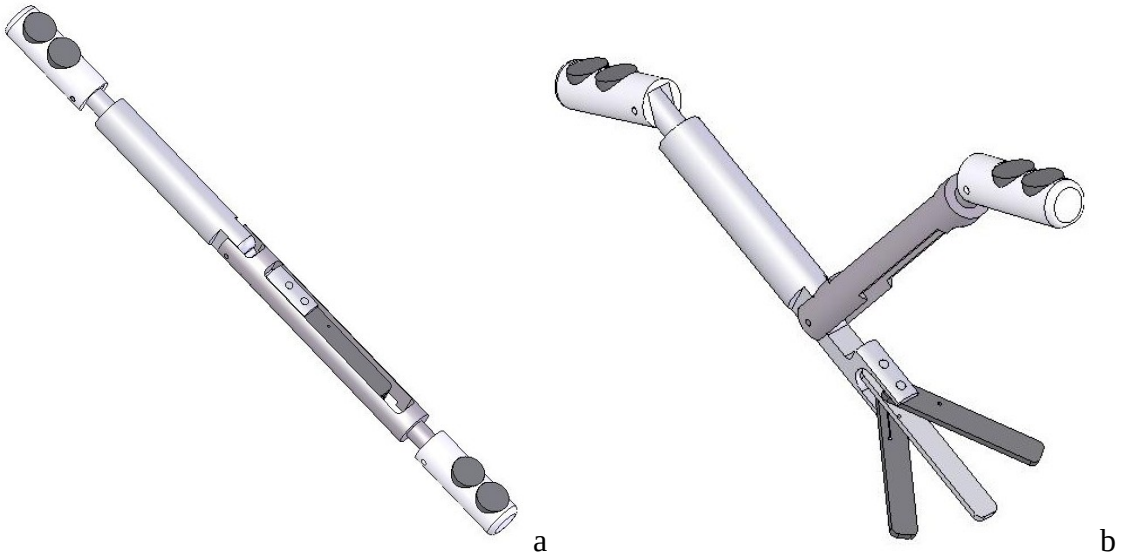

a b

Figure 14. Paddle retractor revision b. For insertion (a), the tool folds to fit through the trocar. After insertion, the tool unfolds (b) and is ready for use.

The third generation paddle retractor (Figure 15) used the valuable testing information gathered from the second generation. The paddle retractor revision c is discussed in detail Chapter 3 Section 8 and Chapter 4 Section 5.3.

a b

Figure 15. Paddle retractor revision c. For insertion (a), the tool folds to fit through the trocar. After insertion, the tool unfolds (b) and is ready for use.

The fourth generation paddle retractor (Figure 16) used the findings up until this point. The tool was built around a smaller bore cylinder that fit the constraints of the trocar better. The paddle retractor revision d is discussed in detail Chapter 3 Section 9 and Chapter 4 Section 5.4.

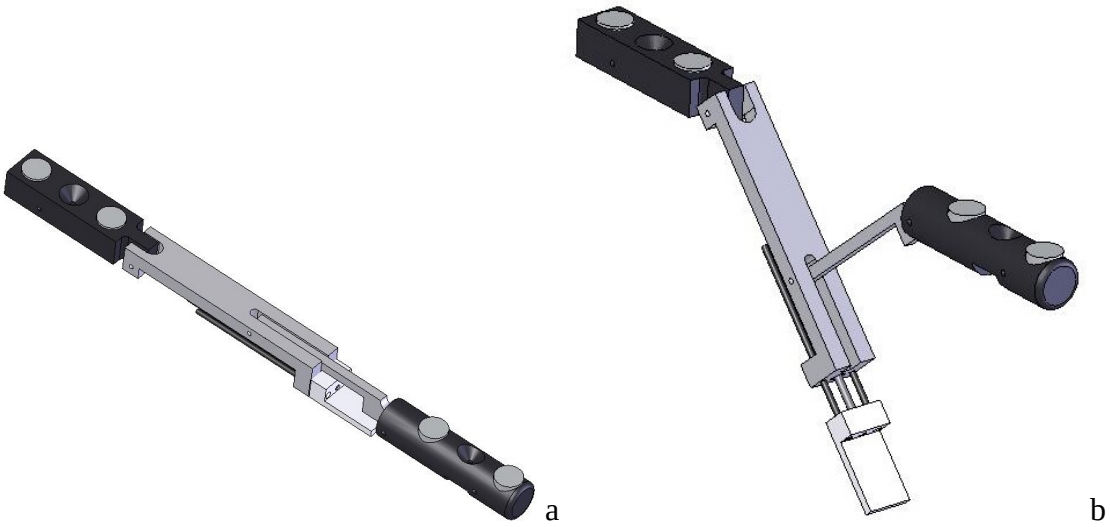

a b

Figure 16. Paddle retractor revision d. For insertion (a), the tool folds to fit through the trocar. After insertion, the tool unfolds (b) and is ready for use.

2.6 Camera System

The camera system is comprised of the actual camera tool, a trocar port light source and a digital editing system. The trocar port light is discussed in greater detail in Chapter 3 Section 11 and Chapter 4 Section 6.2. The digital editing system is discussed in Chapter 4 Section 6.3.

The camera stand prototype (Figure 17) required a conventional tool to aim the camera. The camera stand prototype is discussed in greater detail in Chapter 3 Section 10 and Chapter 4 Section 6.1.

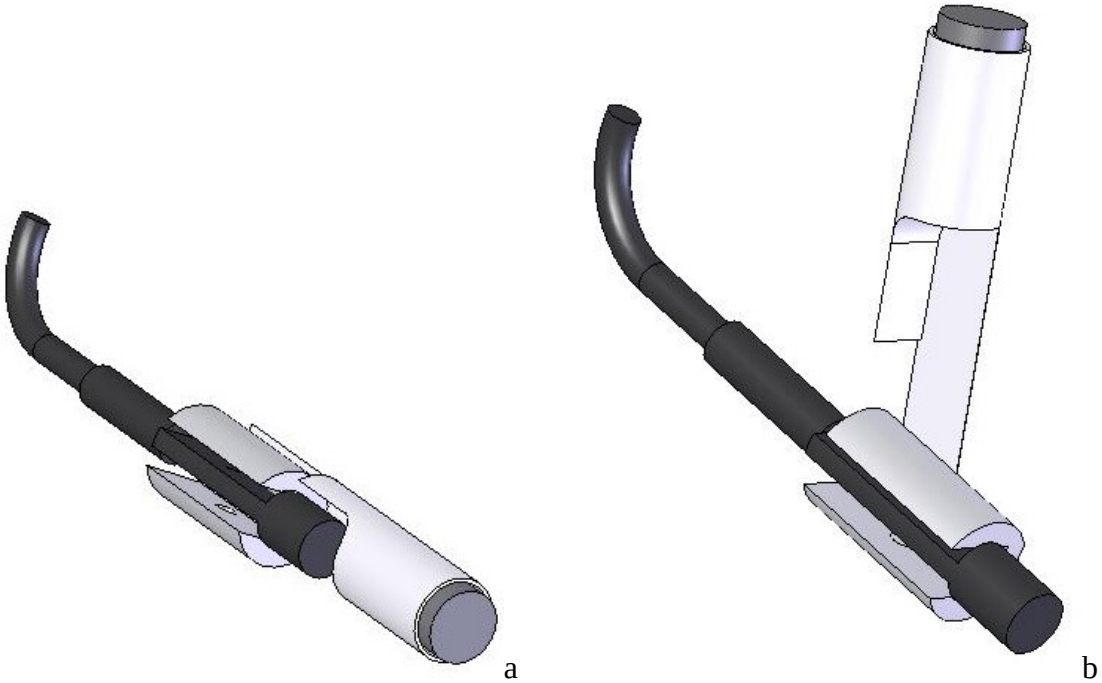

a b

Figure 17. Camera stand prototype. For insertion (a), the tool folds to fit through the trocar. After insertion, the tool unfolds (b) and is ready for use.

The camera stand revision b (Figure 18) was the first truly function camera stand developed. The camera stand revision b is discussed in greater detail in Chapter 3 Section 12 and Chapter 4 Section 6.4.

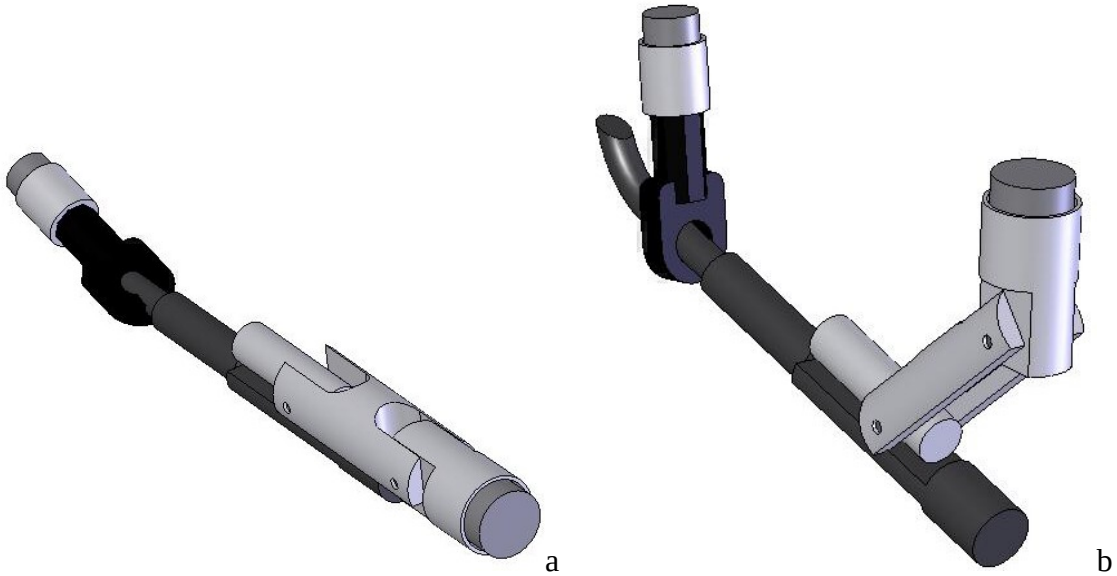

a b

Figure 18. Camera stand revision b. For insertion (a), the tool folds to fit through the trocar. After insertion, the tool unfolds (b) and is ready for use.

Since the dual anchor layout proved to be very beneficial to the camera stand, the concept was carried over to revision c (Figure 19). The camera stand revision c is discussed in greater detail in Chapter 3 Section 13 and Chapter 4 Section 6.5.

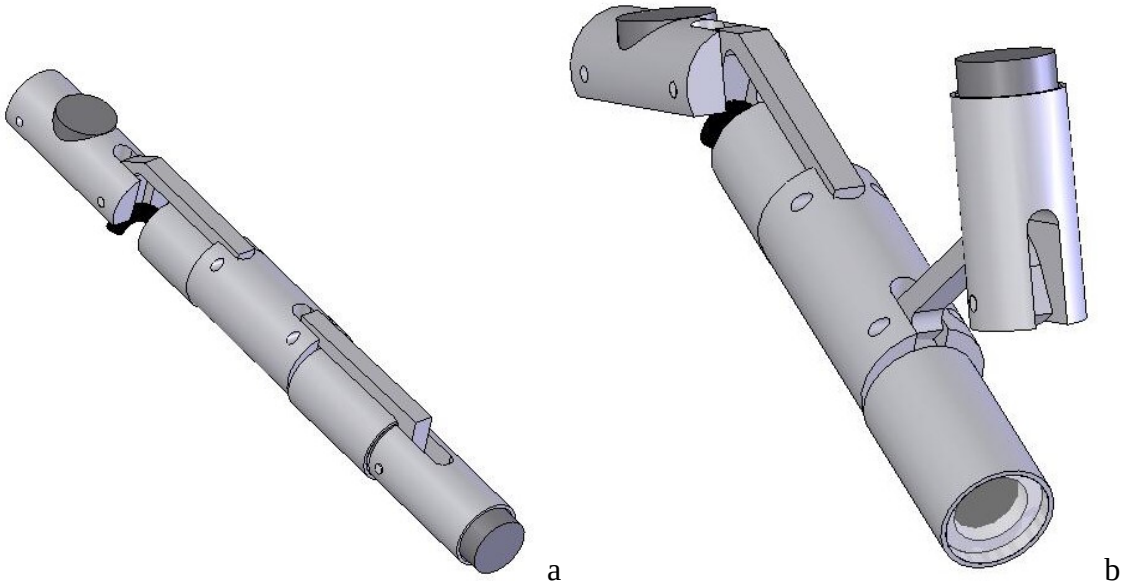

a b

Figure 19. Camera stand revision c. For insertion (a), the tool folds to fit through the trocar. After insertion, the tool unfolds (b) and is ready for use.

With the development of powered anchors, revision d (Figure 20) was reduced to a simple powered anchor. The camera stand revision d is discussed in greater detail in Chapter 3 Section 14 and Chapter 4 Section 6.6.

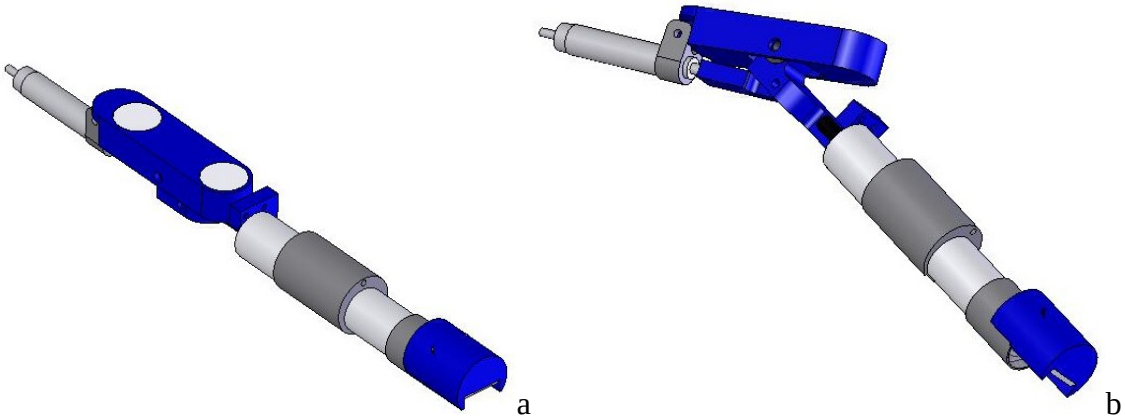

a b

Figure 20. Camera stand revision d. For insertion (a), the tool folds to fit through the trocar. After insertion, the tool unfolds (b) and is ready for use.

2.7 Powered Tooling

With the powered tooling, a control system was needed that allowed input from the surgeon to be translated to motions of the tool. The details of the control system are available in Appendix H, and discussed in Chapter 3 Section 15 and Chapter 4 Section 7.1. The surgeon operated a wireless joystick, which in-turn, was mimicked by the tool.

The pneumatically powered prototype (Figure 21) was designed with the constraints of the trocar in mind, but, more to determine if three on-board degrees of freedom could allow for the motion required to act as a hook cautery. The pneumatically actuated prototype is discussed in greater detail in Chapter 3 Section 16 and Chapter 4 Section 7.2.

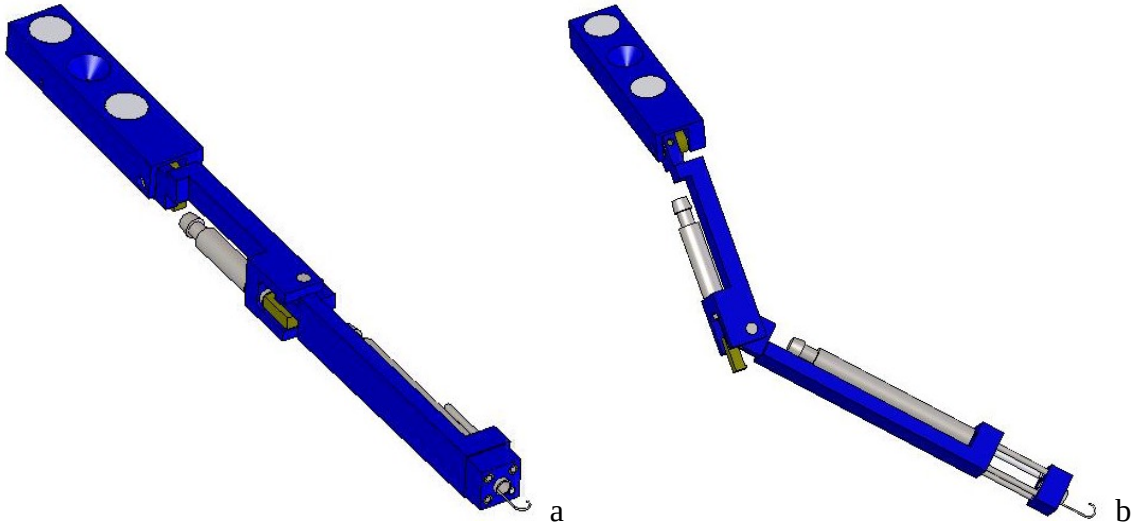

Figure 21. Pneumatically actuated arm prototype. For insertion (a), the tool folds to fit through the trocar. After insertion, the tool unfolds (b) and is ready for use.

The first version of the powered tooling to be used in surgery was the pneumatically actuated revision b (Figure 22). The pneumatically actuated revision b is discussed in greater detail in Chapter 3 Section 17 and Chapter 4 Section 7.3.

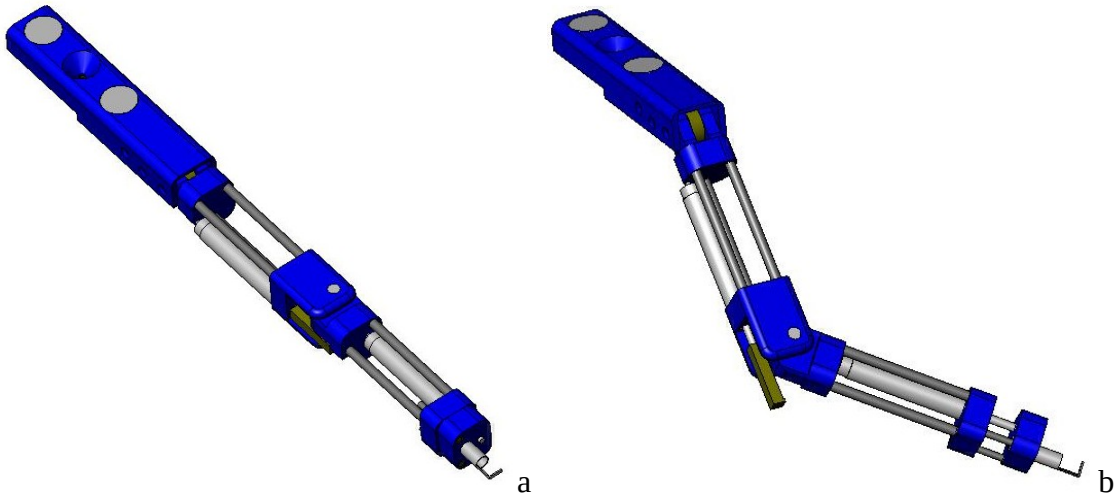

Figure 22. Pneumatically actuated Arm revision b. For insertion (a), the tool folds to fit through the trocar. After insertion, the tool unfolds (b) and is ready for use.

The pneumatically actuated revision c (Figure 23) is a simpler version of the revision b arm. The pneumatically actuated revision c is discussed in greater detail in Chapter 3 Section 18 and Chapter 4 Section 7.4.

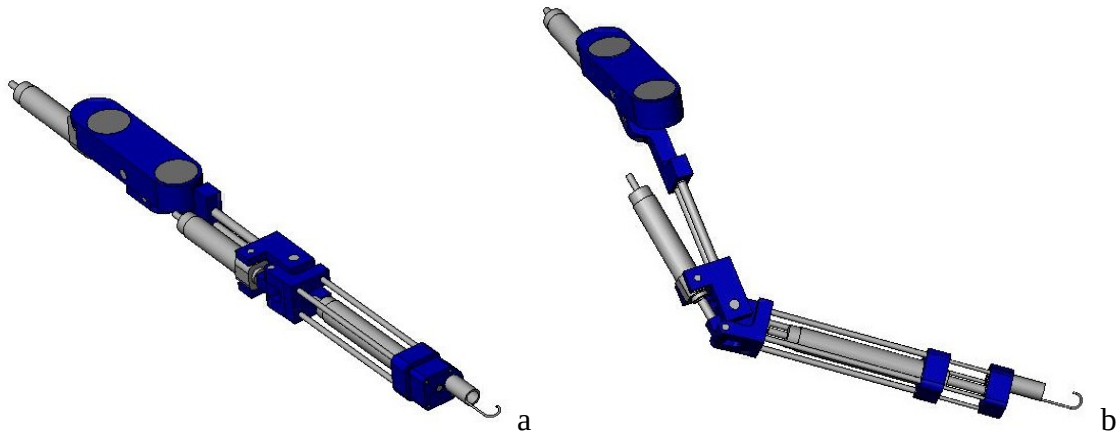

Figure 23. Pneumatically actuated Arm revision c. For insertion (a), the tool folds to fit through the trocar. After insertion, the tool unfolds (b) and is ready for use.

The nitinol actuated prototype (Figure 24) was the first attempt at shape memory alloy powered tooling. The nitinol actuated prototype is discussed in greater detail in Chapter 3 Section 19 and Chapter 4 Section 7.5.

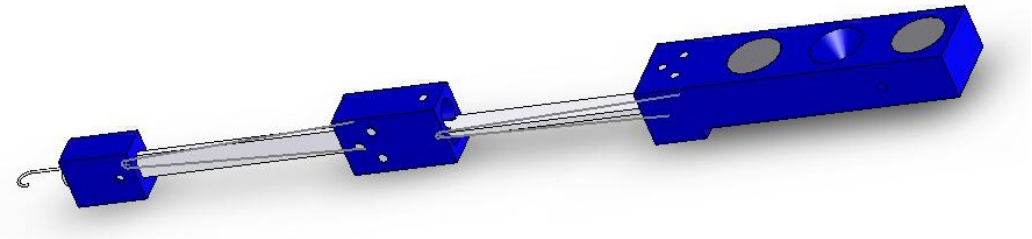

Figure 24. Nitinol actuated arm prototype. The arm's natural, unpowered position was straight, for insertion. Unlike the pneumatic arms, in the prototype, the links bent in only one direction, allowing movement.

The nitinol actuated revision b (Figure 25) was an experimental design to see if the performance of the shape memory alloy could be improved. The nitinol actuated revision b is discussed in greater detail in Chapter 3 Section 20 and Chapter 4 Section 7.6.

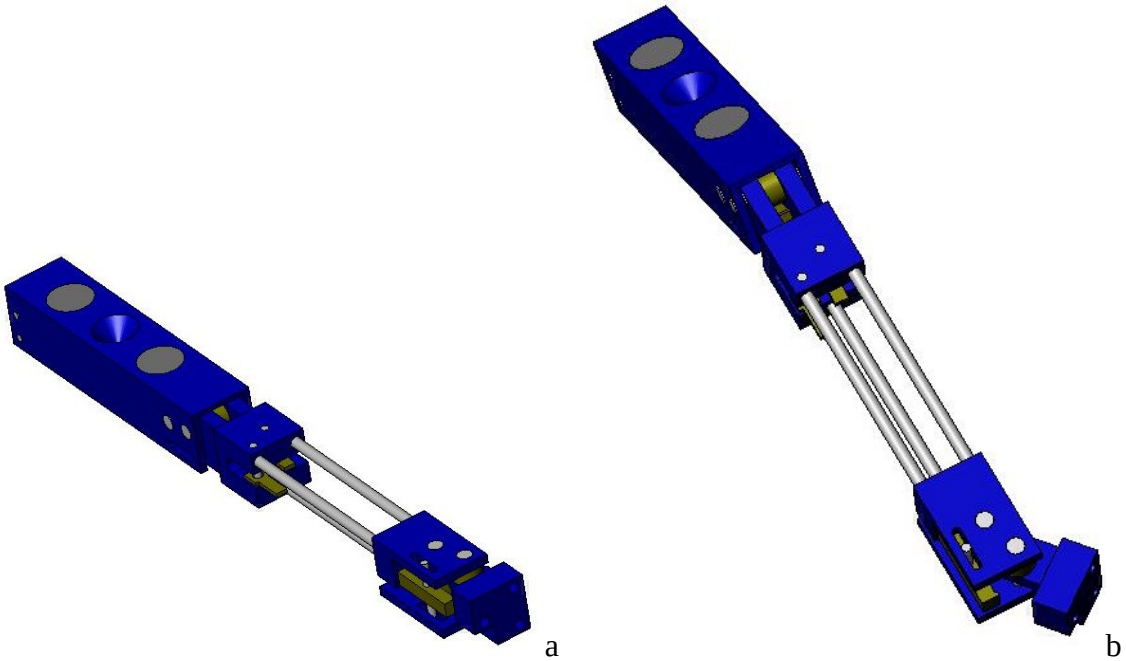

a b

Figure 25. Nitinol actuated arm revision b. For insertion (a), the tool folds to fit through the trocar. After insertion, the tool unfolds (b) and is ready for use.

CHAPTER 3

MATERIALS AND METHODS

While the most successful tools were tested in the animal lab at UTSW, many of the early iterations never made it past design reviews and dry lab testing. For design reviews with Dr. Cadeddu, a simple test structure was built for function testing. The stand was for testing the specific function of the tools, not to simulate tissue.

The test structure (Figure 26) was designed as a platform for the testing of the electromagnets specifically, but its continued used allowed for testing of tools as well. There is a hole in the middle of the upper plate which allowed the electromagnet as well as the permanent magnets be in direct contact with the beef steak for testing of the magnetic attraction force. Later, the stand became useful for demonstrating tool uses and functions. The detailed listing of the materials used in the construction of the test structure is available in Appendix A.

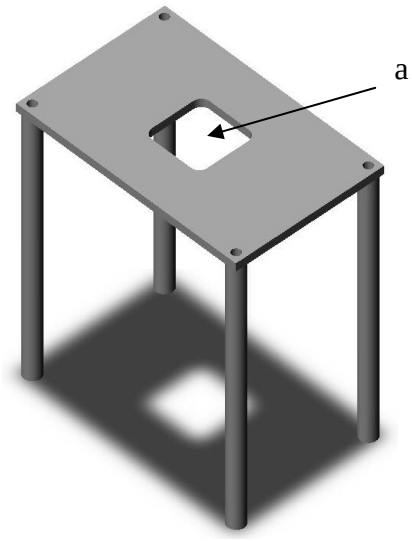

Figure 26. Test structure. The plate served as a support for the beef steak, but also allowed for the magnets to be in direct contact with the steak, as to not skew the test results (a).

3.1 Electromagnet Prototype

For a detailed listing of the materials used in the construction of the electromagnet prototype, please see Appendix B. As shown in Figure 27, the prototype was assembled by threading the two end plates (a) onto the steel rod (b).

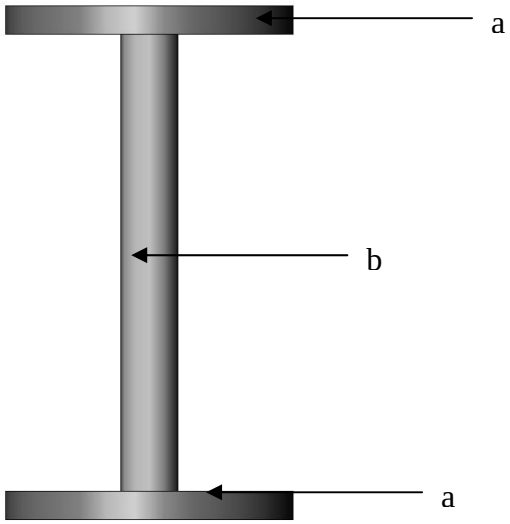

Figure 27. Attachment of plastic end plates to steel core. The ends of the steel and a hole in the end plates were threaded to facilitate assembly.

Then the assembly was inserted into a wire transfer device that was available. The wire was pulled through the hole in the end plate closest to the steel rod, as shown in Figure 28 as point a, until approximately 100 millimeters (4 inch) of wire was free. Then the wire transfer device was started and the wire was guided by hand as tight as possible to minimize losses due to air. When almost all of the wire was wound, the wire was cut and passed through the second hole, as shown in Figure 24 as point b, to keep the wire from uncoiling. The enamel was burned off the ends of the wire and the magnet was ready for use.

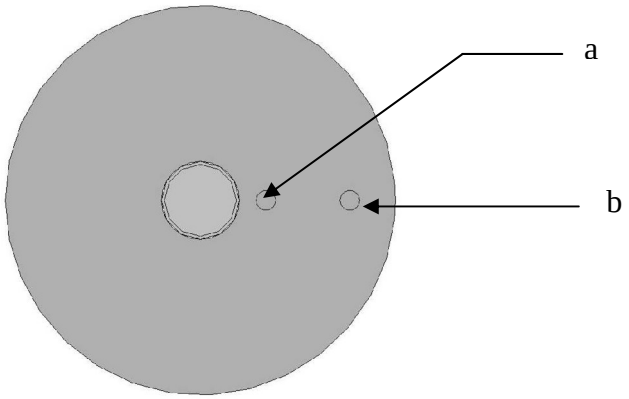

Figure 28. Magnet wire pass-through holes. The wire was pulled through the hole closest to the core (a) until approximately 100 millimeter (4 inch) protruded. After sufficient wire was wound around the core, the wire passed through the outer hole (b) until approximately 4 inches protruded.

3.2 Permanent Magnet Test Structure

For a detailed listing of the materials used in the construction of the permanent magnet test structure, please see Appendix C. One of the magnets was epoxied to the delrin component since delrin in not magnetic and the magnets needed to stay in the delrin piece (Figure 29A). The remaining magnets were then allowed to come in direct contact with the epoxied magnet as well as each other to form the test stack (Figure 29B).

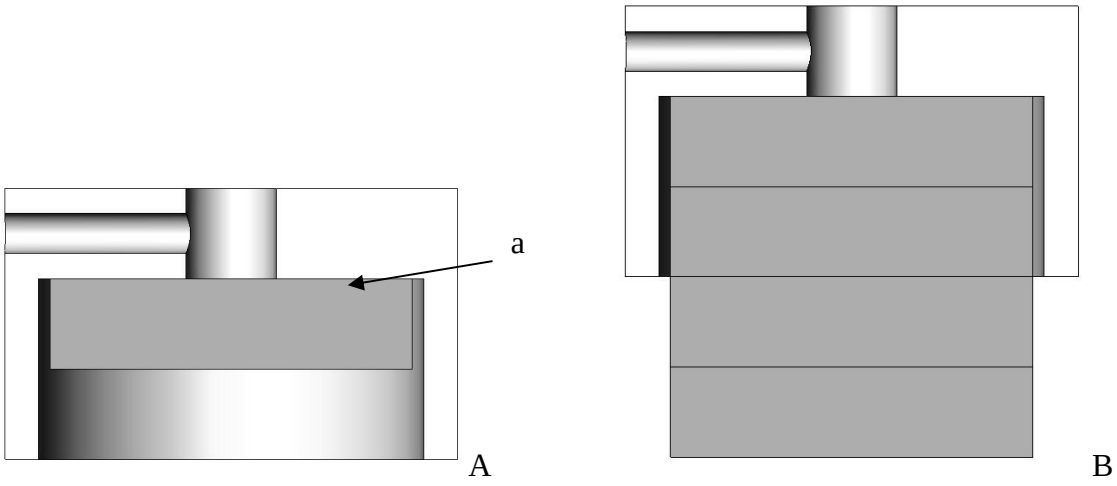

Figure 29. Assembly of magnet stack. Epoxy was applied to the upper surface of the first magnet (a). The remaining magnets were held by their magnetic attraction.

The delrin and magnets were then inserted into the aluminum housing and the thumbscrew was then threaded into the delrin piece to adjust the location of the magnets (Figure 30A). Finally, the clear lexan piece was press-fit into the bottom of the aluminum housing to protect the magnets from the environment (Figure 30B).

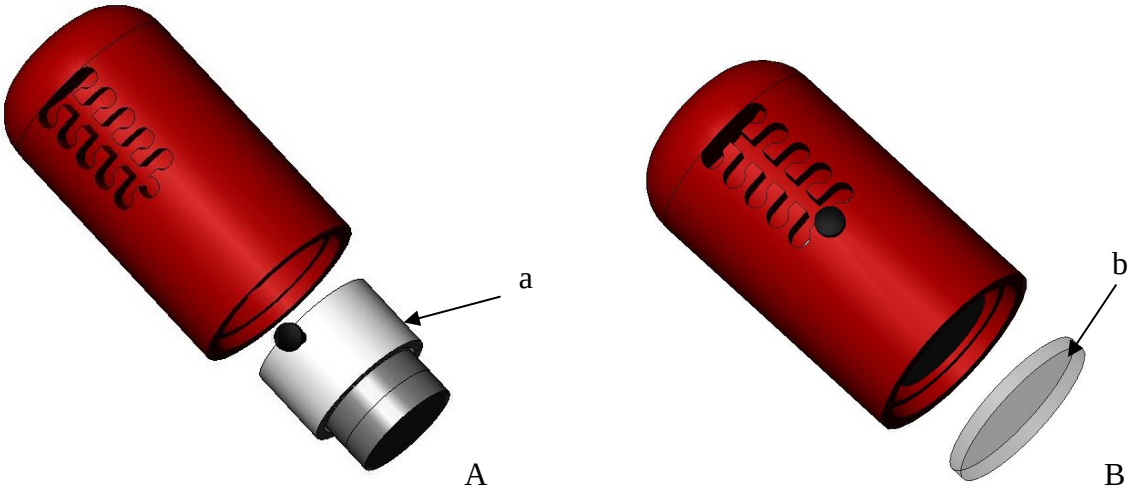

Figure 30. Magnet test structure assembly. The magnetic assembly (a) is slid into the aluminum housing. The lexan disc (b) is pressed into the aluminum housing.

3.3 Permanent Magnet Enclosures

For a detailed listing of the materials used in the construction of the permanent magnet enclosures, please see Appendix D. While there are three distinct types of enclosures, they share many similarities. The nickel plated magnets (Figure 31Aa) were the first to be loaded into the steel tops of the external enclosures because the nickel protects the magnet from corroding. The internal enclosure magnets were always loaded with their polarities opposite that of the external enclosures, as well as the bottom magnet being epoxied into place (Figure 31Bb).

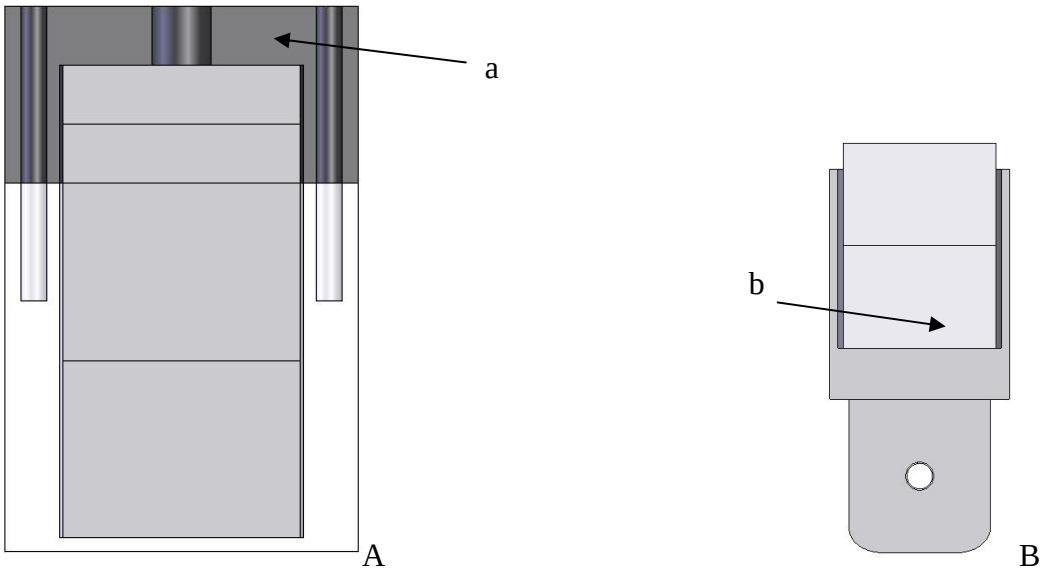

Figure 31. Type 1 external and internal enclosures. Because of the steel used for the top (a) of the external enclosure (A), the internal enclosure (B) requires the magnets to be epoxied into the enclosure (b).

Unlike the Type 1 enclosures, the Type 2 and 3 require a decision on the configuration of the magnets, since the assembly can be either North-North or North-South. For the most part, North-South was used. While knowledge of the poles is not required, the magnets must be installed either in the same direction (North-North) or opposite (North-South). A discussion of the benefits and drawbacks to both configurations is available in Chapter 4, Section 3.

3.4 Sling Retractor Prototype

For a detailed listing of the materials used in the construction of the sling retractor prototype, please see Appendix E. As shown in Figure 32A, the magnet(s) were epoxied to the magnet mount. Once the glue had dried, the magnet mounts were

then threaded into the tube holder until the magnet mount was tight against the tubing (Figure 32B).

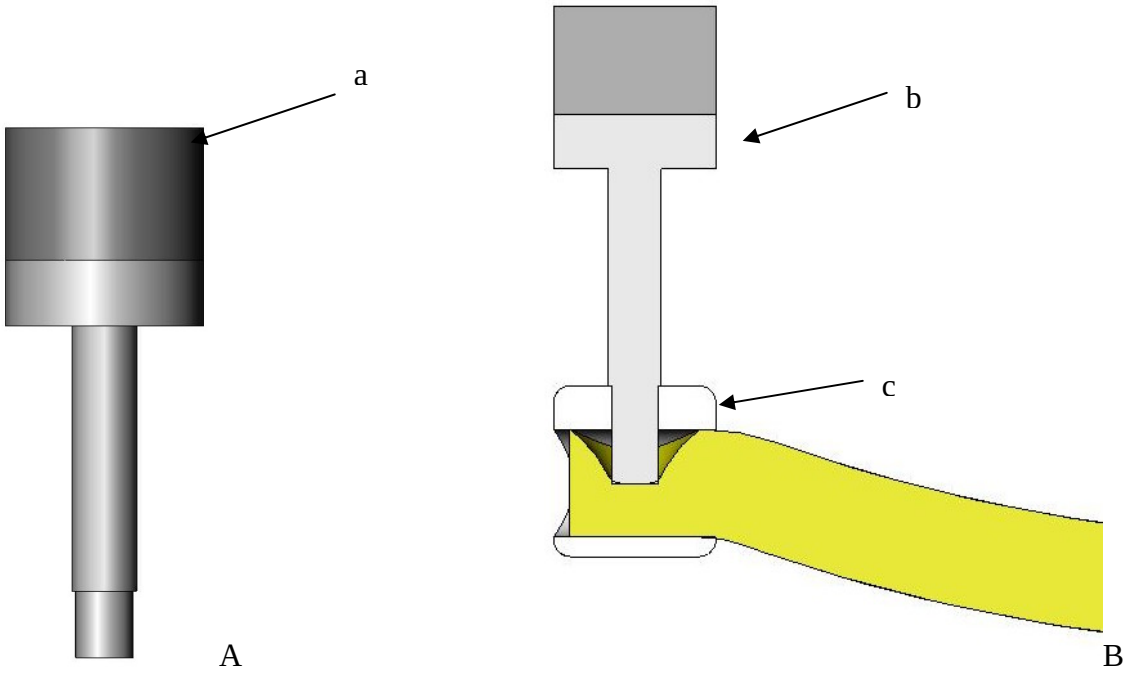

Figure 32. Assembly of sling retractor protoype. The magnet is epoxied onto the magnet mount (a). The magnet mount (b) was threaded into the tube holder (c) until the mount was tight against the tubing.

3.5 Sling Retractor Revision B

For a detailed listing of the materials used in the construction of the sling retractor revision b, please see Appendix E. The magnets were stacked together and allowed to couple to a Type 1 external source. Once coupled, the bottom magnet was epoxied into place in the magnet mount (Figure 33).

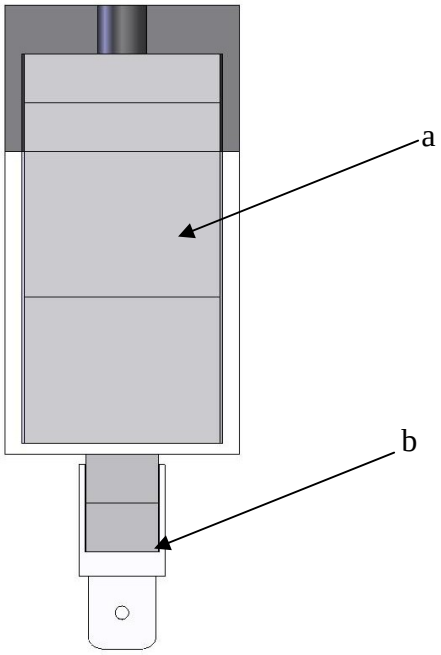

Figure 33. Assembly of type 1 anchor. The magnets are coupled to an external source (a) to ensure proper polarity. The magnet mount is then epoxied to the bottom magnet (b).

The pivot was locked in place by the dowel pin. The barb fitting was installed in the bottom of the pivot, with the tubing then slid onto the barb fitting (Figure 34).

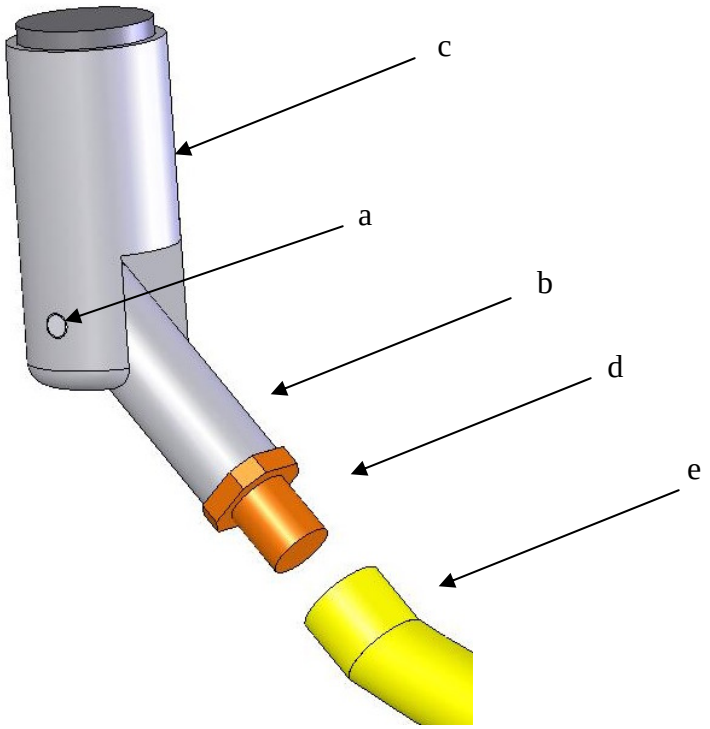

Figure 34. Assembly of sling retractor revision b. The dowel pin (a) is installed to secure the pivot (b) to the magnet mount (c). The barb fitting (d) is installed in the pivot and the tubing (e) is installed onto the barb fitting.

3.6 Paddle Retractor Prototype

For a detailed listing of the materials used in the construction of the paddle retractor prototype, please see Appendix F. The magnets were stacked together into two sets of two magnets and allowed to couple to a Type 1 external source to make sure the polarity was set correctly. Once the magnets were in place, the magnets were then epoxied into place (Figure 33).

3.7 Paddle Retractor Revision B

For a detailed listing of the materials used in the construction of the paddle retractor revision b, please see Appendix F. The magnets were not stacked vertically for this tool. Instead, they were coupled to a Type 2 external source to get the polarity of the magnets correct, then were epoxied into place in the anchors (Figure 35).

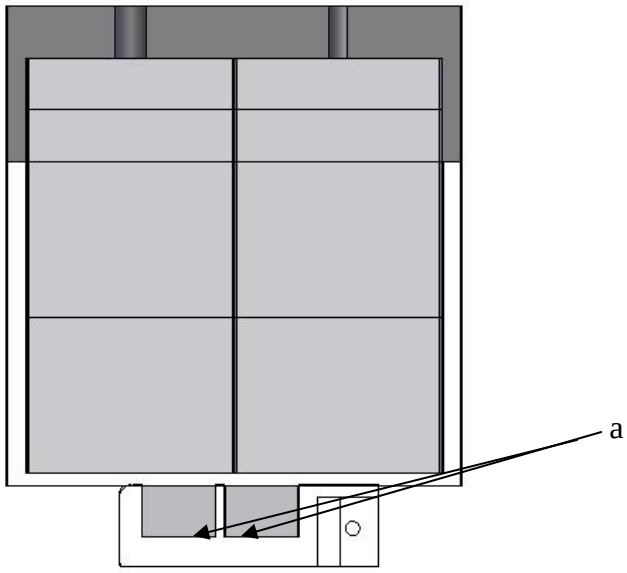

Figure 35. Assembly of type 2 anchor. The magnets were coupled to a Type 2 external source to ensure correct polarity. Then, the magnets were epoxied into place (a).

The 2-56 screws were used to secure the three fingers in the tool, but once the fingers were secure, the caps of the screws were cut off to make the tool fit through the trocar (Figure 36).

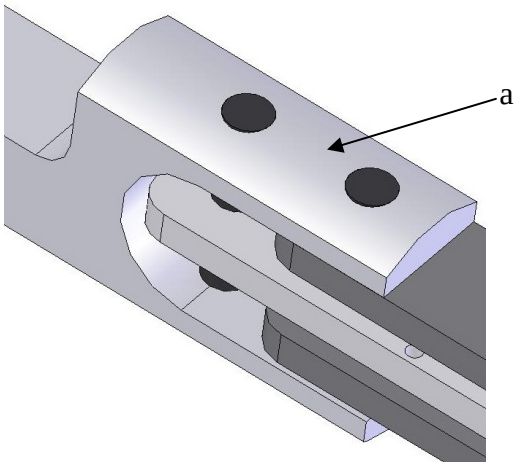

Figure 36. Assembly of paddle. The screws that are inserted into these holes to secure the fingers must have the heads ground off to the surface of the linkage (a) so that the tool fits properly through the trocar.

3.8 Paddle Retractor Revision C

For a detailed listing of the materials used in the construction of the paddle retractor revision c, please see Appendix F. The magnets were not stacked vertically for this tool. Instead, they were coupled to a Type 2 external source to get the polarity of the magnets correct, then were epoxied into place in the anchors (Figure 35). The 2-56 screw was used to secure the two fingers in the tool, but once the fingers were secure, the cap of the screw was cut off to make the tool fit through the trocar. There was not sufficient space available to use a standard fitting for the cylinder. Supply tubing was force into the inlet hole of the cylinder and was able to handle minimal pressures this way. The tool was designed around the need to test the concept of pneumatically actuated tooling, so the problem with the fitting could be tolerated, but needed to be addressed in a fully prepared version (Figure 37).

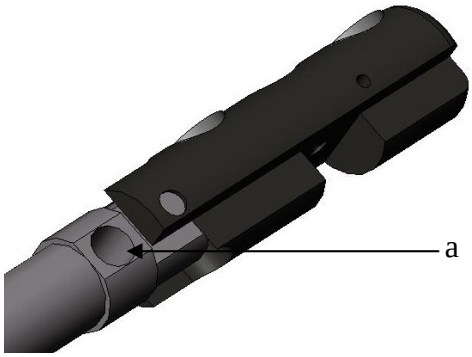

Figure 37. Pneumatic fitting for paddle retractor revision c. The anchor proximal to the trocar port has a passageway for the pneumatic supply line to fit into. Due to the tight size constraints, the pneumatic line was pressed directly into the port on the cylinder (a).

3.9 Paddle Retractor Revision D

For a detailed listing of the materials used in the construction of the paddle retractor revision d, please see Appendix F. The magnets were not stacked vertically for this tool. Instead, they were coupled to a Type 2 external source to get the polarity of the magnets correct, then were epoxied into place in the anchors (Figure 35). The cylinder was modified by removing the factory installed fitting and the rear of the cylinder was bored and tapped to accommodate the smaller 2 millimeter fitting (Figure 38).

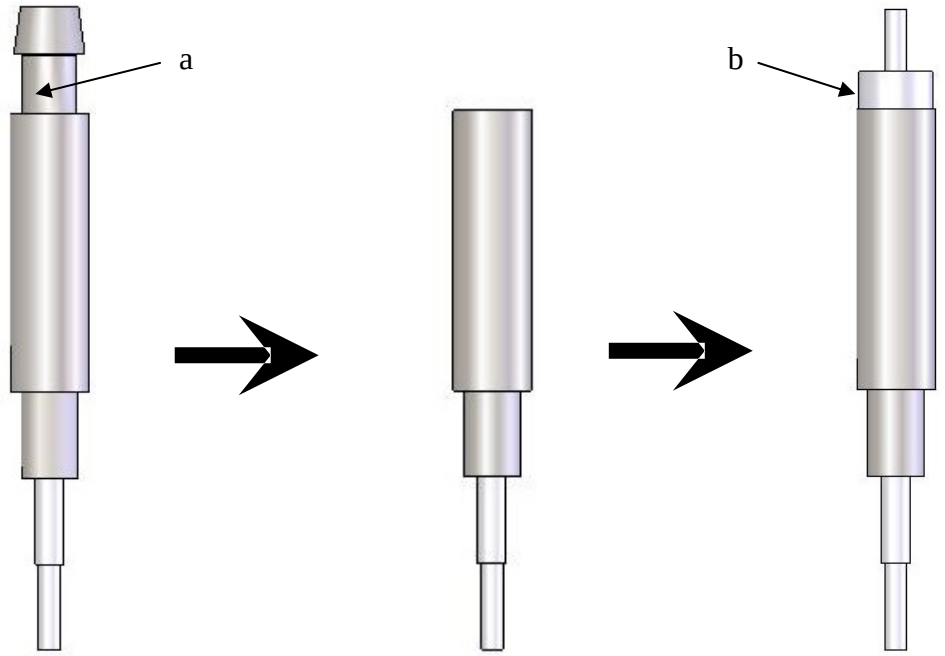

Figure 38. Modification to cylinders. The fitting that is built into the cylinder (a) was removed and the rear of the cylinder was bored and tapped for the 2 millimeter fitting (b).

3.10 Camera Stand Prototype

For a detailed listing of the materials used in the construction of the camera stand prototype, please see Appendix G. The magnets were stacked vertically for this tool. The stack was coupled to a Type 1 external source to get the polarity of the magnets correct, then the bottom magnet was epoxied into place in the anchor (Figure 33).

3.11 Trocar-Light

For a detailed listing of the materials used in the construction of the trocar light, please see Appendix G. The trocar light concept required modification of two conventional trocar ports. The upper portion of the 15 millimeter trocar port was

removed so all that was left was the sleeve itself (Figure 39A). The sleeve was then shortened by cutting off 28 millimeters (1.1 inch) of the distal end and another 9 millimeters (0.35 inch) off the proximal end (Figure 39B).

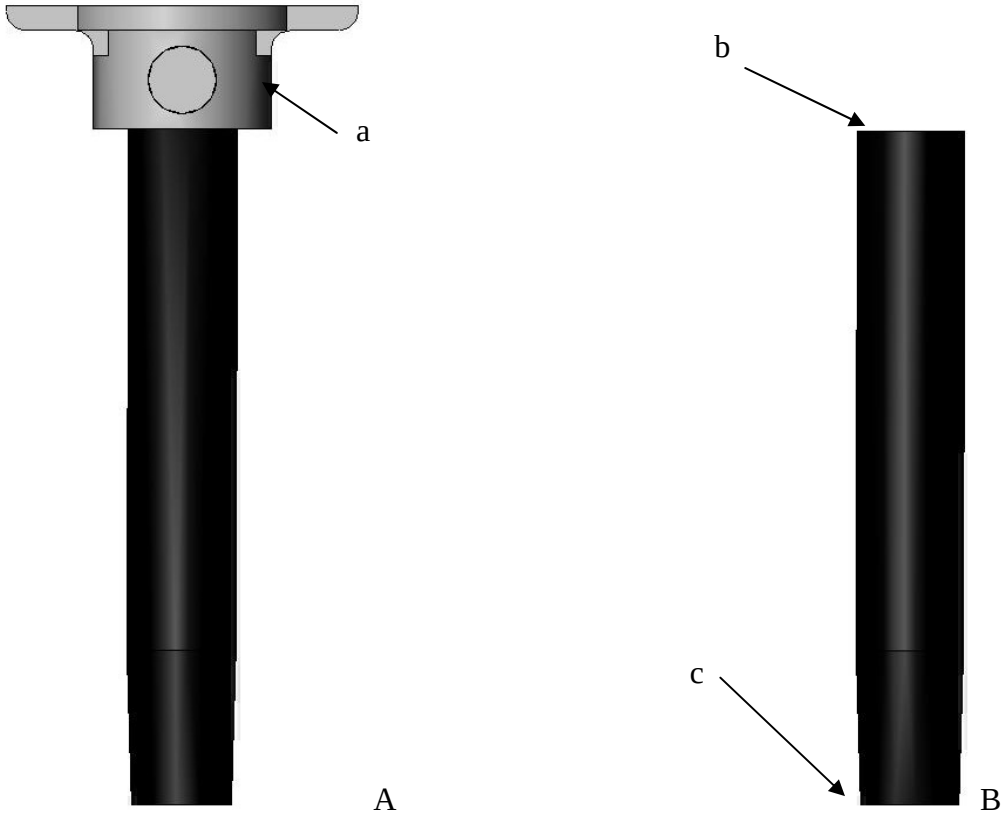

Figure 39. Modification to 15 mm trocar port. The connection at the top of the cannula (a) must be removed from the 15 mm trocar port. The cannula must then be shortened by removing 9 mm of material starting from point b and 28 mm of material starting from point c.

The fiber strips, 61 in total, were placed side by side on the scotch tape to hold them during assembly. The bundle of fibers was then wrapped around the sleeve of the 12 millimeter trocar port (Figure 40A). Finally, the 15 millimeter sleeve was pressed and positioned so that the distal end, with the fibers aligned are after the taper of the 12 millimeter trocar port (Figure 40B).

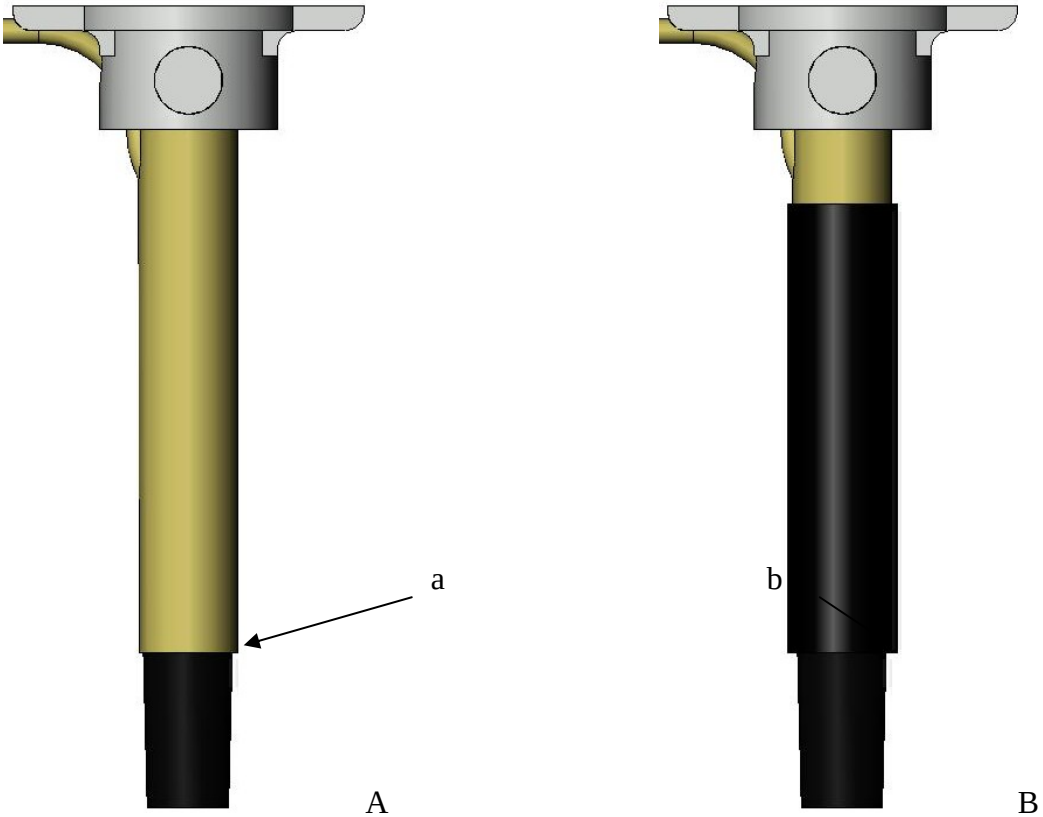

Figure 40. Fiber assembly. The fibers are wrapped around the 12 mm trocar's cannula so that the end of the fibers are aligned with the taper of the cannula (a). The 15 mm trocar cannula is pressed onto the fiber and 12 mm trocar so it too is located at the taper (b).

3.12 Camera Stand Revision B

For a detailed listing of the materials used in the construction of the camera stand revision b, please see Appendix G. The magnets were stacked vertically for this tool. The stack was coupled to a Type 1 external source to get the polarity of the magnets correct, then the bottom magnet was epoxied into place in the anchor(s) (Figure 33). The camera was attached to the support rod by using heat shrink tubing (Figure 41).

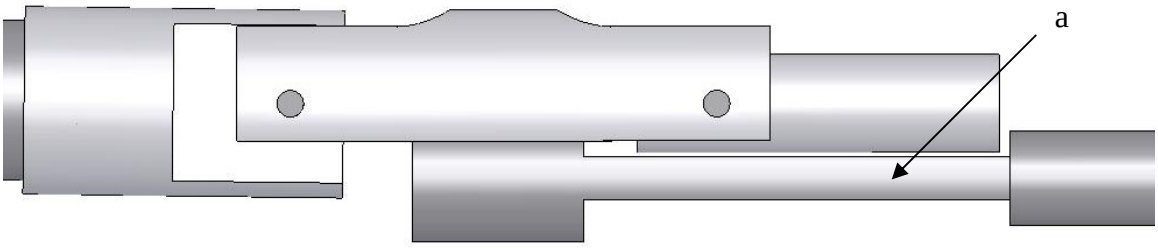

Figure 41. Assembly of camera stand revision b. The body of the camera was attached to the structure by using a piece of heat shrink tubing in the area of point a.

3.13 Camera Stand Revision C

For a detailed listing of the materials used in the construction of the camera stand revision c, please see Appendix G. Due to damage caused to the original camera, it was replaced with a higher resolution version. Two of the magnets were stacked vertically for this tool. The stack was coupled to a Type 1 external source to get the polarity of the magnets correct, then the bottom magnet was epoxied into place in the anchor (Figure 33). The third magnet was coupled to a Type 1 external source, again to get the polarity of the magnet correct, then it was epoxied into place in the second anchor (Figure 33). The glass window was sealed into the end of the camera using a silicon sealant (Figure 42A). The focus of the camera was adjusted so objects approximately 10 millimeters in front of the camera were in focus. The camera was secured to the housing by hot glue (Figure 42B).

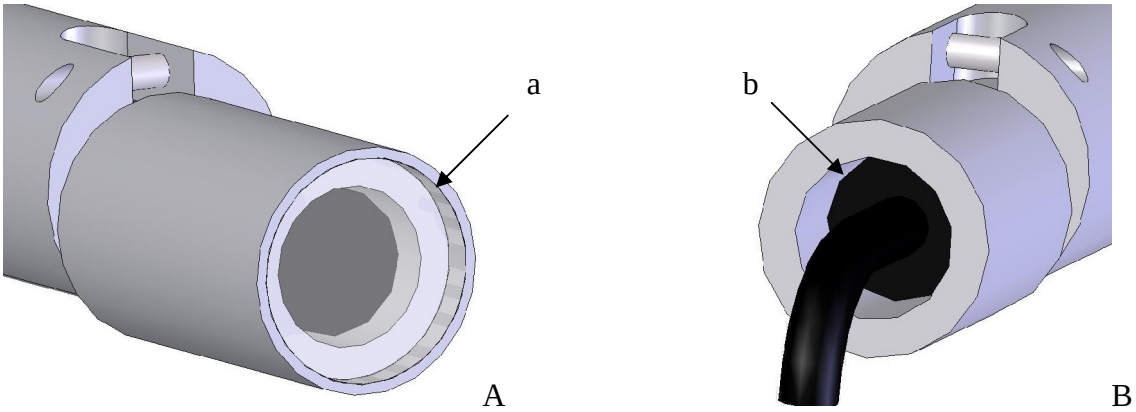

Figure 42. Assembly of camera stand revision c. Silicone sealant was used around the edges of the camera cover to keep fluids from damaging the camera (a). Hot glue was used to seal the rear of the camera tool as well as secure the camera to the enclosure (b).

3.14 Camera Stand Revision D

For a detailed listing of the materials used in the construction of the camera stand revision d, please see Appendix G. The magnets were not stacked vertically for this tool. Instead, they were coupled to a Type 2 external source to get the polarity of the magnets correct, then were epoxied into place in the anchor (Figure 35). The cylinder was modified by removing the factory installed fitting and the rear of the cylinder was bored and tapped to accommodate the smaller 2 millimeter fitting as shown in Figure 38. The glass window was sealed into the end of the camera using a silicon sealant (Figure 42A). The camera was secured to the housing by hot glue (Figure 42B). The mirror was glued into location using super glue. The focus of the camera was adjusted so it was focused on the mirror the best as it could be.

3.15 Powered Tooling Control Box

For a detailed listing of the materials used in the construction of the powered tooling control box, as well as the wiring diagram and the associated Visual Basic program, please see Appendix H.

3.16 Pneumatically Actuated Arm Prototype

For a detailed listing of the materials used in the construction of the pneumatically actuated prototype, please see Appendix I. The magnets were not stacked vertically for this tool. Instead, they were coupled to a Type 2 external source to get the polarity of the magnets correct, then were epoxied into place in the anchor (Figure 35). The 4 millimeter bore cylinder was installed in the anchor. The 2.5 millimeter bore, 5 millimeter stroke cylinder was used in the second joint. The racks had holes drilled and tapped for the 4 millimeter and 2.5 millimeter bore rod ends, respectively.

3.17 Pneumatically Actuated Arm Revision B

For a detailed listing of the materials used in the construction of the pneumatically actuated revision b, please see Appendix I. The magnets were not stacked vertically for this tool. Instead, they were coupled to a Type 2 external source to get the polarity of the magnets correct, then were epoxied into place in the anchor (Figure 35). The cylinders were modified by removing the factory fitting and drilling a tapping a hole for the smaller fitting, as shown in Figure 38. The 20 tooth gears require removal

of the molded hub as well as the bore of the gear enlarged to 4.8 millimeter (0.19 inch) in diameter to facilitate the hub of the 16 tooth gears (Figure 43). These steps must be done twice.

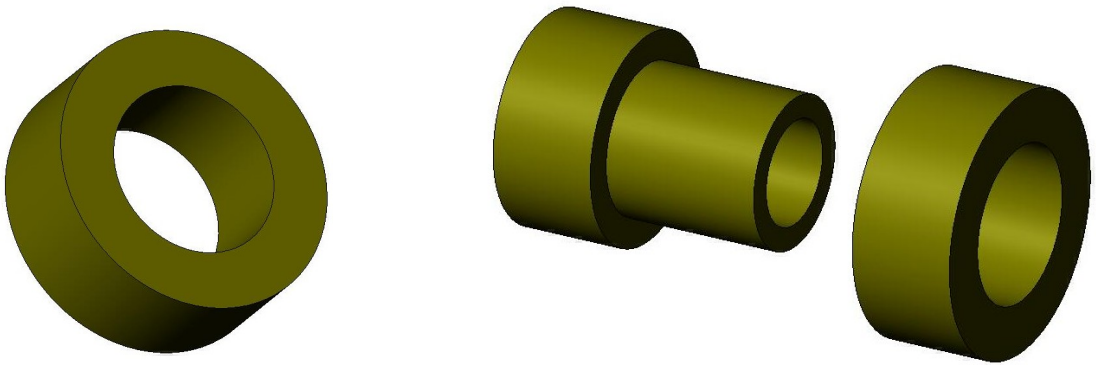

Figure 43. Gear modification. The hub that is molded with the gear needs to be removed and the bore of the gear needs to be enlarged to allow the press-fit of the 16 tooth gear. The 16 tooth gear is pressed into the 20 tooth gear.

The gears were assembled into the drive train for the first joint as shown in Figure 44. One of the 16-20 tooth gear sets was driven by the rack connected to the first cylinder. This gear set, in-turn, drove a second 16-20 tooth gear set, which drove the 24 tooth gear connected to the upper portion of the first link.

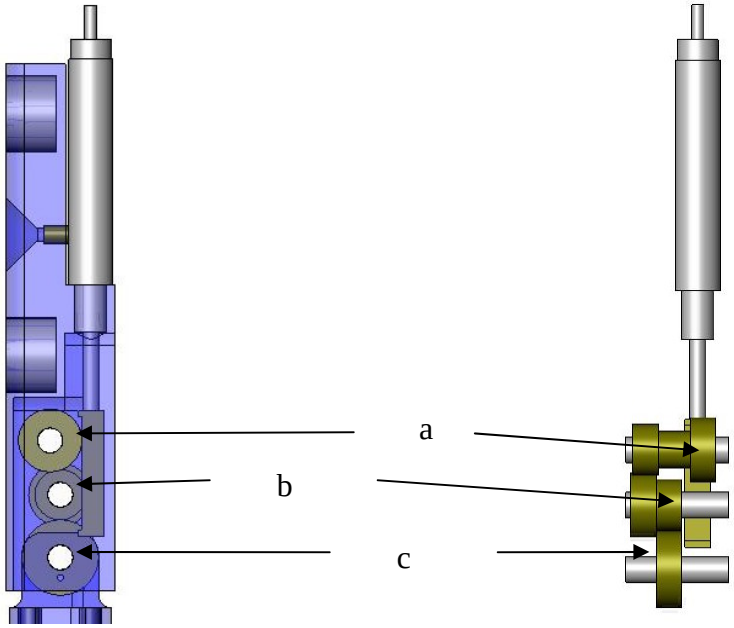

Figure 44. Assembly of gear-train. One set of 16-20 tooth gears (a) was driven directly by the rack connected to the cylinder. A second set of 16-20 tooth gears (b) drove a 24 tooth gear (c) which is connected to the upper portion of the first link (not shown).

The 24 tooth gears require the removal of the molded hub as well. The gears also require a 1.6 millimeter (0.063 inch) diameter hole to the side of the bore of the gear. How this was accomplished is a 2.5 millimeter (0.094 inch) diameter pin was inserted through the gear and the section of arm that it was to be located in and the hole was drilled (Figure 45).

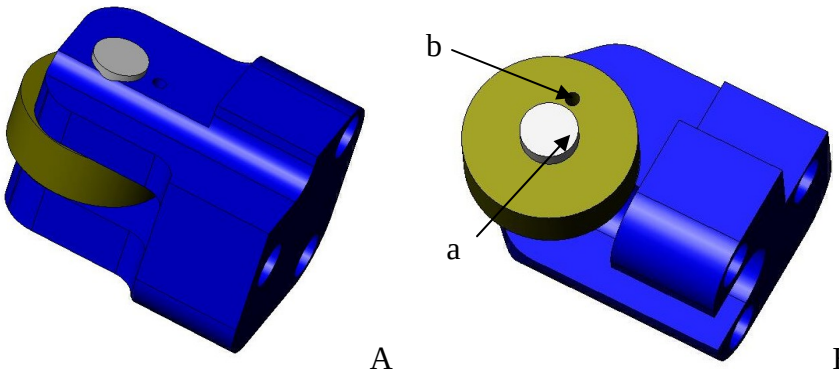

Figure 45. Assembly of geared joint. The drive pin (a) was inserted into the end of the link, the upper link-1 or upper link-2, A and B respectively, and the hole (b) was drilled through the gear and the link part at the same time to ensure proper alignment.

3.18 Pneumatically Actuated Arm Revision C

For a detailed listing of the materials used in the construction of the pneumatically actuated revision c, please see Appendix I. The magnets were not stacked vertically for this tool. Instead, they were coupled to a Type 2 external source to get the polarity of the magnets correct, then were epoxied into place in the anchor (Figure 35). The cylinders were modified by removing the factory fitting and drilling a tapping a hole for the smaller fitting (Figure 38). The 5 millimeter stroke cylinders were used for the first and second joint. The stylus from two of the needles were epoxied into the cutting head of the tool and inserted into the corresponding needle bores to serve as guide pins (Figure 46).

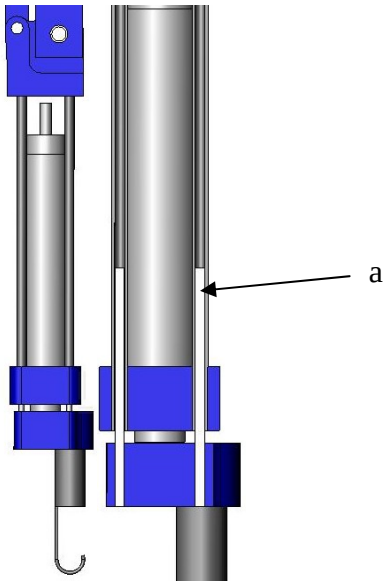

Figure 46. Assembly of guide pins. 18 gauge needles were used as the struts for the lower section of the arm. The stylus (a) was used as guide pins to keep the cauterizer tip oriented the correct way.

3.19 Nitinol Actuated Arm Prototype

For a detailed listing of the materials used in the construction of the Nitinol actuated prototype, please see Appendix I. The magnets were not stacked vertically for this tool. Instead, they were coupled to a Type 2 external source to get the polarity of the magnets correct, then were epoxied into place in the anchor (Figure 35). Assembly of this tool is rather difficult because the distances of the linkages is not specific. One of the ring terminals of the Nitinol is secured at the anchor. The zip tie has a 1.6 millimeter (0.063 inch) hole drilled approximately 6.4 millimeter (0.25 inch) from one end, which is then secured to the anchor. The second ring terminal of the Nitinol wire is secured to the anchor. Then the wire is pulled tight into a “v”, and the zip tie is marked at the apex of the “v”. A second hole is drilled at this location. For the first link, the second joint block is secured at this location (Figure 47).

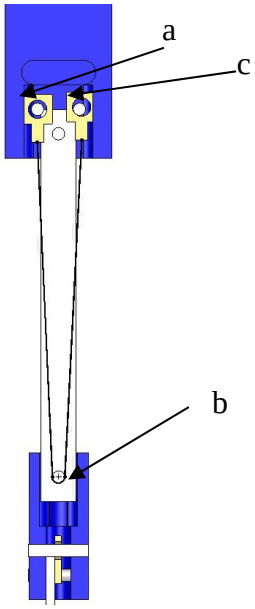

Figure 47. Assembly of nitinol actuated arm prototype. For the first link of the arm, the wire is secured at points a and c in the anchor. Point b is found by pulling the wire tight and inserting a pin at this location. The pin serves as the connection for the second joint.

For the second link the same process of the first link was used. The difference is that the wire was now secured in the second joint block, which serves as points a and c in Figure 47, and the cutting head is attached by the pin located at point b in Figure 47.

3.20 Nitinol Actuated Arm Revision B

For a detailed listing of the materials used in the construction of the nitinol actuated revision b, please see Appendix I. The magnets were not stacked vertically for this tool. Instead, they were coupled to a Type 2 external source to get the polarity of the magnets correct, then were epoxied into place in the anchor (Figure 35). The two racks require a slightly smaller hole than the 1.6 millimeter (0.063 inch) diameter pins

in one end of the rack, and one perpendicular to the rack near the center. The exact location is not very critical because of clearance for the pins in the anchor and the second joint housing (Figure 48).

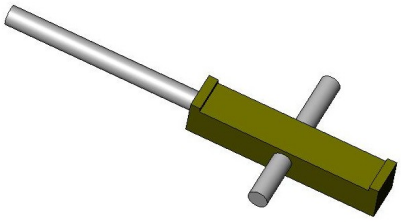

Figure 48. Assembly of rack. The racks that drive the first and second joint require two pins to be installed in it for guidance.

The Nitinol in the anchor is secured on the top pin in the rear of the anchor,is ran down and around the perpendicular pin in the rack and then back to the lower pin in the rear of the anchor. This is done twice, once on the left and once on the right of the anchor. This is done so the power connections for the Nitinol are at the proximal end of the anchor (Figure 49).

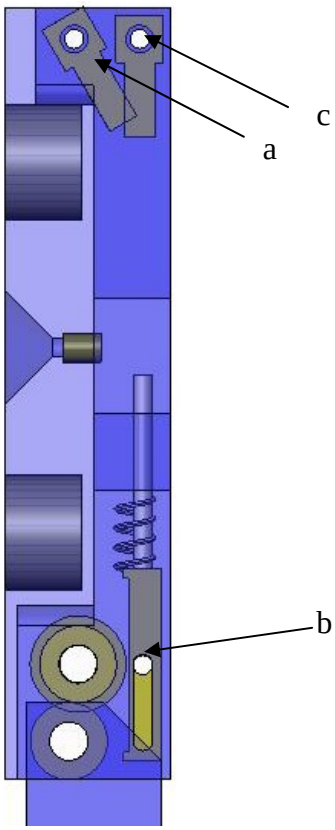

Figure 49. Routing of nitinol for first joint. The Nitinol is secured at points a and c, which allow for power to be connected at the end of the anchor closest to the trocar. The wire is bent around point b to drive the rack, which operates the joint.

For the second joint, one end of the wire is secured on a pin in the upper portion of the second link, ran around the perpendicular pin of the rack in the second joint, then back to the other pin in the upper portion of the second link (Figure 50). The use of the space frame concept allows for fine tuning the length so the wire is loaded properly.

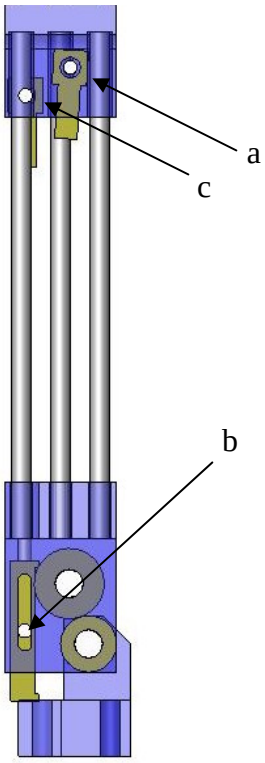

Figure 50. Routing of nitinol for second joint. Like the first link, the wire is secured at point a and c. The wire is bent around the pin at point b, which is connected to the rack, which drives the joint.

CHAPTER 4

RESULTS AND DISCUSSION

The goal of the Magnetic Anchoring System (MAS) project was not specifically to develop fully functional, fully developed tooling, but rather develop multiple tools of reliable and realistic functionality. Once the tool reached a point of reliable function, it was shelved so that other tooling could be attempted. The project was to prove and show that the tooling attached to magnet anchors could be supported, controlled, and used to accomplish real surgery.

In its current embodiment, MAS currently consists of an external magnet assembly, an internal magnet platform which is magnetically coupled to the external magnet assembly, and four different tools that are affixed to an independent internal platform. Each of the tools has unique uses and requirements. However, before any of the tooling could be realized, development and refinement of the method of trans-abdominal magnetic coupling had to be accomplished.

4.1 Electromagnet Development

An electromagnet was originally considered for the external platform due to its ability to generate a variable magnetic field, which in turn varies the holding strength of the magnet. A simple mathematical model was generated to estimate the performance before the magnets were manufactured. While the quantitative accuracy of the model is

unknown, qualitatively it proved to be correct. The model is discussed in detail in Appendix J.

The core of the magnets was made of AISI 1018 carbon steel, which was recommended by the Lord Corporation due to its relative ease of magnetizing. A problem of electromagnets is that a percentage of the magnetic field that is developed is consumed in magnetizing the steel core. The easier the core is to magnetize, the more efficient the magnet is. The steel core is required to focus the magnetic field into something that would be useful for MAS purposes.

The power supply for the electromagnets was limited to a maximum of 60 Watts. The electromagnets were designed to maximize the effectiveness of the power supply. Because of the power supply limitation, the electromagnets are fairly large, but the heat generated was not enough to cause damage to the wiring. A larger power supply, capable of supplying 1,000 Watts was purchased, but was not delivered in time for testing.

4.1.1 Electromagnet Prototype

The electromagnet prototype (Figure 51) was developed using the mathematical model to make a magnet without blindly winding wire. The design was centered around the power capabilities of the power supply, and a design was determined that fit within the constrains with the approximate dimensions of 50 millimeter (2 inch) in diameter by 100 millimeter (4 inch) tall. The specifications determined in the model were the following:

- 54 millimeter (2.13 inch) in diameter by 100 millimeter (4 inch) tall
- AISI 1018 carbon steel core 12 millimeter (0.50 inch) in diameter
- Approximately 3,850 turns of wire
- Approximately 396 meter (1,300 feet) of 22 AWG wire

Figure 51. Electromagnet prototype dry lab testing. Beef steak was used to simulate the abdominal wall.

During dry lab testing, the prototype was capable of lifting 120 grams through 12 millimeter (0.50 inch) of tissue using 0.50 Amps. This performance gave enough confidence to try the first surgical test on March 21st, 2001. During the first surgical test of the magnet, it was mounted to a modified lamp arm to help counter act the weight of the magnet, something not used in dry lab testing. During the surgical test the magnet performed very poorly, for unknown reasons at the time.

Once returned to the dry lab, the lamp arm was disassembled and an inductor was found in the base of the arm. The electrical wires that were originally used for the lamp were reused for the electromagnet. It was determined that the inductor disrupted

the power delivery to the electromagnet. This coupled with the tissue being thicker than expected lowered the performance of the magnet.

4.1.2 Electromagnet Second Prototype

The first prototype showed that magnetic coupling through the abdominal wall is possible with limited success. While the prototype was designed with an abdominal wall with a thickness of 12 millimeters, the degradation due to the increase to 15 millimeters, as well as the inductor, severely hampered the performance of the electromagnet. What was needed was a magnet capable of holding 120 grams or more through 25 millimeters or more, because it would be capable of supporting greater loads at the same distance. Because of the limits of the power supply, the dimensional constraints were relaxed to allow for a prototype that would be capable of better performance.

The fundamental mathematical equation that governs the strength of the magnetic field generated by an electromagnet is the following:

$$B = \frac{\mu \eta I}{2(Ro - Ri)}$$

Where:

μ = Permeability of air, 1.26 x 10^{-6} Tesla-meter/Ampere

η = Number of turns

I = Current, in Amperes

Ro = The outer radius of the coil of wire, in meters

Ri = The inner radius of the coil of wire, in meters

The specifications of the magnet were limited because as the number of turns increased, so did the length of wire used, which increased the resistance, which, due to the limited power delivering ability of the power supply, limited the current that can be delivered to the magnet. The mathematical model was expanded from the simple original version that was used to develop the first prototype to include the cause and effect of increasing certain parameters, e.g., the aforementioned increase in the number of turns, increase in resistance, and reduced current delivery. Using the mathematical model the design of the magnet resulted in the following specifications:

- The magnet coil is 152 millimeter (6 inch) tall, and approximately 89 millimeter (3.50 inch) in diameter.
- The magnet coil is made of approximately 1,981 meter (6,500 feet) of AWG 22 wire. The coil has over 10,000 turns.
- The core is made of AISI 1018 carbon steel with a 25 millimeter (1.0 inch) diameter.

Added to the magnet model was a simple heat transfer model that approximated the temperature of the magnet after a given amount of time, at a given room temperature. To keep the magnet from becoming too hot, it was made larger to give more surface area for cooling, which was also a side effect of using relatively large wire.

Due to the manufacturing time involved with manufacturing the much smaller original prototype, the decision was made to have the second prototype manufactured by an electromagnetic company, namely AEC Magnetics. The specifications derived from the mathematical model were sent, and a couple of weeks later the magnet was delivered.

In testing the second prototype, the performance was much improved over the original prototype. In Figure 52, the increase in lifting capacity is shown as a function of increased current with the tissue medium between the electromagnet and the anchor being beef steak, which was used in the dry lab for mimicking the abdominal wall. As shown, the second prototype is much more capable than the original one.

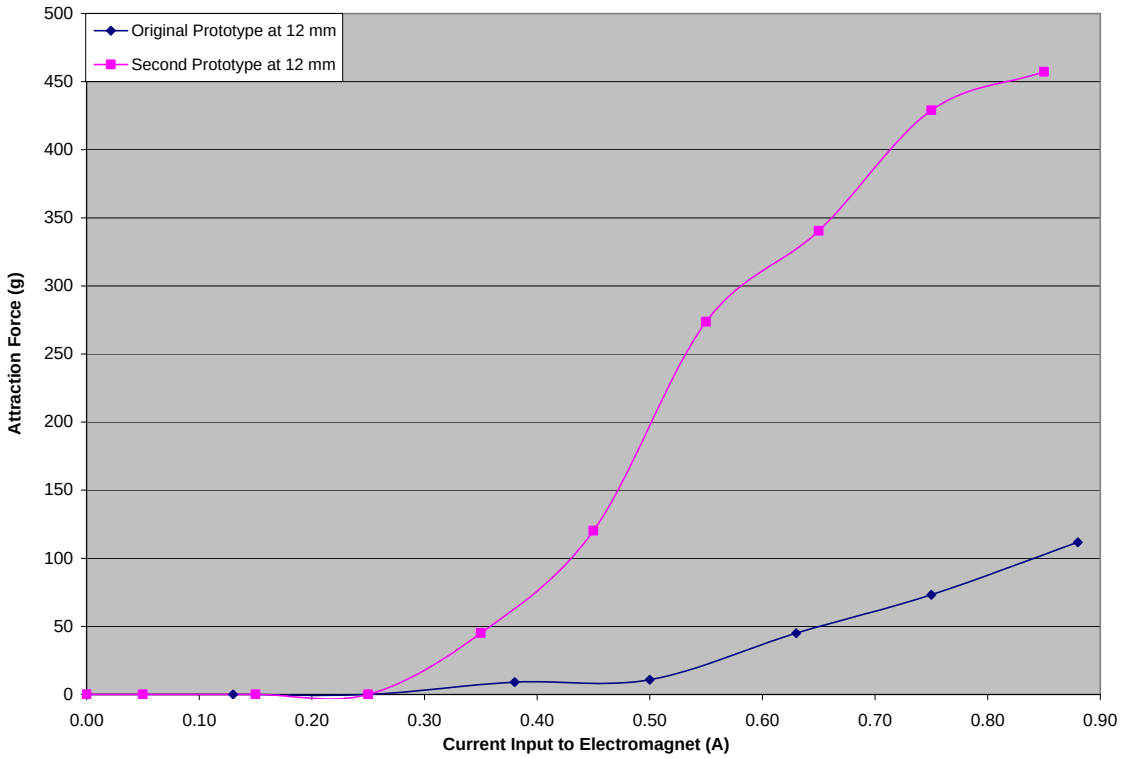

Figure 52. Electromagnet performance. As shown, at 12 millimeter (0.50 inch), the lifting capacity is greatly increased.

With the increased lifting capacity, the team was confident enough to take the electromagnet to the animal lab for a surgical test on May 24, 2001 (Figure 53). To ensure that the inductor was not a problem this time, the electromagnet was directly connected to the power supply. During this test, 200 grams were supported through 12 millimeter (0.50 inch) of tissue at a power of 60 W. While this is not as dramatic of an improvement as Figure 52 would suggest, more lifting capacity was available, but was not accessible due to limited space on the interior surface of the abdominal wall. Also, it should be noted that while the magnet was tilted, the weights were held vertically; the magnet was not only supporting the load, but also holding position.

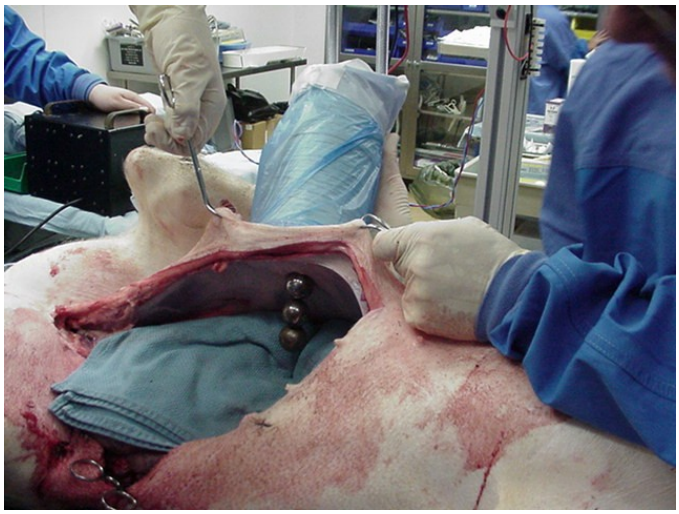

Figure 53. Electromagnet second prototype, surgical test. The magnet supported 200 grams through 12 millimeter (0.50 inch) of tissue.

4.2 Permanent Magnet Development

Electromagnets were originally considered for the external magnetic source because of their ability to have the magnetic strength adjusted relatively quickly and easily. This is important because the force of the magnetic source varies greatly with

distance, and an external source that is designed to work for adults could potentially cause injury to a child. While electromagnets are relatively easy to construct, they are very inefficient due to most of the magnetic field that is developed in the magnet is consumed in magnetizing the core.

To be viable for surgery, the external sources have to have enough attraction force to support tooling securely enough to be positioned successfully, but also be small enough that multiple magnetic sources can be positioned on the abdominal wall with minimal limitation in positioning ability. While the possibility of constructing a more efficient, smaller electromagnet may exist, to expedite the development of external sources that would be capable of supporting tooling, permanent magnets were employed. The concept whether or not a magnet could support a load through the abdominal wall was proven, now the focus was whether or not tooling could be developed that would be functional when designed to work with the magnet.

Permanent magnets are used in many everyday products. Since their magnetic field is always available, a power source, which leads to heat, is not required. Since the entire permanent magnet is magnetic, the magnetic field is much higher density, leading to higher lifting capacity in a much smaller package. The magnets are sold and marketed according to their dimensions, diameter and thickness for example, and the grade of the magnet, which is a rating of the residual flux of the magnet. Further explanation of magnetic terms and properties are available in Appendix K.

4.2.1 Permanent Magnet Testing

To determine whether the change to permanent magnets was viable and would not reduce the performance of the external platforms, some simple, yet informative, tests were conducted to measure the attraction force as a function of distance. One of the perceived advantages of an electromagnet over a permanent magnet is the capability of throttling the attraction force. While the magnetic field of the permanent magnets can be considered fixed, testing with the electromagnet showed that the attraction force of the magnet and its target degrades significantly over distance. A simple housing structure was designed and built with the capability of changing the distance of the magnet and its target.

The magnet test structure (Figure 7) was tested head to head with the electromagnet, varying the distance for the permanent magnets versus the electromagnets varying of current. The test structure (Figure 26) was used for testing had a 6.4 millimeter (0.25 inch) thick aluminum plate, and since there is a 3.2 millimeter (0.13 inch) clear plastic cover over the bottom of the permanent magnet test structure, a spare plastic cover was used to make the distance and the material the same for both sources.

The results of the comparison of the electromagnet and the permanent magnets, shown in Figure 54, show that the permanent magnets are very capable at short distances, specifically, the 12 to 19 millimeter (0.50 to 0.75 inch) range which was the tissue range that had been experienced to this point. It should be noted that the

permanent magnet starts at an offset of 9.5 millimeter (0.38 inch), and the electromagnet is tested at this distance, but the current is varied.

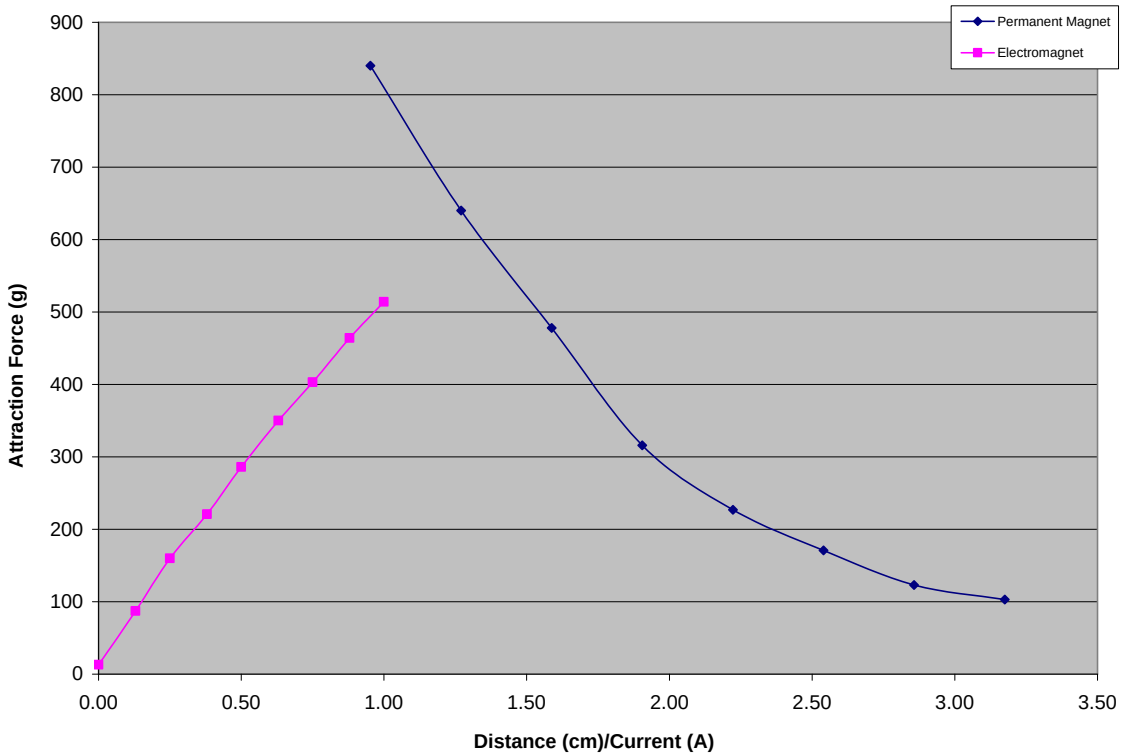

Figure 54. Permanent magnet and electromagnet performance. As shown, the permanent magnet is comparable to the electromagnet, but does not require power input to do so.

The results of this test showed that the permanent magnets were not only more powerful, 840 grams versus a maximum of 500 grams at 90 Watts of power for the electromagnet, but were capable of generating the lifting ability without heat generation and in a much smaller package. This test showed that the permanent magnets could be a replacement for the electromagnet, but what sizes and shape to use was still a question.

4.2.2 Permanent Magnet Modeling, Shape Considerations

The modeling of the permanent magnets was accomplished using a finite element modeling program named Maxwell 2d made by Ansoft. Maxwell 2d is a finite element package that is specifically designed for doing magnetic simulations. While the analysis was limited to 2d problems, e.g., either rectangular or cylindrical modeling, many questions could be answered rather quickly and easily.

One of the first questions was what shape of the magnets to use; rectangular, disc, or ring. Using Maxwell 2d, the different magnet configurations could be tested quickly and easily, as well as viewing determining the differences in the magnet structures. The size, 12 millimeter (0.50 inch) thick by 25 millimeter (1 inch) tall, and material, NdFeB grade 35, was the same for all three types, and were tested in the software the medium around them was specified as air.

The results from the simulation show a very clear difference between the three configurations. A desirable trait for the magnetic sources is to have the magnetic field extend as far as possible, as strong as possible from the poles of the magnet. While the three types have similar field strength from the poles at similar distances, the confirmation of the field is very different and leads to different performance.

Disc magnets tend to deliver a field that dips toward the cylindrical center of the magnet (Figure 55). Rectangular magnets tend to deliver a field that is flat and consistent across the face of the magnet (Figure 56). Ring magnets tend to deliver a field that has a void at the poles of the magnet, which lead to some loss of magnetic strength due to the resistance of the air in the gap (Figure 57).

While there may be a performance benefit from ring magnets, they were dropped from further development due to the suppliers limited offerings of this configuration, i.e., at the time, ring magnets were not available in the size and material grade that is needed for the magnetic source.

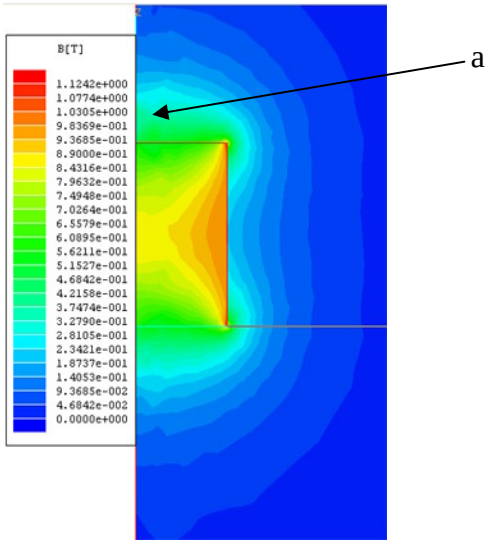

Figure 55. Disc magnet magnetic field. There tends to be a large concentration of magnetic flux along the centerline of the magnet (a).

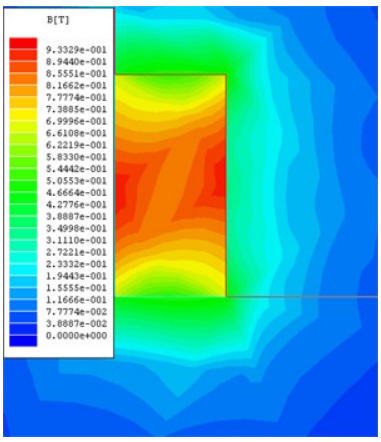

Figure 56. Rectangular magnet magnetic field. The magnetic field tends to be constant across the surface of the magnet.

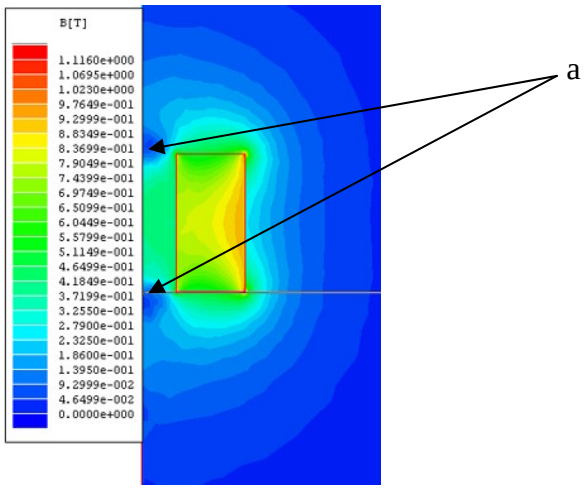

Figure 57. Ring magnet magnetic field. The magnetic field has "dead" zones caused by the magnet being in a ring configuration (a).

A disc and rectangular magnet were purchased with the same material properties and as close as possible size to see how the magnet performed in reality. While lifting capacity is important, control and tracking are also key to the success of manipulating the tooling. In testing, it was found that tracking ability using disc magnets was better than that of rectangular.

One theory for this phenomenon is that the disc magnets have a higher concentration of flux along the centerline of the magnet, while there is a high concentration with rectangular magnets it is usually located more at the edges of the magnets. Since the target tracks the high concentration of magnetic flux, the target tends to stay aligned with the center of the cylindrical magnets, while it tends not to move until the edge of the rectangular magnet comes close to the target. This delay in motion leads to a "dead zone" of motion that causes difficulty in positioning of the tools with rectangular magnets.

Due to the results from the testing, and software analysis, disc magnets proved to be the appropriate choice for the internal and external magnetic sources in respect to the availability, strength, and tracking ability.

4.2.3 Permanent Magnet Modeling, Size Considerations

The second question that needed to be answered was what size of magnets to use. Through testing it was determined that bigger is better, but since the size of the external source is limited due to the other equipment vying for space on the abdomen, the maximum size for the external source was limited. The original target size for the electromagnet was 50 millimeter (2 inch) in diameter and 100 millimeter (4 inch) tall, and this was the size that the permanent magnets had to conform to as well.

The diameter of the magnet for the external source was ranged from 2.5 millimeter (0.1 inch) diameter to 25 millimeter (1.0 inch) diameter, which are the diameters that are readily available from magnet suppliers. Because the different diameters are available at different thicknesses, a uniform thickness of 25 millimeter (1.0 inch) tall was chosen for the external source. While some of the diameters are not available at this thickness, when stacked together, the magnetic flux of the magnets add together, in essence generating same capabilities as a one piece magnet.

The simulations (Figure 58) show that the magnetic flux strength and distribution around the magnet is the same, meaning that it is independent of the diameter of the magnet. However, the distance or “shell” of the magnetic flux around the magnet was found to grow with the increase in diameter. While in Figure 58,

diagram A and B look approximately the same, the 25 millimeter (1 inch) diameter results show the magnet smaller because the magnetic field is further reaching. The 12 millimeter (0.5 inch) magnet (Figure 58B) has the same magnetic flux strength at11.9 millimeter (0.47 inch) from the bottom surface as the 25 millimeter (1.0 inch) magnet (Figure 58A) has at 19 millimeter (0.75 inch) away.

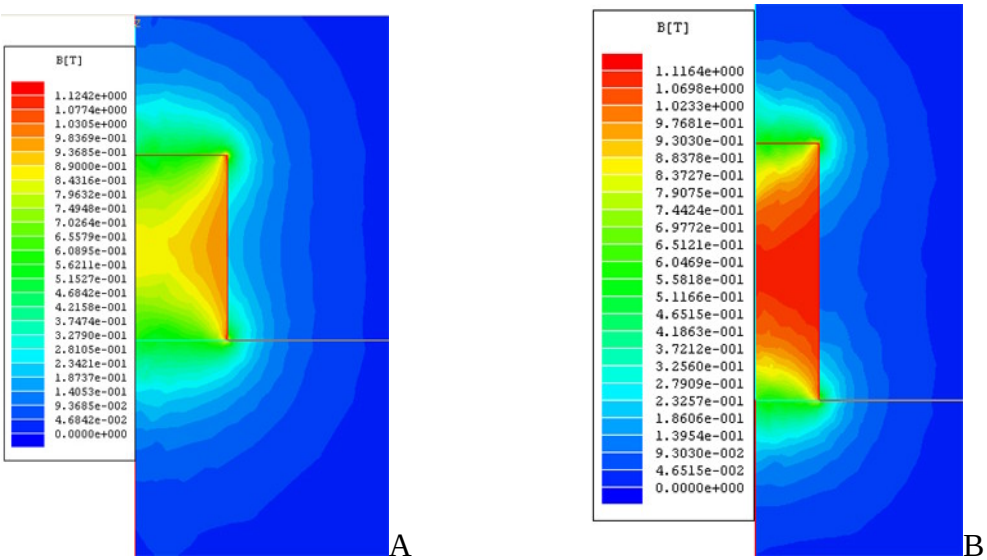

Figure 58. Magnet diameter effects. Magnet A is 25 millimeter (1.0 inch) in diameter, magnet B is 12 millimeter (0.5 inch) in diameter. While they look to have the same performance, the distance from the magnet is much different.

Since the concept of magnetic coupling very dependent upon the strength of the magnetic field at some distance from the surface of the magnet, it was determined that the larger the diameter, the better. Since 25 millimeter (1.0 inch) diameter NdFeB, magnets were readily available, and were also available in a wide assortment of thicknesses and grades, they were chosen as the diameter for the external magnet source.

4.2.4 Permanent Magnet Modeling, Internal Target

While most of the concentration was centered on the external source, the internal target needed to be considered as well. Two different concepts were approached for the target, a permanent magnet or a ferromagnetic object. Since custom permanent magnets are cost and time prohibitive, unlike ferromagnetic materials, an appropriate size for the target was determined by taking into account that it would need to pass through a 15 millimeter trocar port, off the centerline of the port due to the equipment attached to it, and be small enough that it could pass through the port with excess room around the target for coupling to the equipment. Through some rough approximation, it was determined that a diameter of 9.5 millimeter by 6.4 millimeter (0.375 inch by 0.25 inch) thick would be as large as what could be comfortably packaged within the confines of the trocar port.

In simulation, a target was placed 15 millimeters below the external source, which the newly determined 25 millimeter (1 inch) diameter was used with a 25 millimeter (1 inch) thickness since the model was readily available. The distance from the source was a rough approximation of a tissue thickness, but a material other than air was not included in these early simulations. For the magnet version of the target, a grade 30 NdFeB magnet was used. For the ferromagnetic, 1010 carbon steel was used since the data was readily available in Maxwell, and the density is comparable to NdFeB, 7.87 g/cc for 1010 carbon steel, 7.4 g/cc for NdFeB. The density is important to consider since if the coupling strength is high, but most of the force is used to hold the target, there is little benefit.

The differences in the results are quickly apparent with this test when the plots of the magnetic field were taken (Figure 59). Since the coupling force is dependent upon the magnetic field available, the more the better, and since the magnet is an additional magnetic source, it would stand to reason that the forces would be higher between them. According to the simulation, the attraction force between the magnets is 290 grams, versus 65 grams for the steel. The benefit of increased attraction force, requiring no power, generating no heat and the ability to be purchased in a nickel plated version made the decision quite clear in favor of the magnetic target.

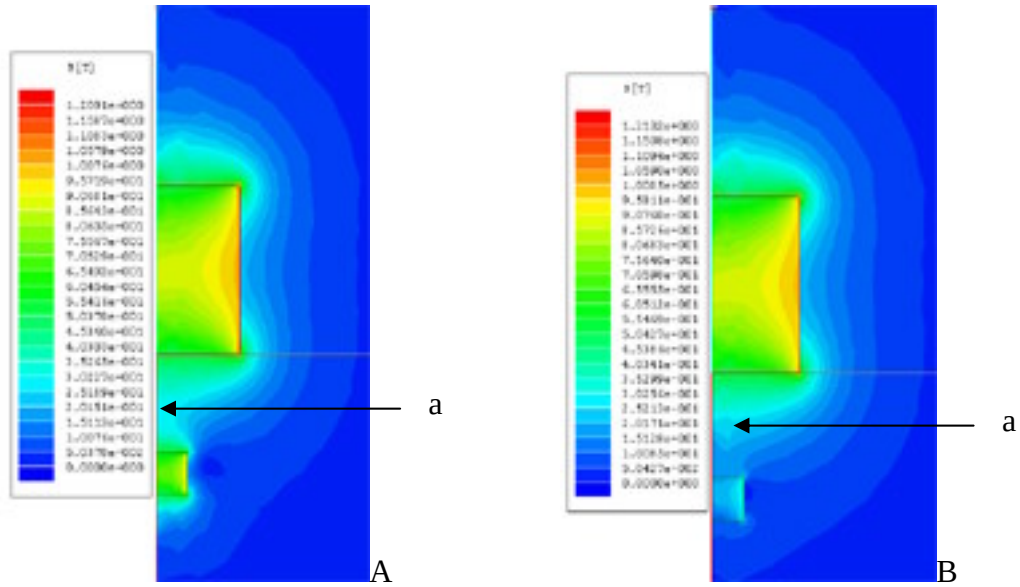

Figure 59. Internal target. The magnetic field (a) between the external and internal magnet (A) is much greater than with the 1010 steel target (B).

While development stopped here, it was later determined that additional coupling force would be beneficial. For some anchor configurations, it is possible to increase the amount of magnetic material inside the anchor by stacking small magnets together to fit the contours of the trocar port more efficiently. While never built,

according to the simulations, there is significant attractive force increases, about 25%, without significant size increase (Figure 60).

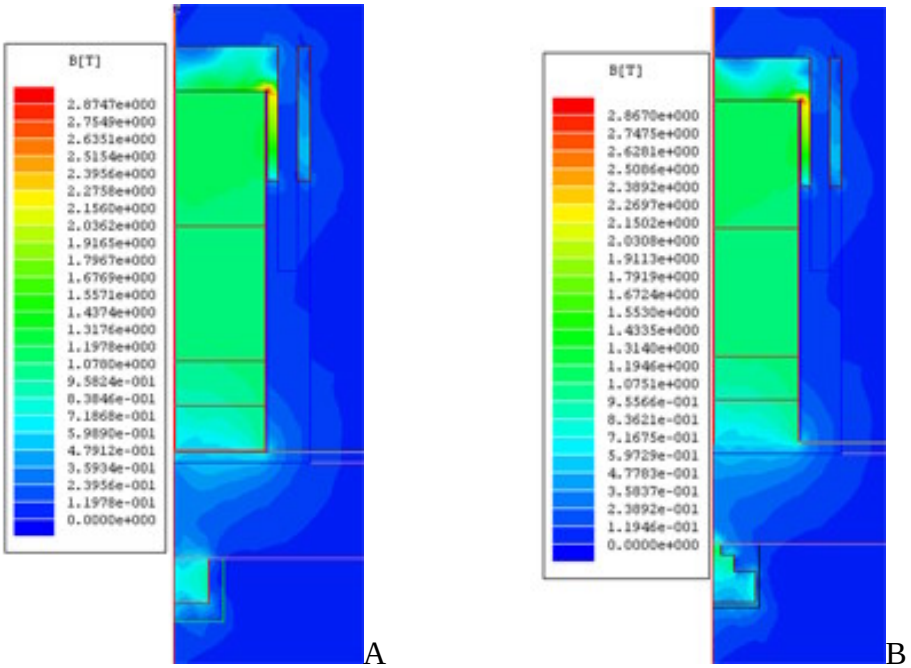

A B

Figure 60. Composite internal target. The composite magnets (B) use the space more efficiently in the anchor than just a simple magnet (A).

4.2.5 Permanent Magnet Modeling, External Source Thickness

Since the diameter of the external magnet was determined, as well as the target for the external source, it was time to determine the thickness, or height of the external source. The distance of 15 millimeters between the external source and target was used since it is large enough to be a challenge for the magnets, but also be bio-medically plausible. For these tests however, the gap between the source and target was filled with sea water to approximate tissue. While not truly representative of tissue, the detrimental effects are thought to be similar, i.e., the magnetic permeability was similar.

To test whether or not this was a fair assumption, a tissue test was conducted using beef steak which was cut to a thickness of 12 millimeter (0.50 inch) and then frozen. The attraction force was measured as 518 grams and the software calculated 424 grams at the same distance through the water. While there is a difference in the measurement and simulation, it is difficult to measure the magnetic properties of tissue. The results from the simulation were used as a benchmark to verify whether a change offered a benefit or not. Also, it the simulation was not over estimating the force available, which meant there would be at least that amount available.

The thickness of the external source was ranged from 2.5 to 100 millimeter (0.1 to 4 inch) to find the best thickness for our uses. When this analysis was started, the assumption was that a 100 millimeter (4 inch) long magnet would generate the greatest lifting capacity. As shown in Figure 61, the attractive force increases rapidly at first but around a length of 50 millimeter (2 inch) the increase is very modest at best. For example, according to the simulations, a magnet 25 millimeter (1 inch) in diameter and 50 millimeter (2 inch) thick will generate a lifting capacity of 331 grams through 15 millimeter (0.59 inch) of sea water, while increasing the length to 100 millimeter (4 inch), generates only an additional 25 grams. The cause for this modest increase is the losses of magnetic energy due to the additional air that the magnetic flux must pass through, i.e., like electrical energy, resistance causes power losses.

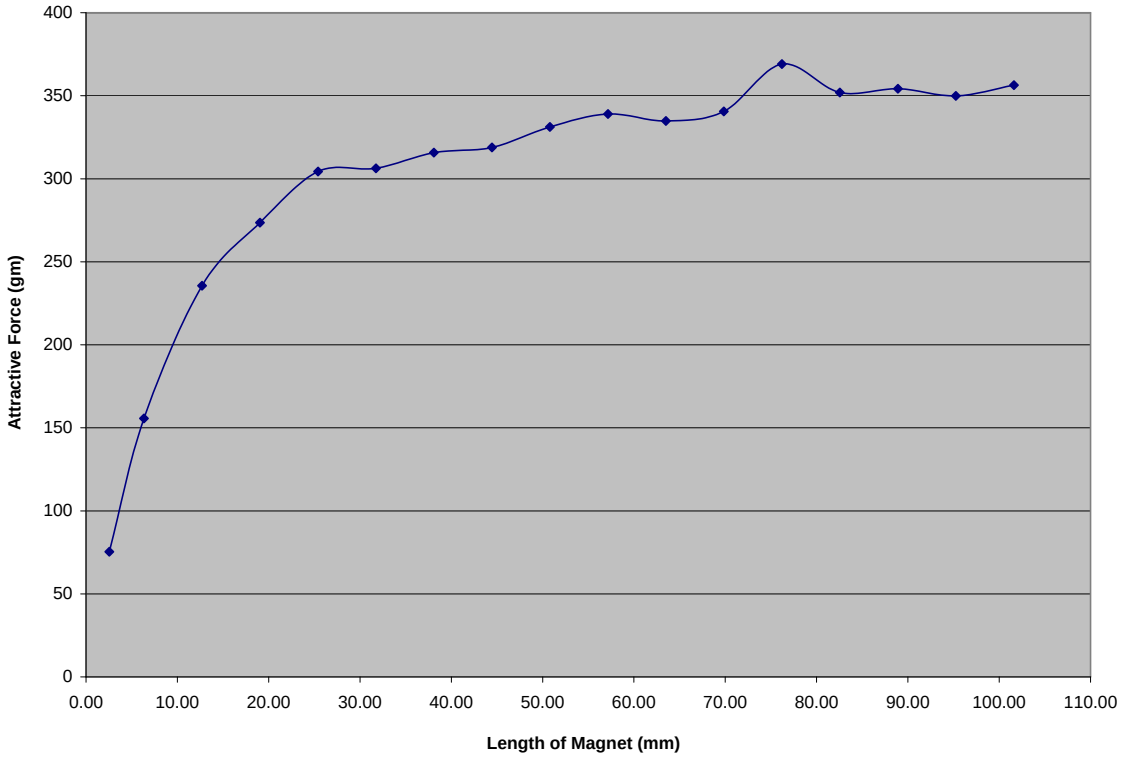

Figure 61. Attractive force vs. magnet length. There is a steady increase until approximately 50 millimeter (2 inch) in length.

There is a desire to keep the external source as small as possible so that more tools can be used at the same time, as well as limiting interference caused by the trocar port(s). Using the data collected from the simulations, a magnetic length of 50 millimeter (2 inch) was chosen because the increases past that point require a larger device with only modest gains.

4.2.6 Permanent Magnet Modeling, Magnetic Flux Control

At this point the size and shape of the external source, as well as the internal target were known and the design of holders to protect the magnets from the patient and vice-versa could be started. When the first external platforms were developed, there was a

problem that was not able to be simulated because of the 2d limitation: interaction between the external sources. The first tooling to be developed used two internal targets, referred to as anchors, and two external sources because the force required at that time was an unknown, and the first tools were mechanically actuated by the motion of the magnets. The magnetic field surrounding the external sources was strong enough that when arranged so that they repelled each other they would not stay, unless forced, any closer than 150 millimeters (6 inches). Set to repel was chosen as the safest configuration for the user since the attraction can pinch fingers of the operator.

Returning to the simulations of the magnets, it was found that a large magnetic field existed along the length of the magnets (Figure 62). This field is what was causing the violent repulsion and needed to be dealt with since most of the tooling required the sources to be within 25 to 50 millimeter (1 to 2 inch) of each other.

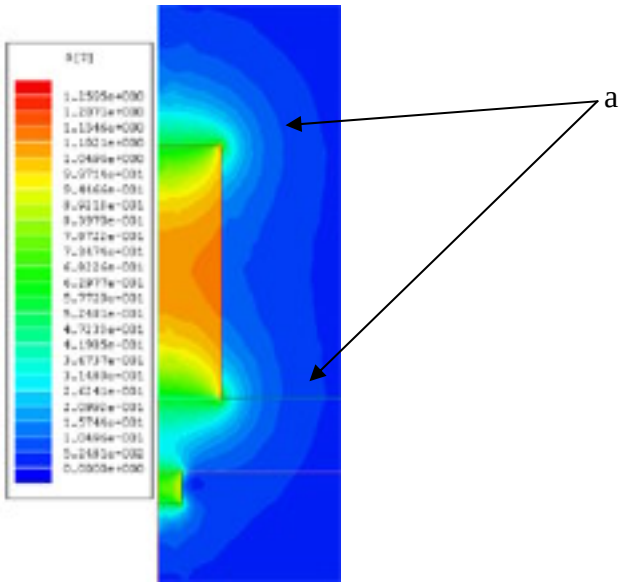

Figure 62. Rogue magnetic field. The magnetic field 63.5 millimeter (2.5 inch) from the magnet centerline was strong enough to cause the severe repulsion (a).

An analogy between electricity and magnetic flux can be used when discussing the path the magnetic field will take is the path of least resistance. The concept that was tested in simulation was to give the magnetic field a desired path that would keep it closer to the magnet. Multiple attempts were made to accomplish task, ranging from steel collars that the magnets were inserted into to, to flat steel discs that were placed on the top of the stack.

As stated earlier, the concept of the magnetic anchoring system relies on the magnetic field extending past the magnetic surface. In the simulations multiple approaches to limiting the field along the length of the magnet were tested, but many were rejected because the magnetic field was drawn to the “shielding”, which lead to a lower magnetic field where it was needed. A balance was needed between lifting capacity, manufacturability, and the reduction of the “rogue” magnetic field.

This balance came in the shape of a steel top that is designed to fit atop the stack of magnets in the external source (Figure 63). The size and spacing of this top, while not optimum, was simulated multiple times to make sure that it was large enough to fix the problem, but small enough as to not severely limit the lifting capacity. The design that was that proved to be the best balance brought the magnetic field closer to the magnet stack, but as a result, reduced the lifting capacity by 29 grams, to a total of 302 grams through 15 millimeter (0.59 inch) of sea water. There may be a better way to solve this problem, but this solution solved the problem enough that tool development could continue.

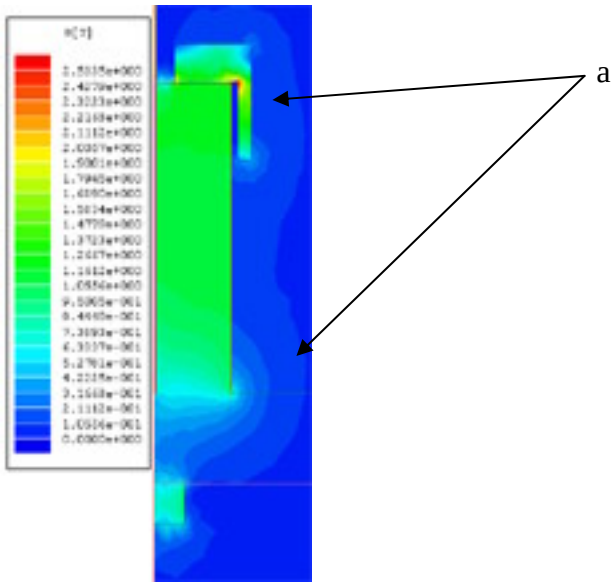

Figure 63. Effect of steel top. The rogue magnetic field (a) was brought significantly closer to the magnet stack, without the steel the field was 63.5 millimeter (2.5 inch) from the centerline, while with the steel, it is only 25 millimeter (1.0 inch) away.

4.2.7 Magnetic Coupling Strength Surgical Viability

A reoccurring criticism and concern of the MAS concept is whether or not the magnet couplers develop sufficient attraction force to allow for surgery to be possible. The only way to truly determine this is to study the abdominal wall tissue thickness of patients and compare it to what the magnets can generate. While gathering this information was not part of the MAS project, comparable data was found in studies performed for other purposes.

Doctors at Northwestern University Medical School (MP, Milad) used spinal needles to measure the abdominal walls before inserting trocar ports. What they were trying to determine is whether the body mass index could be used to predict the abdominal wall thickness of a patient in obese women. Their findings, while not

directly related to this project give real measurements of a patient population, which allow for a comparison of what the magnets are capable of delivering and what thicknesses would be seen in medical use (Figure 64).

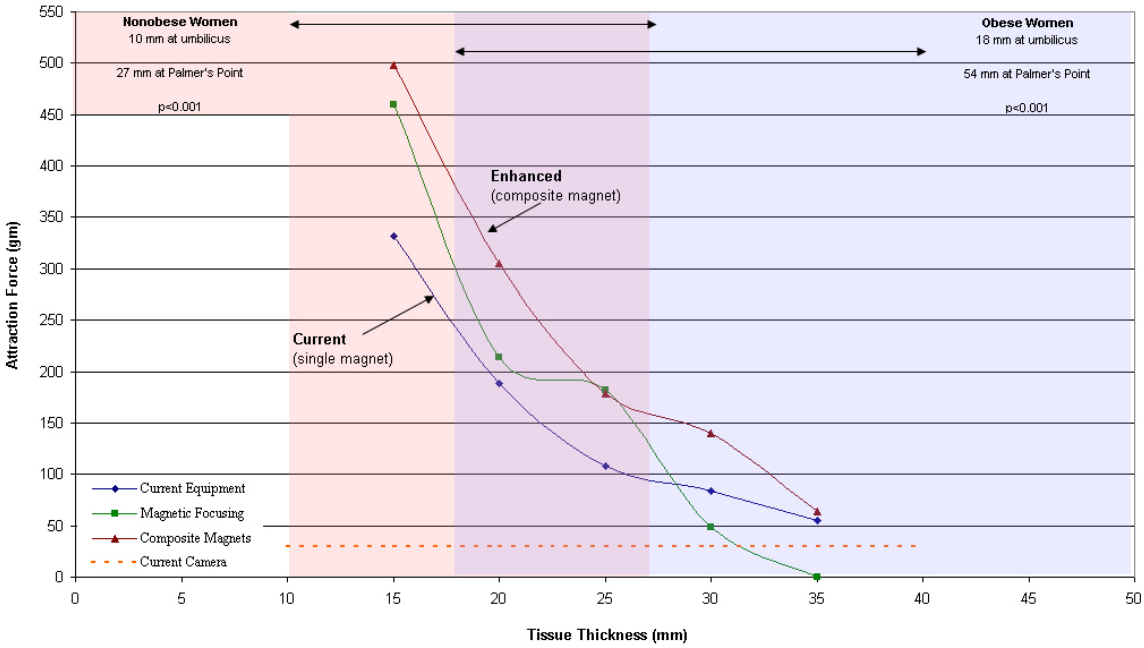

Figure 64. Surgical viability. The weight of the Camera Stand Revision D is shown as a dashed line, and the coupling strength of the current magnet setup as well as simple improvements are shown across measured tissue thicknesses.

It should be noted that the results in Figure 64 are from simulations of the magnets coupling through sea water approximations of tissue. Also, is should be noted that due to software limitations, the results shown are equivalent to a Type 1 coupling or approximately half of what a Type 2 coupling would be. The camera stand revision d was shown since it is one of the tools that would be used no matter the operation being attempted. According to the simulation, the camera should be able to be confidently supported through 35 millimeter (1.38 inch) of tissue, with a factor of safety of approximately 2, since the camera stand uses a Type 2 anchor. The pneumatically

actuated revision c cauterizer weighs approximately the same as the camera stand, and has the same Type 2 anchor. As shown in Figure 64, the magnets are capable of supporting tooling through a significant range of tissue thicknesses to be a viable alternative to conventional equipment.

Due to the shielding effect of the steel cap, the external sources were considered complete. While the design may not be the most efficient, the performance was deemed adequate and all development time and energy was redirected to developing the tooling to be supported.

4.3 Permanent Magnet Enclosure Development

During the development of the magnetic sources and anchors, an attempt was made to standardize the tooling to help with mass production and to keep the equipment as simple as possible. A naming convention was assigned to the equipment based on the number of magnet assembly, referred to as “stacks”, in the device. The electromagnet prototype was used as a benchmark since its performance through tissue was known.

4.3.1 Type 1 External and Internal Enclosures

Of the internal and external equipment developed, the Type 1 internal and external platforms are the simplest (Figure 8). The key improvements in respect to the electromagnet prototype are the following:

- A much larger lifting capacity. The electromagnet prototype could support 200 grams through 12 millimeter (0.50 inch) of tissue, while a Type 1 internal and external pair can support around 396 grams through 11 millimeter (0.43 inch) of tissue.
- The Type 1 external enclosure is much smaller. The electromagnet has external dimensions of a 100 millimeter (4 inch) diameter by 178 millimeter (7 inch) tall, while the Type 1 is 31.8 millimeter (1.25 inch) in diameter by 57 millimeter (2.25 inch) tall. The smaller size helps with maneuvering around the abdominal wall.

Type 1 internal and external equipment have very high tracking ability because the magnets in the anchor try to align their magnetic pole to the pole of the external device. Because there is a single pole to attract to, there is very high fidelity in tracking, but since there is only one magnetic pole, it is not possible to transfer torque from the external source to the internal anchor, or hold orientation in relation to the rotation about the center of the magnets. Because of the high fidelity of tracking, a derivative of the Type 1 external source was developed for the camera using slightly smaller magnets since the camera requires much lower lifting capacity.

The Type 1 internal anchor is very simple and can be used for times where pure lifting or high fidelity of motion is needed. The magnets are either press-fitted to the housing, or epoxied in place to ensure that they do not separate from the anchor. A pivot pin is supplied on the bottom end of the anchor for attachment of a variety of tools.

4.3.2 Type 2 External and Internal Enclosures

The Type 2 external enclosure and anchors (Figure 9) were developed for tooling that requires a more stable platform than available from the Type 1 anchors. The Type 2 external enclosure can have the magnet stacks arranged in one of two ways, either North-North or North-South configuration, which refers to the orientations of the poles of the stacks.

In the North-North configuration, the external enclosure's force should be double that of a Type 1 enclosure, but testing was not done to confirm this assumption. This is because the magnetic fields of the two stacks repel each other, distorting the field and making more of the magnetic field available further from the enclosure, thus increasing lifting capacity. However, while lifting capacity is increased, fidelity of tracking is lost to a high degree because there is not a clear pole for the internal magnets to attract to. For tools with dual Type 2 internal anchors, this is not such a problem because the anchors work together to achieve the desired location.

In the North-South configuration, the lifting capacity of the magnets increased to 589 grams at 11 mm of tissue. This configuration was used extensively in testing the MAS tools since there is a high fidelity of motion transmitted across the abdominal wall, as well as the capacity for transmitting torque. For tools such as the camera stand revision d, where there is only one Type 2 anchor, and the torque transmission is very useful for aiming of the camera.

The development of the Type 2 anchors was, originally, directly related to the needs of the organ retractors. While the sling type retractor works very well with the

Type 1 equipment, a paddle retractor requires the ability to press down on tissue, as well as to lift. With the first version of the paddle retractor, it was determined that Type 1 equipment was not capable of resisting the side loads to the anchors. The Type 2 anchors have a much lower profile which resists the forces along the length of the anchor, but not perpendicular to it. As stated with the information concerning the Type 2 external enclosure, the orientation of the magnets lends itself to the ability to transmit torque across the abdominal wall. While the original form of this anchor is not used in the later tooling, the concept has been successful.

4.3.3 Type 3/Anchoring Needle External and Internal Enclosures

With tooling like an organ retractor that does not need to move around the abdomen dynamically, the concept of a mechanism that would lock the anchor to the abdomen was conceived. Because the anchor would be locked to the abdominal wall, the external enclosure could be removed, which is less clutter on the external surface, and the holding force of the anchor was not a function of the strength of the magnetic attraction, instead it was a function of the material properties due to the stress induced in the locking mechanism.

The concept revolved around a slightly modified Type 2 external and internal platform. The Type 2 platforms were chosen because the anchor aligns itself very well with the external enclosure, and there is material between the internal magnets which would lend itself to the locking mechanism. The magnets in the external enclosure had to be moved away from each other slightly to make room for the passage of a rigid

structure to pass through. The rigid structure was chosen to be an 18 gauge needle, or equivalent stainless steel rod. While this rigid structure does not allow dynamic motion across the abdominal wall, the trauma induced is significantly less than that of a trocar port.

The development of the Type 3 anchor (Figure 10) revolved around the use of a threaded lock. A cam-style locking mechanism was conceptually developed, but due to problems with unlocking, it was abandoned for the simpler threaded version.

The threaded lock was perceived as a very simple, yet effective, way of locking and unlocking the anchor because unlike the cam, force downward onto the anchor was not required, and accidental locking onto the wrong surface was not possible. This concept was much easier to lock and unlock since all that was required was to insert the needle into the anchor, then "thread" the needle into it. Due to dry lab success, on August 22nd, 2003, a test of the anchoring needle concept was done under surgical situations (Figure 65). While in dry lab testing the concept worked quite well, under real conditions the alignment and tracking of the anchor to the external enclosure was not sufficient to lock the anchor without much trial and error. One theory to explain the difficulty of locking is that the porcine model's skin is much harder to puncture than the dry lab's silicone rubber skin.

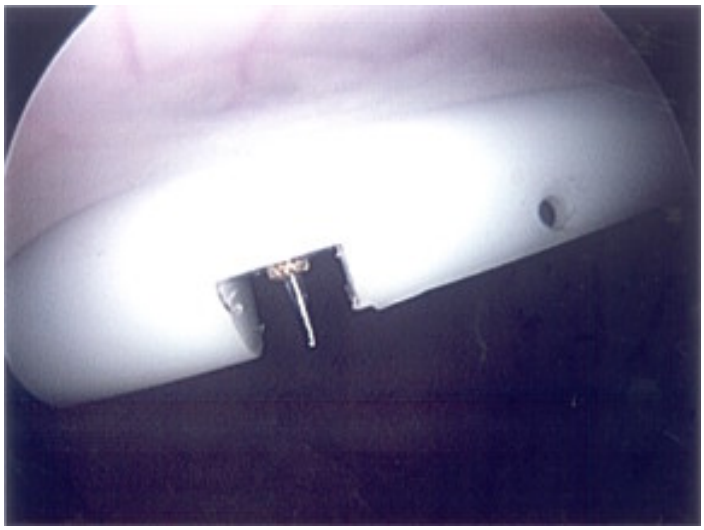

Figure 65. Needle anchor surgical test. While the anchor was successfully locked, it was much more difficult than in the dry lab conditions.

4.4 Sling Retractor Development

The first tool that was developed was what is called a sling-retractor. Composed of two Type 1 internal and external enclosures linked internally by a flexible polymeric tubing, this tool is very strong, light, and easy to use.

4.4.1 Sling Retractor Prototype

The sling retractor prototype (Figure 11) was the first tool to be developed to use the MAS concept. During dry lab testing, it was found that when the tubing was loaded, the anchors tended to lean, reducing the coupling force. This lead to the decision to couple the polymeric tubing to a jointed section of the anchor so that the anchor can stay aligned while the tubing can bend as required. Also, a second internal magnet per anchor was added to increase the attraction force.

4.4.2 Sling Retractor Revision B

While not perfect, the prototype showed that the concept warranted another attempt. In the second generation (Figure 12), a second magnet was added per anchor to increase lift, as well as a pivot for the tube mounts. In dry lab testing the second generation proved to be much more capable and the major problems with the prototype had been resolved.

In the dry lab the tool proved to be very easy to use and worked quite well. The decision was made to test the tool under real conditions in the animal lab at UTSW on a porcine model. While not exactly mimicking a human, the size and weight of the tissues in the abdominal cavity are close to that of an adult human. Also, it would give valuable information on the ease of use of the tool, and the MAS concept in general, under real operation conditions. On May 9th, 2002, the tool was tested with success (Figure 66).

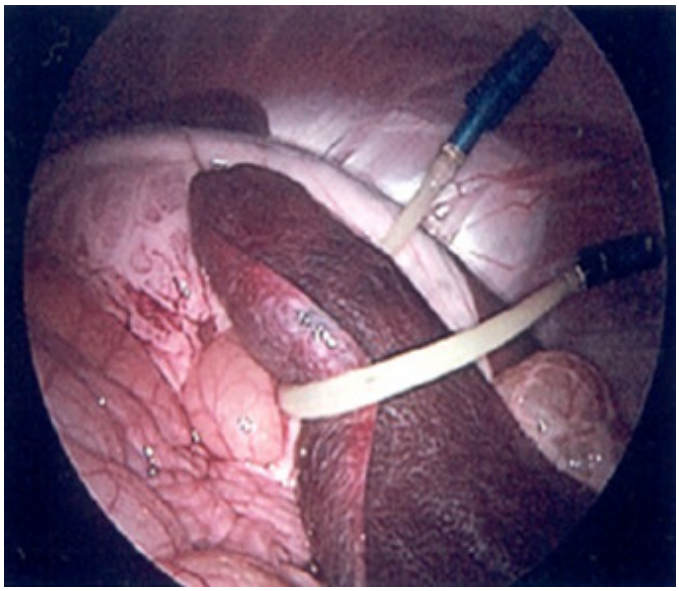

Figure 66. Sling retractor revision b surgical test. The sling retractor revision b successfully supported and positioned a section of a porcine liver.

The mobility and fidelity of tracking of the internal anchors was found to be satisfactory. When “loading” the tool, for example with the liver, all that is required is to position the medium between the anchors near the target, then use a graspers to place the tissue on the medium. Once this is accomplished, moving the external magnets manipulates the tissue.

While the tool performed as intended, it showed that the sizing of the medium between the anchors can be quite difficult. If the length of material is too much, the distance the magnets must travel could be more than what the abdominal cavity will allow. If the length of the material is too short, there may not be enough room to get a good “grip” on the tissue which does not allow the tool to work properly. While the natural rubber tubing worked well, when loaded it tended to stretch, which made sizing

more difficult and required more than ideal motion of the magnets to make the tissue move.

4.5 Paddle Retractor Development

A paddle retractor is slightly different than a sling retractor in the sense that a rigid structure is present that is capable of lifting or lowering tissues, as well as pulling or pushing. A conventional paddle retractor consists of a large diameter rod, usually just one or two millimeters smaller in diameter than the trocar port, which either has metallic fingers or an expandable cloth covered surface. The tissue is manipulated by moving the handle with the paddle against the tissue in question.

For the MAS concept, a paddle retractor with a rigid link protruding through the trocar port was out of the question. Instead, the concept of using the external magnets to maneuver not only the tool, but the tissue was employed. By not having a rigid connection to the outside, the tool is capable of moving completely independent of the trocar port, allowing it to not only be positioned where it is needed, but freeing the entry point to be used to introduce other tooling.

4.5.1 Paddle Retractor Prototype

The paddle retractor prototype (Figure 13) consisted of two Type 1 platforms because their performance under real conditions was known. During dry lab testing, the concept works as intended, but it was determined that there was a problem related to the

anchors: the Type 1 anchors can not withstand loads that are perpendicular to the axis of the magnets.

In dry lab testing this did not seem to be a problem because the tool was tested in only lifting or lowering tissue with the magnets coupling through a flat surface that was not very thick, only about 6.4 millimeter (0.25 inch). When the abdomen is inflated, the internal wall is dome shaped, which cause the magnets to be at an angle relative to eachother, which causes the angle between the anchor and the linkage connected to become more acute, resulting in more of the load being transmitted perpendicular to the anchor. Also, the abdominal wall of the porcine model was approximately 12 to 15 millimeter (0.50 to 0.59 inch) thick, which causes the coupling force between the internal and external magnets to be less than the dry lab tests.

While the limitations of Type 1 anchors lead to the tool not working as intended, it did show that the dual link concept would work. The dual link concept is that the position of the paddle can be manipulated by changing the distance between the anchors, which will raise and lower the primary link, thus raising and lowering the paddle and the tissue in question (Figure 13). The tool was able to show the promise of this design, but the anchors were inadequate for the tool to function properly, and a need for an anchor which can withstand loading perpendicular to the magnetic coupling, at least in one direction, which all lead to the development of the Type 2 platforms.

4.5.2 Paddle Retractor Revision B

The development of the Type 2 platform delayed the development of the second generation paddle retractor (Figure 14), but the delay was worth it. The Type 2's lay down anchor was exactly what is needed for the paddle retractor to be successful since the Type 2 layout resists forces perpendicular to the magnetic coupling along the length of the tool. The original anchors that were employed were not very efficient because the spacing of the magnets on the anchor did not match the external platform's spacing. While it did work, it was not as strong as it could have been. With the spacing changed to match the external spacing, which is 25 millimeter (1 inch) on center, the anchors couple very strongly and the tool could actually be tested.

The anchors were not the only significant improvement in Revision B. A three-fingered, spring-loaded paddle was added to the distal end of the primary link. The concept with this paddle is that it would fold up when the tool was pulled into the trocar port, and the fingers would slide into the secondary link. While the introduction and extraction of the tool works very well, the tool itself is hard to maneuver once delivered due to the length of the linkages.

The length of the tool is the result of the requirements of the tool. It must reach from the internal abdominal wall are reach tissue level, which we approximated to be 80 to 100 millimeters (3.1 to 4 inch). The fingers are only 15 to 20 millimeters (0.59 to .79 inch) in length, so the primary link must make up the rest of the length. The secondary link has to enclose the fingers and be long enough to reach a point on the primary link for the pivot with gives control of the angle of the paddle. Added to the length of these

two linkages are the Type 2 anchors, which are approximately 30 millimeter (1.18 inch) each and the tool is very cumbersome to use. When deployed the anchors would spread from one side of the abdomen to the other, which made it difficult to use.

The tool was successfully tested in a MAS test session on August 22, 2003 (Figure 67). While the paddle worked well, limits on the rotation of the fingers were needed because they spread too far and made it difficult to manipulate soft tissue such as intestine. Also, an improvement in the length of the tool when deployed was desperately needed.

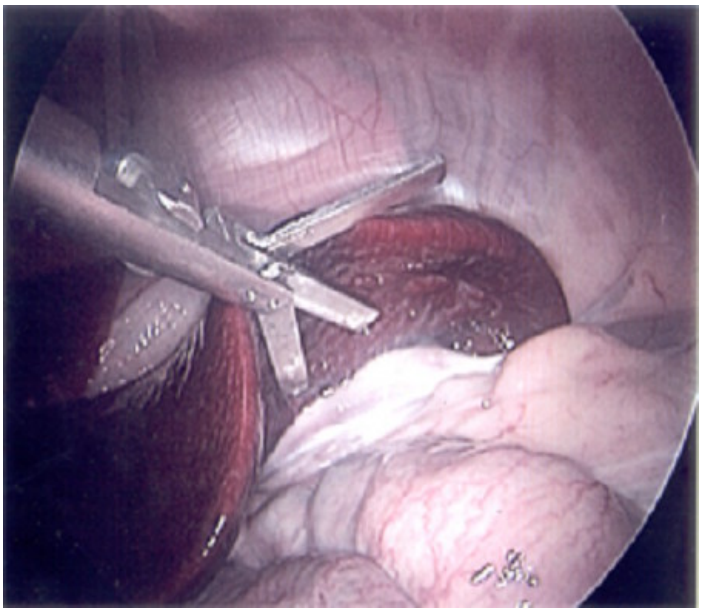

Figure 67. Paddle retractor revision b surgical test. The paddle retractor revision b successfully supported and positioned a section of a porcine liver.

4.5.3 Paddle Retractor Revision C

The revision b paddle retractor was capable of fulfilling its intended job, but it also demonstrated problems in the design. First, the tool required two external magnets

at all times, which limited room on the external surface of the abdomen which was a problem when another tool needed to be repositioned. Secondly, the paddle fingers had to be limited in their spread, or replaced with something else entirely. Thirdly, the tool needed to be shortened to increase maneuverability in the abdomen.

The first problem prompted the development of the anchoring needle, or Type 3 platforms. The concept revolved around the requirements of the paddle retractors anchors: the retractor was not a dynamic tool. Since it was essentially a "lock and forget" tool, the external magnets were not needed to move the tool, only support it in the abdomen. Another benefit of the anchoring needle is that the holding strength of the retractor is greatly improved because the coupling strength of the magnets is not what holds the tissue in place, but rather a rigid rod or needle. While the early versions of the anchoring needle or Type 3 platforms were difficult to use, it showed the possibility of this technique.

The second problem was first approached by reducing the number of fingers from three to two. The fingers were designed to only move out +/-45 degrees, and overlap in the middle.

The third problem is the hardest to solve. The concept of a telescoping primary link was approached as a possible approach to shortening the tool. The primary link was replaced by a single acting pneumatic cylinder. Since the cylinder had a spring internally that caused the cylinder to normally be retracted, varying the input pressure to balance the spring gives a simple but not precise position control. Since there was uncertainty of whether or not this concept would work, a simple, yet functional, tool

was put together to test the concept, resulting in the paddle retractor revision c (Figure 15). While the cylinder used was too big to fit through a conventional trocar and had to be inserted through the incision directly with the pneumatic tubing passed alongside the trocar port, the testing in-vivo showed that the tool would function and should be attempted with equipment that could be passed through a trocar proper.

4.5.4 Paddle Retractor Revision D

Revision C showed that not only was a telescoping link a viable solution, but showed that pneumatic tooling could be delivered successfully, even though the tool was not delivered via trocar port. One of the problems with the pneumatic cylinder that presented itself was what is referred to as “memory” or specifically the bend radius of the tubing connected to the cylinder. The tubing used for revision c was fairly stiff and caused problems when trying to deliver the tool properly.

The original cylinder was replaced with a significantly smaller unit: 11 millimeter bore to a 4 millimeter bore. Along with the smaller diameter came a much shorter package, even with longer stroke. While the commercially available cylinder has a fitting for 4 millimeter inner diameter tubing, this tubing would not bend in a small enough radius to be viable for use. Instead, the cylinders were modified, as discussed in Chapter 3 Section 9, by cutting off the factory fitting, and drilling and tapping the rear of the cylinder to accept a fitting that would allow 2 millimeter inner diameter tubing. (Figure 38).

While in principle, the rotating fingers will give a larger surface to manipulate tissue, lowering the stresses induced in and on the tissue, the ideal size for packaging and tissue manipulation was something that could pass through the trocar port. The decision was made to abandon the rotating or expanding paddle in favor of a fixed size paddle since it was easier to manufacture and use.

The paddle retractor revision d was tested during a MAS field test on May 27th, 2004 (Figure 68). The tool was delivered through a 15 millimeter trocar that was then removed from the porcine model and slid along the pneumatic supply line. A second trocar was inserted into the incision so that the pneumatic tubing was sandwiched in-between the abdominal wall and the wall of the trocar port. This was done because conventional trocar ports are not capable of having two objects pass through them at the same time and seal properly. This trocar port location was used to insert the MAS camera, which was inserted with the same procedure. This port was ultimately used for the graspers during the surgery. When attempts were made to have the supply lines and/or wires pass through a conventional trocar port along side a conventional tool, the port's seals leak.

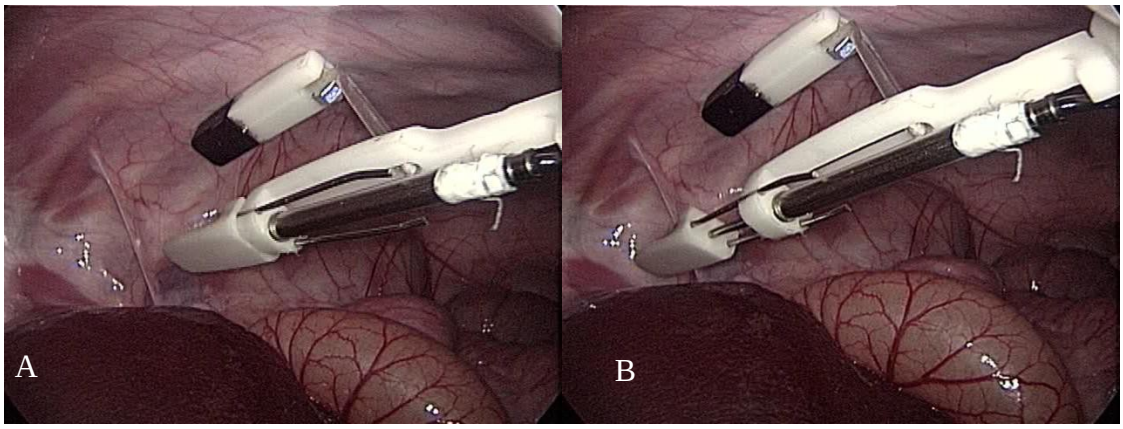

Figure 68. Paddle retractor revision d surgical test. The cylinder allowed for the length of the tool to be short (A) or variable length (B) depending upon what was needed.

4.6 Camera System Development

One of the more ambitious developments for MAS, and one of the most successful was the development of the camera system. As with the other tools that were developed, the concept revolved around taking a conventional tool and attaching it to a magnetic anchor. However, with the camera, there is another part to the tool that must be delivered at the same time, namely a light source.

A conventional laparoscopic camera has a glass cylinder surrounded by fiber optics. The glass cylinder is used to "transmit" the image back to the camera which is attached to the end of the tool. There is a mirror at a fixed angle at the end of the glass tube which allows for the camera to not be required to point directly at the area the surgeon wants to look at. The fiber optic deliver the light parallel to the axis of the camera to reduce shadowing in the image used for surgery. The MAS camera would need to deliver light, and somehow deliver an image to a monitor for the surgeon to use.

The true concept for the camera would consist of a CCD array, wireless transmitter and on-board light source, making the tool completely free of the trocar. In extensive searching of suppliers, a camera consisting of these specs was not available.

Developments by Given Imaging and RF Norika have shown that this technology is possible, but it is not available as an off the shelf component. While this concept is the ultimate goal for the tool, lack of expertise in the fields required meant that the tool, for now, would have to be limited to what is commercially available.

One of the first concepts looked into was fiber optics for not only light delivery, but for image delivery as well. While in concept this is the simplest solution, there are problems with this technique: the flexibility of the fiber optic and what is referred to as "honeycombing".

Honeycombing (Figure 69) is the result of the image being split among the fibers and the camera seeing the split. While the effect is worse when there are only a few fibers used, increasing the number increases the rigidity of the bundle, making it harder to bend. Bend radius is important for any MAS tool since the tool's tether must come out of the trocar port and bend toward the tool, or allow for the tether to bend easy enough to coil slack in the abdomen. While exaggerated, the following pictures show the difference between the fiber optic image system and the conventional camera. Since MAS was to be a valid replacement for conventional tools, the decision was made to use a remote camera head that would give good image quality and demonstrate the possibilities.

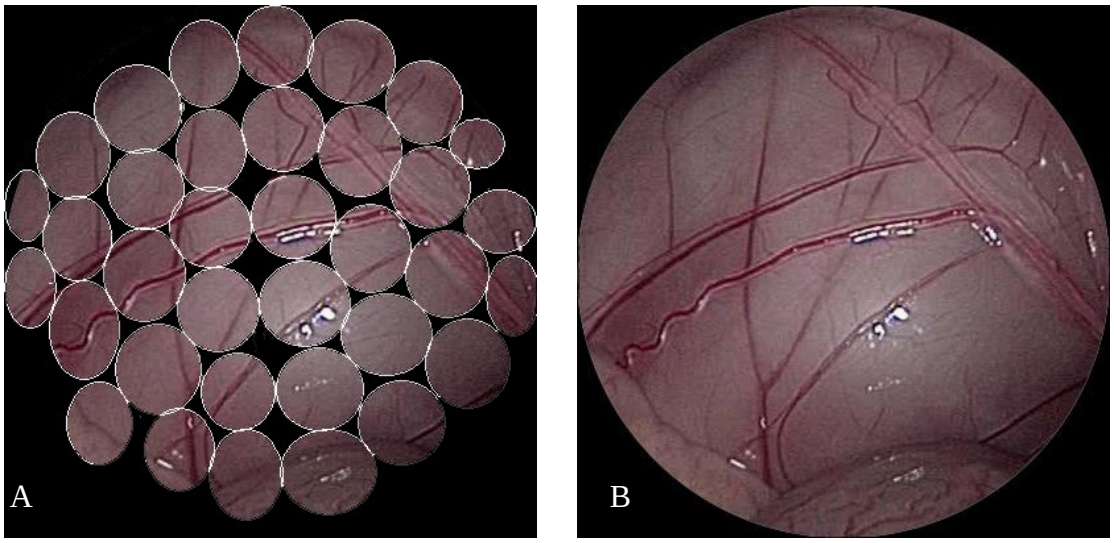

Figure 69. Honeycombing effect. Image A represents a simulated honeycombed image, while image B shows what a conventional camera would see.

In searching for the ideal camera, two small CCD cameras were found that would fulfill at least a proof of concept design. While the cameras were different resolutions, abilities and cost, they were approximately the same size: 7 millimeter (0.28 inch) in diameter by approximately 50 millimeter (2 inch) in length. The diameter was the major dimensional constraint because something to support the camera would need to pass through the trocar with the camera because assembling the camera onto a structure in the abdomen is very difficult since one cannot see what is happening.

4.6.1 Camera Stand Prototype

The camera stand prototype (Figure 17) consisted of a single Type 1 anchor with a pivot on the distal end for positioning the camera. The angle of the camera was controlled by moving the camera itself or the cable coming from the camera. The

position was held by friction of the pivot. While this setup worked, it was not practical since the camera and cable were difficult to see and the position the camera was adjusted to was not held well. It did allow for the first video to be captured from a MAS camera stand on May 9th, 2002 (Figure 70). The light was delivered by pointing the conventional endoscope to the area of interest.

Figure 70. Camera stand prototype image. While the image quality is not that of a conventional laparoscope, the image was deemed sufficient for surgical use.

4.6.2 Light Delivery

Among possible improvements to the camera stand itself, a need for a light source became very apparent during the surgical test. For light delivery, multiple concepts were devised, but were not tried due to either fundamental problems, or added too much complication to be useful.

One concept was to develop tools that consisted of a string of lights. This concept would use the anchoring needle to power the lights without having a tether.

However, without these lights, the camera is useless and the tools cannot be seen. This concept was dropped because of this problem.

The easiest concept is to mount the light source on the camera tool directly. The problem that develops is that the camera requires more light than what can be comfortably housed on the camera tool. As stated earlier, the camera is approximately 7 millimeter in diameter and it must pass through a 15 millimeter trocar port with the structure attached. In testing, light emitting diodes (LED) were considered for delivering the light for the camera, but due to their size, enough to be truly effective are difficult to package with the camera.

The solution that was used for most of the testing was the concept of a trocar light (Figure 71). At least one trocar port will be required to use the medical tools. Since a trocar is needed for inserting the tools, at the light needs to be delivered before the camera, the decision to combine the trocar and light source into one tool.

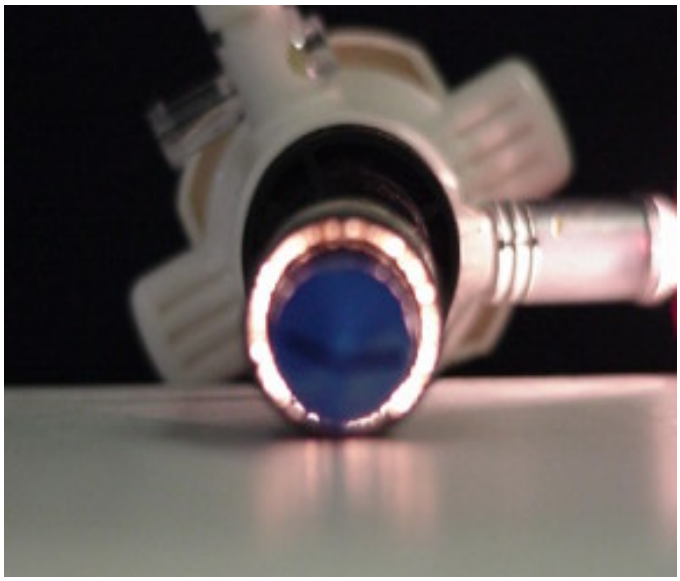

Figure 71. The trocar-light. Since the trocar has to be inserted before the camera, it was deemed natural that it be used as a light source as well as an entry point.

This was accomplished by taking a 15 millimeter trocar, cutting the shank and pressing it over a 12 millimeter trocar with small fiber optic lining the walls of the trocar. The trocar has a fitting that allows for it to directly connect to a conventional light source. The trocar light performs well enough that there is enough light delivered for the camera to see in the surgical area. This concept is not perfect because the light is delivered off axis with the camera, causing shadowing.

4.6.3 Digital Manipulation

A conventional laparoscopic camera tool is heavily dynamic because zooming and horizon correction are done by physically repositioning the camera. While these abilities were desired in the MAS camera tool, they are very difficult to achieve mechanically due to space requirements for an optical zooming solution, and because

there was not a rigid link to the outside world, it is difficult to cause the camera to rotate as needed. Zoom could be accomplished simply by moving the camera closer or farther away from the target, but by moving closer to the target, the tool is in a position where it could interfere with the other surgical tools.

Digital manipulation was employed to solve the horizontal correction as well as zooming without increasing the size and/or complexity of the tool itself. The most difficult part of the use of digital editing the video from the camera is that it must be done in real-time so that there is little to no noticeable delay in the video images since the surgeon relies on that information. Most digital editing systems on the market are capable of digitally manipulating the video, but only after it has been digitized and stored on a computer.

A broadcast quality digital editing system was employed to manipulate the video from the camera. The digital zooming (Figure 72A) is accomplished by over-sampling the image, i.e., taking one pixel and breaking it into nine pixels. While the resolution of the picture degrades, only on the most severe zooming does the image degrade to the point that it becomes a problem. Because the space of the abdomen is fairly small, the camera was able to be digitally zoomed without problems with the image quality.

Horizon correction (Figure 72B) is accomplished by rotating the image about an axis. This is done by applying a transformation to the pixels and causing them to be repositioned. All this is done without a noticeable time lag with a fairly easy to use system. While not as high quality as optical zooming or mechanical manipulation of

the camera, it is useful enough to allow for the tool to function properly in surgical testing.

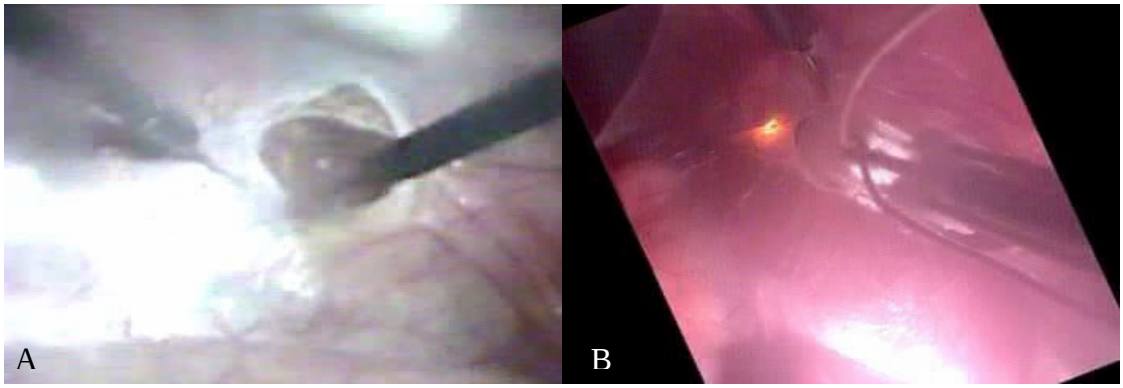

Figure 72. Digitally manipulated samples. Image A demonstrates a digitally zoomed image, image B demonstrates a digitally rotated image.

4.6.4 Camera Stand Revision B

The prototype camera stand showed that the concept was valid, but changes in controlling the camera itself were needed. While the addition of the trocar light and digital manipulation of the video helped with some of the problems, the tool itself required major changes.

One of the problems that needed to be tackled was to make the camera stand more stable. With just one anchoring point, the tool proved to be fairly easy to tip or deflect with just movement of the cable. The concept that was employed was to increase the number of anchoring points to make the tool more stable along the axis of the camera, and cable. A secondary anchor was added to the rear of the camera to help with stability and as an added benefit helps with the second problem of aiming the camera, which resulted in the camera stand revision b (Figure 18).

Since there are two anchors, one can move them together which moves the camera and holds the camera in orientation. If one magnet is moved along the axis of the camera while the other is held still, one can change the inclination/declination of the camera head. This allows for the adjustment to be accomplished externally, which makes it easier to adjust since the camera and/or cable does not have to be grasped.

4.6.5 Camera Stand Revision C

While revision b was an improvement, the performance of the stand itself was rather clumsy. The secondary anchor worked well for adding stability and positioning, but did not work well during introduction and extraction of the tool because of having to fold the cable of the camera to make the anchor fit with the cable.

During testing of revision b, the original camera was damaged beyond repair. The camera was not protected and was exposed to body fluids and an alcohol bath that damaged the electrical connections for the CCD array.

From the onset of the design, revision c (Figure 19) was planned to enclose the camera in a water tight enclosure. This was done to not only protect the camera from the abdominal environment and the cleaning afterward, but also from the warming baths that are used to bring the camera up to body temperature to limit fogging of the lens. The lens cover of the camera enclosure is sealed by using Teflon tape and threading the cover to the front of the housing. This was done to allow for adjustment of the focus of the camera without having to completely remove the camera, as well as allow for changing of the lens since the focal length to use was an unknown. The rear of the

enclosure was sealed by using hot glue. Hot glue was used because of its ability to be squeezed into any gaps, but more importantly, it would not react chemically with the camera and the camera cable.

The dual anchor arrangement was continued with revision c, but with improvements. A modified Type 2 anchor that had only one magnet was used for the rear anchor because of its low profile. The low profile of the anchor allows for the camera cable and the rear anchor to pass through the trocar port easier than with revision b. The low profile also helps with maximizing the angle that the camera can be lowered and raised to.

The linkages are connected to the camera enclosure by a loose coupler. This was done to allow the camera enclosure to rotate independently relative to the anchors to lower the twisting stress in the camera cable so that it does not side load the camera tool. While the coupler is not loose enough to allow horizon correction, it is loose enough to allow the enclosure to rotate, relaxing the camera cable.

Figure 73 shows the camera stand revision c during one of the multiple surgical tests it was subjected to. It should be noted that the camera is completely free of the trocar port that it was delivered in. All that protrudes the abdominal wall is the cable for the camera. With sufficient cable slack, the tool can transverse anywhere the surgeon needs it within the abdominal cavity.

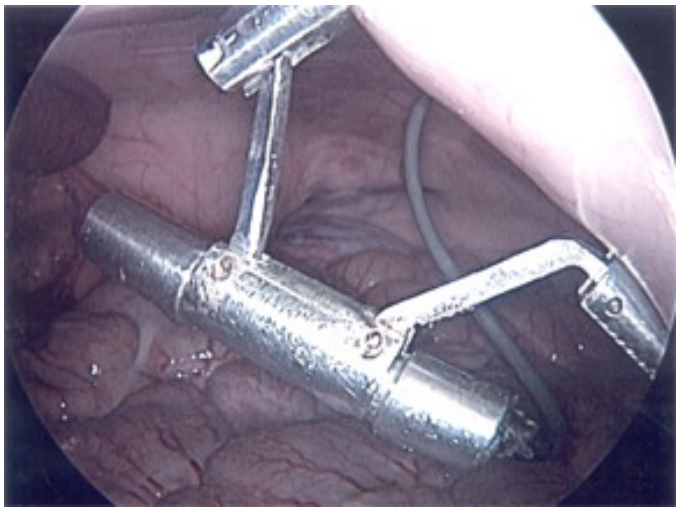

Figure 73. Camera stand revision c surgical test. Notice the camera is located away from its entry point, allowing other tools to enter the same port.

4.6.6 Camera Stand Revision D

Revision c is very reliable and has been used for multiple surgeries without damage being caused to the camera. Since the tool worked very well, there were two improvements that would increase the functionality of the camera tool: using a powered anchor for inclination/declination control and an angled mirror in front of the camera lens.

From testing the camera tool and the retractors, using two anchors, while functional is cumbersome. With the success of pneumatically powered anchors, the decision was made to connect a camera enclosure to a powered anchor. The pneumatic powered anchors work because the spring in the cylinder combined with the weight of the camera enclosure balance the force developed by the pneumatic pressure. By using

variable pressure, one is capable of changing the angle of the camera with only one anchor.

A conventional laparoscopic camera has an angled mirror in front of the camera so that the camera does not have to be pointed directly at the target. Having the angled mirror, keeps the camera from being located in the surgical arena. One of the problems with revision c is that the camera must be pointed at the target area directly. A mirror angled at 30 degrees was located in front of the camera's lens. While the concept should have worked, the position of the mirror was calculated incorrectly and the camera could not focus properly on the mirror.

During the surgical test of the camera stand revision d (Figure 20), the mirror assembly was removed so that the camera could function normally. With the removal of the mirror, the powered anchor could be tested as a means of moving the camera, with success.

4.7 Powered Tooling Development

The dual anchor system, that allows for a mechanically driven tools, works well but it is cumbersome to use. The question was raised whether tool maneuvering could be powered by electrical or fluid powered actuators. The needle anchor concept was proven to be able to deliver electrical power directly to the anchor, making this type of tool possibly wireless. The problem was that for each actuator, a needle pair would have to pass through the abdominal wall, and couple to the anchor. In theory, this is not a problem, but in practice the anchor would be large and difficult to use. For a single

actuator tool, this concept would work, but the goal was a minimum of two degrees of motion. Furthermore, the needle anchor concept worked against the principle of easy maneuverability of the internal tools by manipulation of the external magnet assembly.

Tethers, whether electrical wire or pneumatic tubing, presented a challenge for delivering the tools. Conventional trocar ports do not have seals that work with more than one circular object passing through them at a time. This presented a problem since the trocar was to be used for delivery, and conventional tooling. What was done to get around this problem was to use a conventional trocar port to introduce the tool into the surgical area, then, once secure, remove the trocar port and slide it up the tether. A different trocar port was then inserted into the incision that could be used to introduce another tool, or for the conventional tool to pass through. This concept was first tested with the camera tool with reasonable success, and was successful at delivering the active tooling as well.

While the concept of the magnetic anchoring system had proven capable of supporting passive tooling, e.g., tooling that required motion of one or both of the anchors to drive the tool end, to truly accomplish a reduced trocar port surgery, active tooling, i.e. able to move relative to an anchor, was needed. Since the tools would move relative to the anchor, one failure point for the tool would be if there was a power failure. All the tools to be developed must be able to be introduced and removed through a trocar port without being powered. Before the attempt to switch from passive to active tooling, questions concerning which modality to use for actuation, control, command as well as which tool to attempt to mimic became important.

It should be noted that a tool was developed and built that used externally located actuators to provide motion for the arm. The actuators used were simple hobby servos, which were connected to flexible stainless steel cables. While in the dry lab, this concept proved to be functional, there was a fundamental problem with this approach: the cables were required to have tension at all times. To supply the tension a hard cover, much like a bicycle brake cable, was looked at but would not bend sufficiently to be viable. In the dry lab the tension was developed by maintaining a distance from the actuator(s) and the anchor by use of the anchoring needle. However, it was determined that while this worked in the dry lab, biological tissue would not support the loads required to maintain tension and would cause significant tissue damage. As such, the determination was made that the actuators needed to be housed on the tool itself.

One of the major constraints for the actuator to be used was the volume of the actuator. Due to the size requirements of being able to pass through the 15 mm trocar port, the cross sectional area was of concern. Once passed through the trocar port, the length of the tools was a concern for mobility, so the actuators needed to not only have a small cross sectional area, but also a short length. Also, the ease of coupling to the actuator was considered since space is at a premium for packaging.

One of the main goals for the MAS development was to reduce the number of trocar ports used during surgery. In the porcine model, the use of a paddle retractor is not required, which reduced the replaceable tools to a camera which was functional in

either the revision c or d variant, a graspers and the cutting tool, which could be either a scissor tool, or hook cautery.

The graspers have multiple degrees of freedom and complexity that was deemed to difficult to be in a first version active tooling. A scissor tool was also looked at, but driving the scissors with enough force drew concerns, so it was rejected as well. A hook cautery, however, does not require as extensive degrees of freedom as other tools, and the tool tip does not require any mechanical motion, just an electrical connection.

4.7.1 Control System

Before development of the powered tooling was started, the control system for the tools was constructed. Originally, there was a desire to keep the control system as simple as possible, because the tooling would be very complex by themselves. However, the addition of a computer offered many advantages over the cumbersome "simple" solution: adjustability, capability of controlling all required functions, more professional look and feel, and increased reliability.

Adjustability of the effects of the output from the control device is useful for correcting responses from the user. As started earlier an off-the-shelf gaming joystick was used for the user input device. The specific joystick used has 4 proportional axes, as well as 10 push buttons that can be used for any purpose required. The "mapping" or definition of the buttons on the joystick can be changed to accommodate more functions, or change which buttons control different functions. The proportional axes were used to control the motion of the arm, and due to the adjustability that was

available, the sensitivity as well as limits on the motion could be adjusted quickly and easily.

The three actuation modalities were going to be applied for different arm configurations, namely electric motors, shape memory alloys, and pneumatic cylinders. Each of these technologies has advantages and disadvantages, which are discussed in Appendix L.

The position control of the electric motor was a by-product of the gear head that was installed on the motor. The gear reduction was great enough as to have enough drag that driving the output shaft to operate the motor was extremely difficult. The motor command consisted of full speed either clockwise or counter clockwise until the button that controlled it was released. While the control system and software has components to drive the electric motor, it is not connected due to lack of available output channels on the data acquisition card and lack of need.

For the pneumatics, the user commands were taken from three of the joystick's proportional axes and converted to corresponding pressures. Position control with the pneumatics is possible because the cylinder has a spring that generates a restoring force for the cylinder. By varying the pressure, one can balance the force of the spring and make the cylinder extend in a rudimentary position control scheme.

For the shape memory alloy, trans-conduction amplifiers were used, which two of the proportional axes were converted to a variable current output. As the current flowed through the shape memory alloy, the heat generated caused the wire to contract. While the position control of the shape memory alloy was not well defined, proportional

functions were available. It should be noted that the shape memory and pneumatics were not meant to operate at the same time due to sharing of the axes of the joystick.

While the other points are valid, the most important thing was reliability. Due to the time and resources that went into setting up one of the MAS field tests, having questionable equipment was not acceptable. Because the control scheme was converted to more commercially available components, an inherent reliability can be expected.

For each of these technologies, the power control devices needed to be housed in a platform capable of interfacing with the computer. This was accomplished by using a digital to analog card with capabilities to control 8 different outputs at the same time. The wiring diagram for the control box that was built, as well as the program that drives the equipment is shown in Appendix H.

4.7.2 Pneumatically Actuated Arm Prototype

The hook cautery was designed to mimic the motions of Dr. Cadeddu, who was one of the principle investigators of the technology, and chief tester of the equipment. The required motions dictated a 3 degree of freedom arm: inclination and declination, left and center and telescoping ability. The requirement of left and center was based on the desire to mimic a conventional cautery, which Dr. Cadeddu operated with his right hand. This simplification was done to improve the reliability and function of the arm.

The pneumatically actuated arm prototype (Figure 21) was designed with the idea of being sized properly for surgical use, but was never used in this fashion because it was mainly a proof of concept. Before a full scale, surgery prepped, robotic arm was

to be commissioned, a verification of the limited degrees of freedom were still enough to accomplish the required motions. Also, the prototype would be used to tune and configure the control system for the surgery ready, second generation.

Some of the key features of the prototype are the inclusion of an anchoring needle lock mechanism, the use of a rack and pinion drive system, and solid linkages in between the different joints. The anchoring needle concept was included because there was concern in whether or not the magnets could withstand the loading on the tip of the arm. The rack and pinion drive was used to help with packaging of the pneumatic cylinders since the drive mechanisms were packaged at the pivot point and the cylinder body was stationary. The linkages were very difficult to manufacture because the shape of the linkages was fairly complex as well as very thin to minimize weight.

While generating losses due to gearing, as well as friction, the rack and pinion assembly worked for driving the arm. The friction arose from the size of the components in the rack and pinion setup, which did not allow a bearing or bushing to be used. As with conventional robotics, the first joint of the arm must have the most power since it must be able to maneuver the structure that comes after the first pivot. A 4 millimeter bore cylinder was used as the actuator to drive the first joint due to the increased area for the pressure act on. However, while the first joint was capable of lifting the arm, more torque was required. This would be addressed in the surgery ready version.

For a surgery ready arm, the linkages needed to be lighter, simpler and stronger. While delrin is fairly light, in order to machine the material, some areas needed to be

thick enough to be held within the machine. There was a failure in the first pivot of the arm due to the limited thickness of material available. The issues with the linkages would be addressed in a surgical version of the arm.

While the arm had multiple problems, the function of the arm was deemed satisfactory. While the control of the arm was not as precise as it could be, the control system was still being fine tuned and the problems that limited the performance would be addressed in the surgical version.

4.7.3 Pneumatically Actuated Arm Revision B

The prototype showed that a functional 3 degree of freedom robotic arm that fit through a 15 millimeter trocar port was possible, but there were key improvements that needed to be made, namely: more flexible tubing, more torque available from the first joint, more torque at the second joint, a better linkage system and better range of motion.

The cylinders from SMC come with fittings molded into the cylinder body to fit 4 millimeter tubing. This tubing, while highly flexible for normal industrial applications was too stiff for MAS uses because of its bend radius. What was needed was more flexible tubing, or smaller diameter tubing. More flexible tubing was not available due to the pressures that were being used, 620 to 689 kPa (90 to 100 psi). Smaller tubing, 2 millimeter, was readily available from SMC, as well as fittings. However, the cylinders were not available with this fitting pre-installed. To use the more desirable smaller tubing the factory fitting was removed and the rear of the

housing was drilled and threaded to fit the smaller fitting, as discussed in Chapter 3 Section 9. While this had to be done with great care to minimize leaks as well as hold up to tugging and such that was bound to happen. Because of this modification, the pneumatic arm is viable since the minimum bend radius of the smaller tubing is well within the range required for the MAS tools.

The first surgical iteration of the pneumatic arm was defined by the first joint of the arm. Since the diameter of the cylinder cannot easily be increased due to packaging concerns, and the pressure was close to the limits of the cylinders and tubing, gearing was incorporated to increase the torque developed in the first joint of the arm. According to the calculations, the first joint of the prototype was generating 22 N-mm (3.12 oz-in) of torque from 620 k Pa (80 psi). The gear train that was designed should have generated 52 N-mm (7.30 oz-in) of torque, but, as with the prototype, due to the size of the components, bushings and bearings were not able to be installed. As such, when the arm was operated, much of the torque generated was consumed in the friction of the gear train. However, the benefits of the gears was visible since the arm was longer and heavier than the prototype, increasing the torque requirements, but the same cylinder was able to raise and lower the arm with less trouble than the prototype.

The second joint, which acts as an “elbow”, required more torque as well. The prototype used a 2.5 millimeter bore cylinder for the second joint, which proved too weak for controlling the tool tip. A 4 millimeter bore cylinder was used instead, which increased the torque on its own. However, the pinion gear was replaced with a larger

gear, 16 tooth to 20 tooth respectively. These two improvements increased the torque applied to the second joint from 9 N-mm (1.22 oz-in) to 33 N-mm (4.68 oz-in).

A new linkage system was devised to improve durability, as well as make the part(s) simpler for manufacturing. Referred to as the "space frame", the solid links of the prototype were replaced with the concept of essentially two plates with threaded rods in-between them. The benefit to this design is that the end plates are much simpler to machine, while also allowing for freedom of placement with the cylinders since most of the volume of the linkage was not used. While the concept was useful, the arm turned out heavier simply because it was overbuilt: the threaded rods used were 2.4 millimeter (0.094 inch) diameter 304 stainless steel. Three rods were used, not because of bending of the arm, but for fear of the arm twisting under load. Once built, it was apparent that twisting was not as much of a concern, and fewer threaded rods were required.

Along with the space that is gained by using the space frame concept is the routing for the pneumatic supply lines as well as the power connections for the cauterizer tip. Grooves were added to sections of the arm for routing during assembly because there is a desire to keep the arm as short as possible. Even with CAD versions of all components used, the exact paths for the hoses and wires was not truly known until the arm was pieced together. Trimming the parts and making cut outs allowed for the arm to be much shorter than originally predicted from the software model.

The arm when assembled and straightened for passing through the trocar port is 178 millimeter (7 inch) in length. A large portion of this length was due to the anchor,

67 millimeter (2.64 inch) by itself, most of which was consumed in the gear train of the first joint.

On May 27th 2004, the second generation pneumatically actuated 3 degree of freedom robotic arm was tested in-vivo (Figure 74). Since conventional trocar port gaskets cannot seal properly with multiple objects being passed through the port, the arm was introduced in a conventional 15 millimeter trocar port and once magnetically coupled and positioned away from the incision, the trocar was slid down the supply lines of the arm and a new trocar port was passed through the incision. The supply lines were pressed against the tissue and the outer surface of the new trocar port which was used as an access point for conventional tools, specifically the graspers.

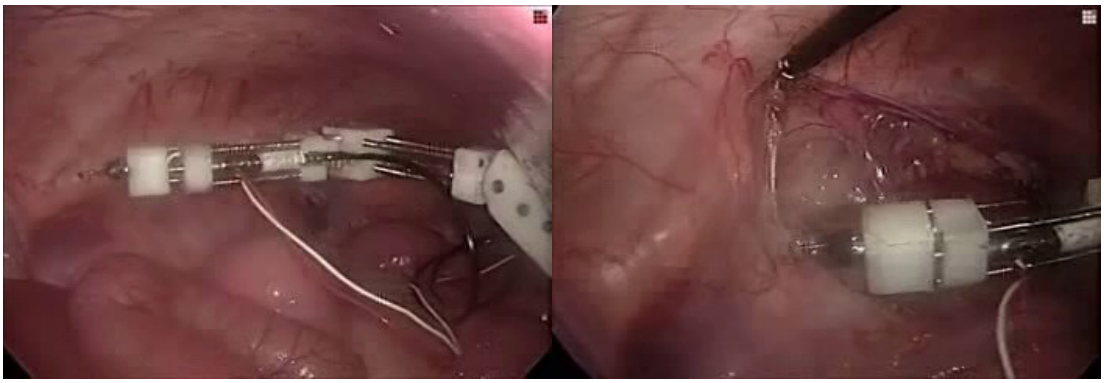

Figure 74. Pneumatically actuated arm revision b surgical test. The arm was used to successfully cut the tissue surrounding the kidney.

4.7.4 Pneumatically Actuated Arm Revision C

The space frame concept proved its usefulness in the second generation arm, and was deemed useful enough to be used in the third generation arm. With the experience gained from the second generation arm, it was determined that the size and

number of struts used in the arm could be reduced. Reducing the size and number of the struts used would allow the ends of the linkages to be smaller, thus reducing the load on the cylinders and reducing the need for the complex gear system.

There were two decisions that lead to the significant changes between the second and third generation: removal of needle anchor and removal of gear system. The needle anchor area consumed the center of the anchor, not allowing the pivot to be located in-between the two lift magnets. This caused an imbalance in the loading of the magnets which lead to coupling problems through thicker tissues.

The removal of the gear system allowed for installation of high precision bearings that reduced the friction in the drive train allowing for more of the force generated by the cylinder to transfer to driving the arm. Instead of the gears, a “direct drive” linkage system was used to transmit the linear motion of the cylinders piston to rotational motion of the links. This required that the cylinder body was mobile relative to the anchor, but the required motion is not great enough to cause problems.

While the rack and pinion drive for the second joint worked well, the increased weight of the joint caused unnecessary loading on the first joint. The same approach to using a direct drive linkage system was used on the second joint as well. Due to packaging problems, only one bearing was able to be used in the second joint, but even with one bearing, the motion was smoother than that of the second generation. There was some difficulty in working out the kinetics of the joint so that the cylinder was positioned correctly for easy ingress and egress of the tool through the trocar port, and being able to generate sufficient range of motion. While the range of motion is not as

large as desired, the target being 90 degrees, the joint is capable of approximately 60 degrees which is sufficient for its purposes.

Many upgrades were applied to the last section of the arm due to problems that arose from the second generation arm. One of the first problems was that the struts for this section of the arm caused a large load on the first joint because of their relatively long distance from the first pivot. A desire to either reduce the number of struts or their diameter was primary to the redesign. The second problem was the guide pins that were used to keep the cauterizer tip from rotating were causing tissue interference problems. The cauterizer tip was attached to the piston of a pneumatic cylinder which caused the telescopic action that was desired. The problem was that the cylinders do not have a mechanism to not allow rotation of the piston, so this guidance needs to be supplied by the arm itself.

The two main problems with the second generation arm were solved with the use of 18 gauge needles and their styluses as the struts for the lower section of the arm and the guide pins, respectively. The needles are smaller in diameter than the solid struts used the second generation arm, but are also hollow. The stylus is made to pass through the inner diameter of the needle by the manufacturer, so they could be used as the guide pins without modification. While the second generation arm used three larger struts, this generation uses four struts, not because of strength issues, but for packaging. In order to route the pneumatic supply lines, the telescoping cylinder was located closer to the axis of the arm. Because of this, a three strut design could not be comfortably fit into the confines of the arm, but four could be located in the corners of the end plates.

Also, using the smaller struts allowed for the endplates of the arm to be smaller, helping to reduce the load on the different joints.

While the improvements to the pneumatically actuated revision c (Figure 23) arm would help performance, there was a concern with its length when straightened to pass through the trocar port into the abdominal cavity. While the second generation fit within the abdominal cavity, it was fairly large and did not have much room to maneuver. The third generation is 136 millimeter (5.4 inch) long from the proximal end of the anchor to the distal end of the arm, or 158 millimeter (6.2 inch) long from the proximal end of the first joint's cylinder to the distal end of the arm. While this was shorter than the 178 millimeter (7 inch) length of the second generation, the hope was that the arm would have been shorter, but the other gains made compensated for the not as dramatic improvement in tool length.

On September 10th 2004, the third generation pneumatically actuated 3 degree of freedom robotic arm was tested in-vivo (Figure 75). As with the second generation arm, the conventional trocar port gaskets cannot seal properly with multiple objects being passed through the port, the arm was introduced in a conventional 15 millimeter trocar port and once magnetically coupled and positioned away from the incision, the trocar was slid down the supply lines of the arm and a new trocar port was passed through the incision. The supply lines were pressed against the tissue and the outer surface of the new trocar port which was used as an access point for conventional tools, specifically the graspers.

Figure 75. Pneumatically actuated arm revision c surgical test. The arm's motion was greatly improved over the previous version in terms of speed and smoothness.

While the performance of the third generation was improved over the second generation arm, there was a problem with the telescopic section during the surgery. The arm was repeatedly tested in dry lab conditions and was fully functional before the surgery. However, either during transportation to the animal lab or during the procedure, one of the guide pins became bent and became stuck. After the surgery the problem was corrected and now the arm is full functional.

4.7.5 Nitinol Actuated Arm Prototype

The development of the powered tooling took two concurrent paths, pneumatically based and shape memory alloy based. Ultimately, the pneumatics received the lion's share of the development time because there are fundamental hurdles that must be overcome with the nitinol to be used as a viable actuator in the project. This being said, nitinol has an advantage in force that can be generated and cross

sectional area. The benefits and limitations are discussed in more detail in Appendix 12.

The nitinol actuated prototype arm (Figure 24) was developed concurrently with the pneumatically powered prototype, and like the pneumatic arm, was not intended for surgical use, but was designed with these constraints in mind. The prototype used a uni-axial spine that allowed for displacement in one axis only. The arm moved because the spine bent in this direction, making the entire mechanism light weight. The spring constant of the spine was used as the restoring force for the Nitinol, which must be kept in tension at all times. The displacement of the links was increased slightly by using zip ties at certain locations along the spine, which held the wire closer to the spine and increasing the arc generated.

Unlike the pneumatic prototype, the Nitinol arm only had 2 degrees of freedom because for the development of the arms, especially the prototypes, the desire was to deal with the requirements and problems of one technology at a time. Also, due to the bending of the linkage, instead of rigid link rotation, there was a length change in the arm.

The prototype, much like the pneumatic prototype, was instrumental in configuring the controls for the later built Nitinol powered equipment. However, the actuation time of the Nitinol became an apparent problem, especially when compared to the much faster responding pneumatic powered arm. However, as stated earlier, the force per cross sectional area of the Nitinol actuators is very impressive and a second

generation arm was attempted to see if the nitinol's shortcomings could be minimized or eliminated altogether.

4.7.6 Nitinol Actuated Arm Revision B

Again, as with the prototypes, the second generation pneumatic arm and the second generation Nitinol arm were developed concurrently, and, like with the prototypes, most of the development time was spent specifically on the pneumatic tool. While the prototype Nitinol arm showed that a functional arm was possible, key concerns needed to be addressed; water resistance of the wire, protecting the tissue from the wire, actuation time and displacement.

One of the key concerns of the Nitinol was the potential for the wire to electrically short if it was exposed to body fluids, something that was highly probable. One of the first steps to protect the expensive equipment that drove the arm, and more importantly the patient, was to install fast blowing low amperage fuses on the output to the arm. While the fuses would not stop an electrical short from happening, they would minimize damage. The water resistance of the wire was not solved, but what was done is to cover the wire in insulating material to minimize the chance of the wire's shorting if they contacted each other, and would give some protection from the elements since the only exposed portion of the wire is where the main electrical connection and the wire were joined.

There was a concern early on of exposing the wire, which has a transition temperature of 90 degrees Celsius to the tissue. At this temperature damage to the

tissue would be severe. However, in testing the wire, one can put their finger on this wire and not be injured. One theory as to why this is so is that the wire has an extremely small cross section and mass, so there may not be enough mass there to sufficiently warrant a response from the body. To fully protect the tissue from the wire and vice-versa, the wire was located fully within the anchor so the possibilities of tissue and wire making contact were extremely limited, so much so that for the most part a structural failure in the anchor would have to happen for contact to be a problem.

Actuation time and displacement were combated by the inclusion of gearing in the drive system. The actuation time of the Nitinol wire favors heavily the relaxation time of the wire. This is because the contracting stage of the wire is actively driven, i.e., a driving current causes the wire to heat, and thus contraction. The relaxation time is the time that the wire takes to dump the excess heat to the environment so that it can expand to its natural shape and/or size. A potential problem that may need to be looked into further is the effect of locating the wire in a protective jacket and whether or not the wire is capable of dumping its thermal energy reliably. The displacement of the wire is 5-10% of its length, which either requires a long piece of wire, or a large lever ratio to amplify any and all movement, both of which would be difficult to package. In determining the gear ratios for the pneumatic arm, a gear ratio was determined for the second generation Nitinol arm as well.

Unlike the pneumatic arm, the Nitinol did not require amplification of its force output, but rather its displacement. A benefit of the Nitinol actuators is that their small cross section allows multiple wires to be used in a relatively small area. As such, the

reduction in force output could be minimized by increasing the number of actuators driving the arm. The gearing that was used was a rack and pinion setup, but the pinion gear was chosen to be larger than the output gear that was attached to the first link of the arm. Using the gear ratio a small motion of the rack would be amplified so any small motion of the wire would be immediately available. While this concept works, due to power supply limitations, the amount of current required to drive the additional wires needed to make up the loss in force was not possible.

Due to the power supply issues, the Nitinol actuated revision b arm (Figure 25) was never used in surgical tests. During dry lab testing the motion of the arm, while not as fast as the pneumatics, was substantially faster than the prototype. With a larger power supply and additional wires, this arm would be well suited for high force load applications. Also, the arm was missing the cautery section of the arm because it was designed with the ability to share parts with the second generation pneumatic arm. As such, it was redundant to develop a lower section of the arm when the two arms cannot be used at the same time due to the command system configuration.

CHAPTER 5

CONCLUSION

Minimally invasive surgery is a growing field, with new procedures, tools and applications being added every year. While these developments have made minimally invasive surgery more desirable for the patient, there is room for advancement to benefit not only the patient, but the surgeon as well.

Using MAS tools such as described in this thesis, the surgeon gains a larger work volume for each tool used as well as more degrees of freedom. With the added flexibility of the MAS tools, new and improved surgical procedures may be possible since some limitations of current tools are counterbalanced. For the patient, there are fewer incisions required, and while there may be no significant physiological advantages, there are psychological benefits.

While the tools as described may not be the most efficient designs, nor as small as some might like, they are useful in proving the basic concepts of magnetic anchoring, e.g., employing tools that do not require dedicated trocar ports. There is room for improvement, but as is, the existing tools validate the concept. Their development should be continued.

The MAS tools were tested in experimental laparoscopic procedures employing porcine models at the University of Texas Southwestern Medical Center's animal lab. Porcine models are widely accepted as relevant testing grounds for new technologies.

Due to U.S. Food and Drug Administration regulations, the tooling was not tested on human subjects.

Successful development of the equipment was demonstrated in the completion of several two-trocar port nephrectomies using the MAS camera and cauterizer. While two trocar ports were installed into the animal subject, only one was used during the surgery for the grasper-based manipulations. The other port was used only for image documentation purposes.

5.1 MAS Specific Conclusions

One of the original objectives of the MAS concept was to determine if the magnets were capable of attracting a target small enough to pass through a conventional trocar port with enough force that useful equipment could be attached to the target. While the performance of the original electromagnets was experimentally determined to be sufficient to warrant further research, permanent magnets were found to offer stronger attraction, in smaller packaging. As shown in Figure 62, the attraction force is great enough, across a clinically relevant, large tissue range, that tooling such as the camera and articulated arm can be held securely and positioned well enough to be used in surgical applications.

Tied in with the concern about the attraction force of the magnets was whether or not tissue compression caused by the external magnet source and internal target would cause ischemia and necrosis. While quantitative results of whether tissue compression is a problem or not, qualitatively, there seems to be no appreciable tissue

compression problem. If such a problem were observed in a specific instance, relocating the tooling to a different location, much like what is required with conventional equipment, could be carried out.

While the attraction force of the magnets is key to the proper working of any tool, very high attraction forcer is required for the sling and paddle retractor. Currently, the attraction force in that case is sufficient for some tissue manipulation, but not for demanding manipulations such as lifting the liver, for example. However, for low force tool requirements, such as manipulation of the camera and cauterizer, the coupling force is sufficient for a wide range of tissue thicknesses.

Part of the driving force for the development of this technology is to be as compatible with conventional laparoscopic equipment as possible. As such, the tools themselves have been designed to mimic their conventional counterparts so as to expedite their integration into the surgical armamentarium. Since the UT Southwestern animal lab is equipped with conventional laparoscopic equipment, verification of compatibility with conventional equipment was accomplished by direct comparison to make sure functions that were required were faithfully replicated.

5.2 Challenges Faced

The two key features of this technology proved to be the two largest hurdles to development, namely the magnetic coupling and the specifics of tool design.

Conventional magnetic coupling is done in direct contact with the object to be magnetically supported, or over a very small distance. In MAS uses, the internal

tooling will always be an appreciable distance from the external source: up to 30 millimeter (1.18 inch) or more in the case of morbidly obese patients. The degradation due to separation distance of the attractive force can be modeled as a decaying exponential. While methods may exist to slow this degradation, they are beyond the understanding of the author. Instead, what has been incorporated is methods of shifting the degradation vertically, thus increasing lifting capacity over the same distance range, or shifting the degradation to the right, thus increasing the working distance, as shown in Figure 76. These concepts are promising, but the proof of concept will need to include the tools to be used, as well as magnet development.

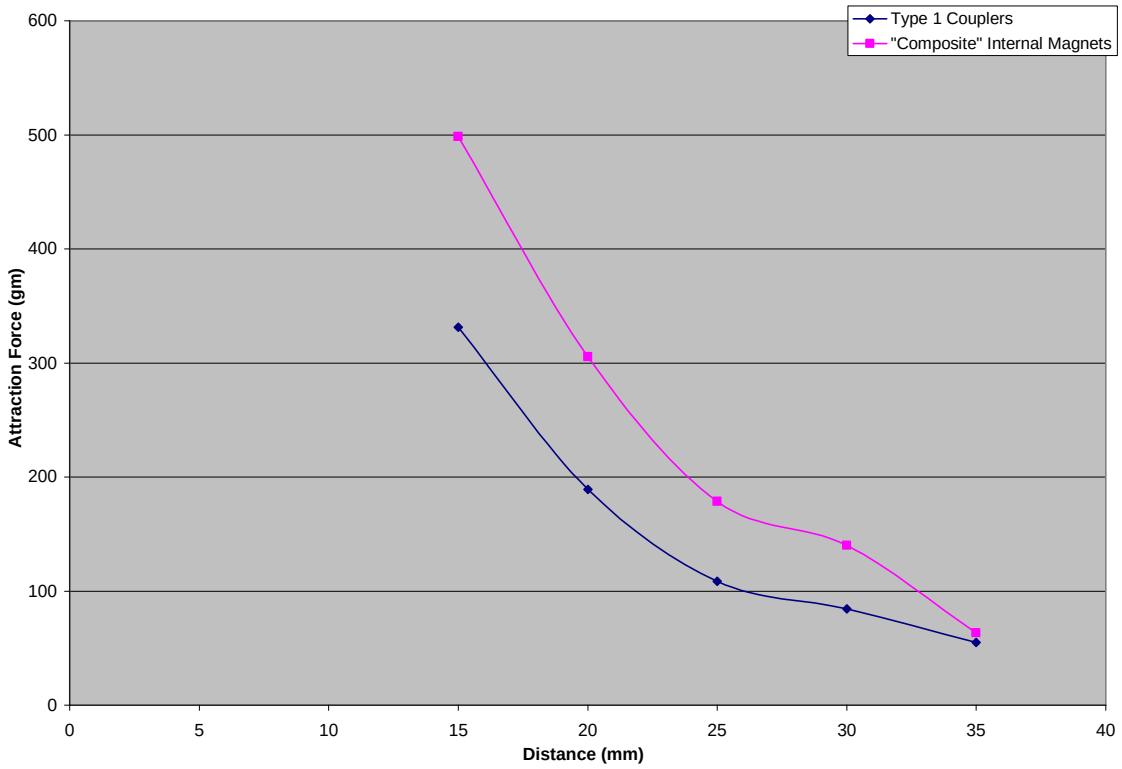

Figure 76. Magnetic force improvements. As shown, the implementation of the "composite" magnets results in shifting the capabilities of the magnetic couplers vertically (same distance, more force) and horizontally (same force, greater distance).

While the drive to make surgical, as well as industrial and consumer equipment smaller and easier to manipulate, unfortunately, the MAS equipment falls into a realm where the availability of technology and off-the-shelf components is extremely limited. Micro Electro-Mechanical devices (MEMs) are one of the latest trends, but are too small and/or do not deliver enough power to drive the intended surgical tools. Conventional or industrial equipment is too large for this use. Therefore, much of the equipment developed for this thesis had to be custom made or was purchased and

heavily modified. This has lead to limitations in features available for tools, frankly due to packaging problems.

CHAPTER 6

RECOMMENDATIONS FOR FUTURE WORK

This thesis is centered on the proving the basic concepts of the Magnetic Anchoring System, by developing functional magnetic couplers and rudimentary tools to demonstrate the possibilities of this technology. While there are multiple areas for future work, the magnetic couplers affect everything else, are the primary limiting factor to successful deployment, and thus define the most important area for future work.

While the current magnetic couplers have been successful in proving the technology, they are far from optimal for any patient attempted. They are capable of supporting tools like the camera and cauterizer out to tissue thicknesses of 30 millimeter (1.18 inch). However the magnets are not capable of generating sufficient coupling strength for tools like the retractors when they are heavily loaded by large or tightly constrained tissue. Two possibilities exist to enhance the magnetic attraction: composite magnets and magnetic focusing.

Analysis shows that the composite magnets will give a dramatic increase in lifting capacity, however more may be done to increase the coupling by employing magnetic focusing. This requires more study as well, since as stated earlier, if the magnetic field can be distorted to increase the field strength across the tissue, the lifting force will increase as well. Electromagnets were looked into as a possible mechanism for focusing, but sufficient magnetic field to disrupt the permanent magnets was not

developed, and the associated heating was counter productive. A concept that may prove more useful is the use of permanent magnets placed perpendicular to the magnet stack. According to simulation data, the local attraction force is noticeably increased by this means, but then drops off at greater distances. There may be a need for adjustments of these perpendicular magnets to increase the field at these distances.

The utility of the retractors would benefit greatly from an attraction force increase. While in testing the usefulness of the sling retractor was limited, a tool with this function may be more useful for other surgical procedures. As such, the medium between the anchors either needs to be a predetermined length of a semi rigid material, or an onboard adjustability allowing the tool to be sized on site, inside the body, must be devised. For the paddle retractor, a stronger coupling force is also required as well as a reduction in size. One possibility would be to make the paddle retractor an anchoring needle tool that is actuated so the onboard actuators are what cause the tissue to be manipulated, instead of repositioning the magnets. However, this defeats, in part, the attractiveness of the MAS mobility.

The camera would benefit greatly by reduction to the essential features required, lens and CCD array only, or minimal processing at the camera head location; it would also benefit by conversion to wireless function. Wireless function would eliminate the need for reinstalling a trocar port into the incision and would allow the camera more freedom of deployment than the current tool. Reducing the camera to the essential features would reduce weight as well as complexity making the tool more reliable and easier to package.

The pneumatic articulated arm could benefit from refinement of the motion of the arm, as well as by minimizing the length of the tool. While the articulated arm was designed around the constraints of conventional manufacturing practices, rapid prototyping machines are capable of parts that are "printed" rather than machined. As such, the constraints on part complexity could be eased and the tool reduced in size and weight, which would help with performance as well.

The Nitinol articulated arm would benefit greatly from dedicated development time. The second generation arm showed significant improvement in response time, and the concept of "over-gearing" may hold the key to making the Nitinol a more viable actuating modality. This concept could be used to develop a retractor tool capable of manipulating tissue, or simply a tool capable of higher forces than the pneumatics tools.

Like the development of the magnetic couplers, smaller more powerful actuators would be beneficial for the entire project. Currently, pneumatics have the advantage, but there may be the possibility of using low pressure hydraulics, in which saline solution may be a viable fluid. A relatively new technology, electro-active polymers, may also be useful for certain applications.

APPENDIX A

TEST STRUCTURE

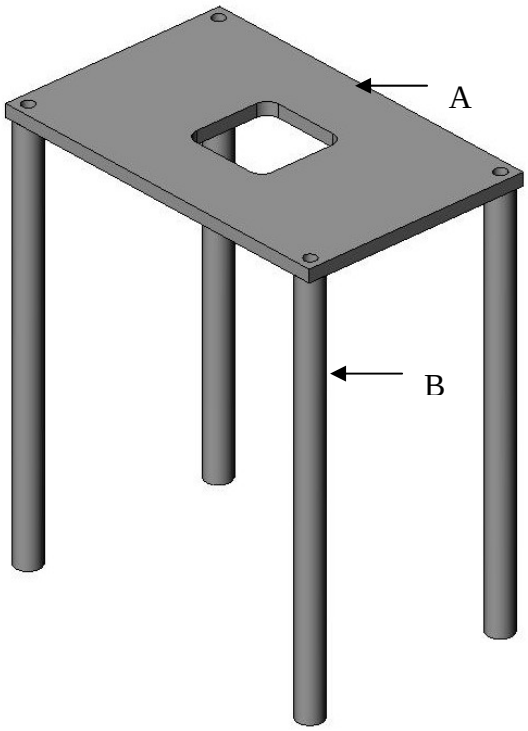

Figure 77. Test structure, assembly

- Misc.
    A. One piece 6061-T6 aluminum 178 by 114 by 6.4 millimeter (7 by 4.5 by 0.25 inch)
    B. Four pieces of 6061-T6 aluminum 12 millimeter (0.50 inch) in diameter by 203 millimeter (8 inch) long
- MSC
    C. Part number 05628052
        - 10-32 Button head cap screws, 12 millimeter (0.50 inch) in length (not shown)
        - 4 are required to secure the legs to the upper plate

APPENDIX B

ELECTROMAGNET PROTOTYPE

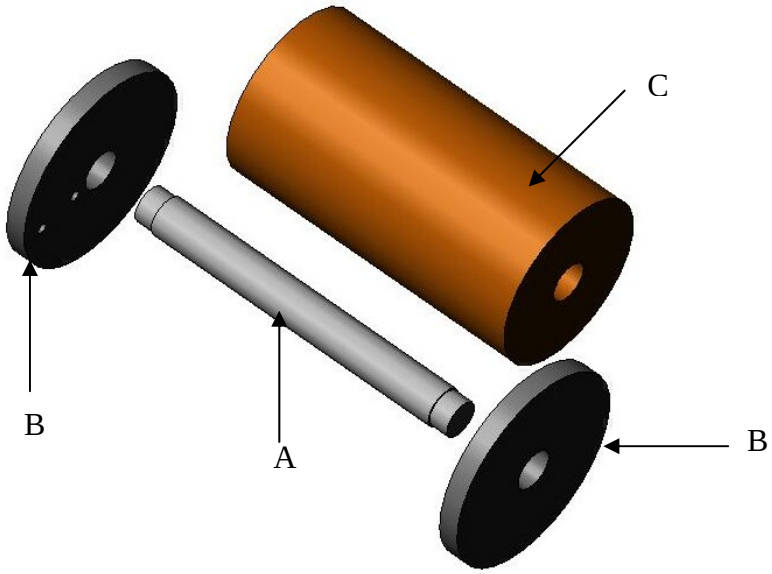

Figure 78. Electromagnet prototype, exploded view

- McMaster-Carr

  A. Part number 8920K15

     - AISI 1018 carbon steel rod, 12 millimeter (0.50 inch) in diameter by 1.8 meter (6 feet) long.
       - A piece of the rod was cut to a length of 114 millimeter (4.50 inch).
       - The ends of the rod was threaded with 7/16-20

  B. Part number 8572K32

     - ABS plastic rod, 63.5 millimeter (2.50 inch) in diameter by 304 millimeter (12 inch) long

- The rod was cut to make two plates, 58 millimeter (2.30 inch) in diameter by 6.4 millimeter (0.25 inch) thick.
- The plates have a hole in the center threaded for 7/16-20.
- There are 2, 3.3 millimeter (0.13 inch) diameter holes drilled in one of the plates. These holes are for the magnet wire to protrude out the top of the magnet.

C. Part number 7588K59

- 396 meter (1,300 feet) of AWG 22 magnet wire.

APPENDIX C

PERMANENT MAGNET TEST STRUCTURE

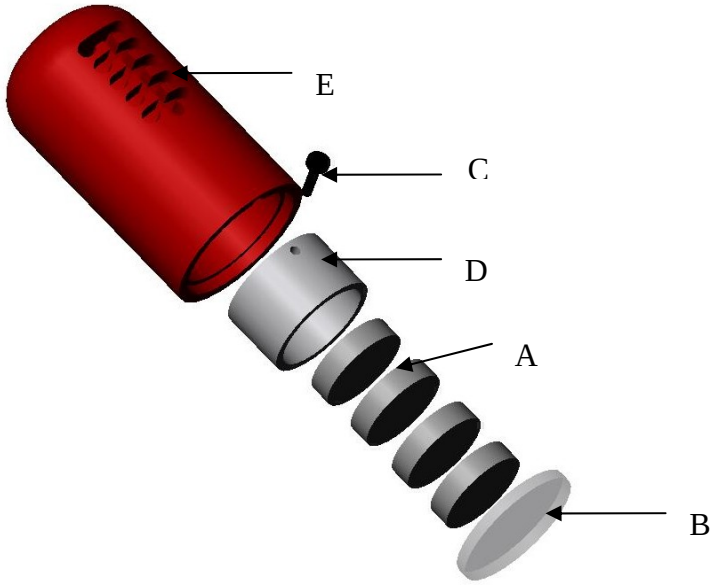

Figure 79. Permanent magnet test structure, exploded view

- Magnet Sales & Manufacturing

  A. Part number 35DNE6416-NI

    - NdFeB Grade 35, 25 millimeter (1 inch) diameter by 6.4 millimeter (0.25 inch) thick, nickel plated permanent magnets
      - Four of these magnets are required for the structure.

- McMaster-Carr

  B. Part number 8571K18

    - 38 millimeter (1.50 inch) diameter by 610 millimeter (24 inch) long clear lexan rod
      - This was cut down to a diameter of 37 millimeter (1.45 inch) by 3.3 millimeter (0.125 inch) thick.

- MSC

    C. Part number 01151414

        - The thumb screw used on the structure to hold the adjustment of the distance.

- Misc.

    D. Delrin Rod

        - The part requires a piece 31.8 millimeter (1.25 inch) in diameter by 19 millimeter (0.75 inch) long.

    E. Aluminum Rod

        - The part requires a piece 43.2 millimeter (1.70 inch) in diameter by 75 millimeter (3.0 inch) long.

APPENDIX D

PERMANENT MAGNET ENCLOSURE

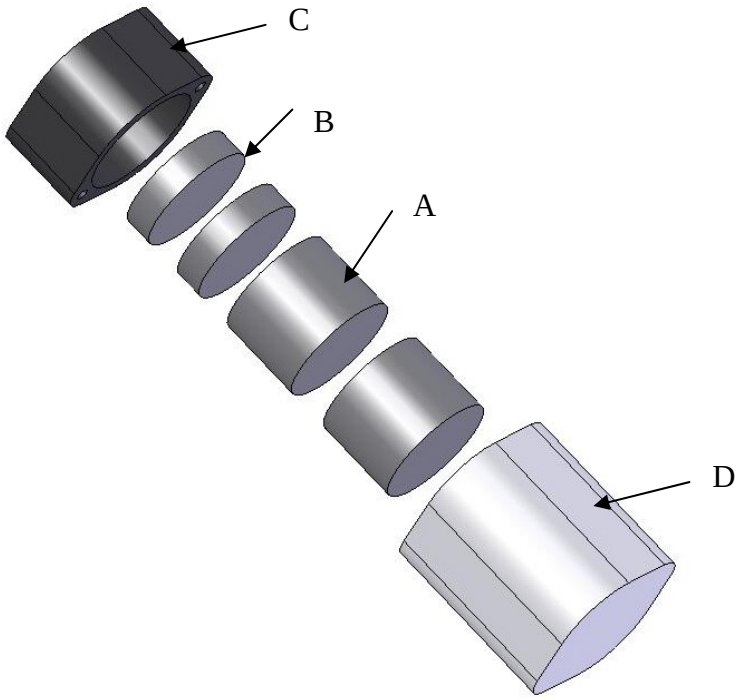

Figure 80. Type 1 external enclosure, exploded view

- Magnet Sales & Manufacturing

  A. Part number 35DNE6448

     - Two, NdFeB Grade 35, 25 millimeter (1 inch) diameter by 19 millimeter (0.75 inch) thick

  B. Part number 35DNE6416-NI

     - Two, NdFeB Grade 35, 25 millimeter (1 inch) diameter by 6.4 millimeter (0.25 inch) thick, nickel plated permanent magnets

- McMaster-Carr

  C. Part number 8920K311

- 38 millimeter (1.50 inch) diameter by 914 millimeter (36 inch) long AISI 1018 carbon steel rod.
    - A piece was machined per the drawing from this material.

- Misc.

D. One piece of delrin approximately 34 millimeter (1.35 inch) in diameter by 40 millimeter (1.57 inch) long

E. Two 4-40 socket head screws that are 25 millimeter (1.0 inch) in length (not shown)

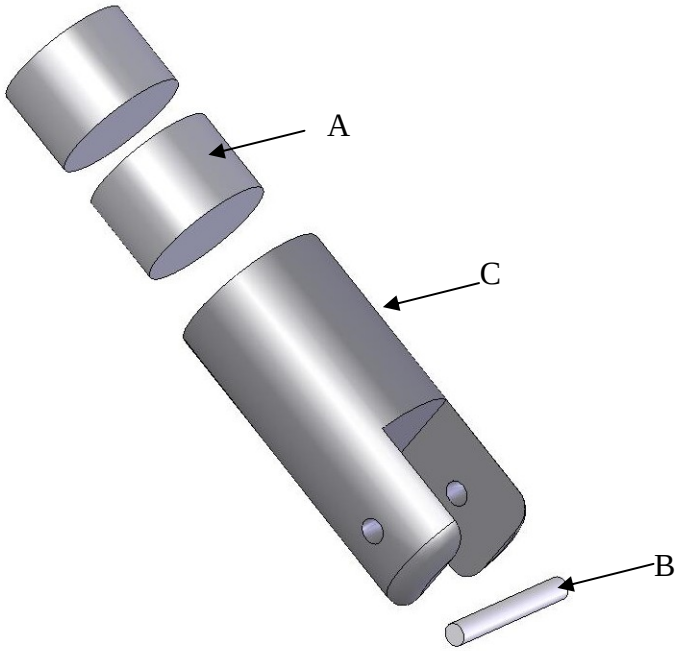

Figure 81. Type 1 internal enclosure, exploded view

- Magnet Sales & Manufacturing

  A. Part number 30DNE2416-NI

     - Two, NdFeB Grade 30, 9.5 millimeter (0.375 inch) diameter by 6.4 millimeter (0.25 inch) thick, nickel plated permanent magnets

- MSC

  B. Part number 60630050

     - 1.6 millimeter (0.063 inch) diameter by 12 millimeter (0.50 inch long) steel dowel pin

- Misc.

  C. One piece of 6061-T6 aluminum approximately 11.4 millimeter (0.45 inch) in diameter by 25 millimeter (1.0 inch long)

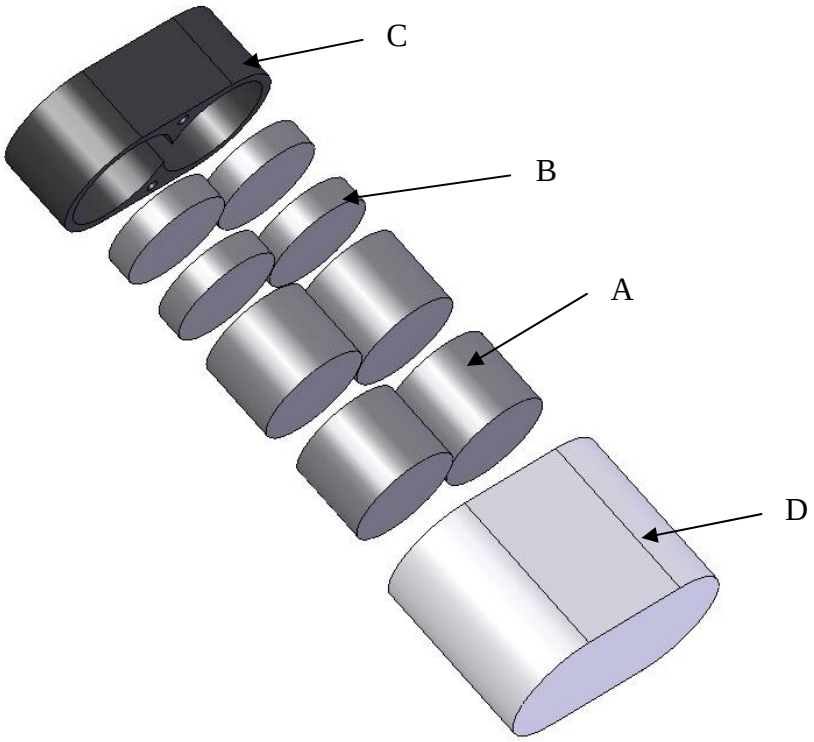

Figure 82. Type 2 external enclosure, exploded view

- Magnet Sales & Manufacturing

  A. Part number 35DNE6448

     - Four, NdFeB Grade 35, 25 millimeter (1 inch) diameter by 19 millimeter (0.75 inch) thick

  B. Part number 35DNE6416-NI

     - Four, NdFeB Grade 35, 25 millimeter (1 inch) diameter by 6.4 millimeter (0.25 inch) thick, nickel plated permanent magnets

- McMaster-Carr

  C. Part number 8920K311

- 38 millimeter (1.50 inch) diameter by 914 millimeter (36 inch) long AISI 1018 carbon steel rod.
    - A piece was machined per the drawing from this material.

- Misc.

D. One piece of delrin approximately 57 by 30 by 40 millimeter (2.25 by 1.20 by 1.57 inch)

E. Two 4-40 socket head screws that are 25 millimeter (1.0 inch) in length (not shown)

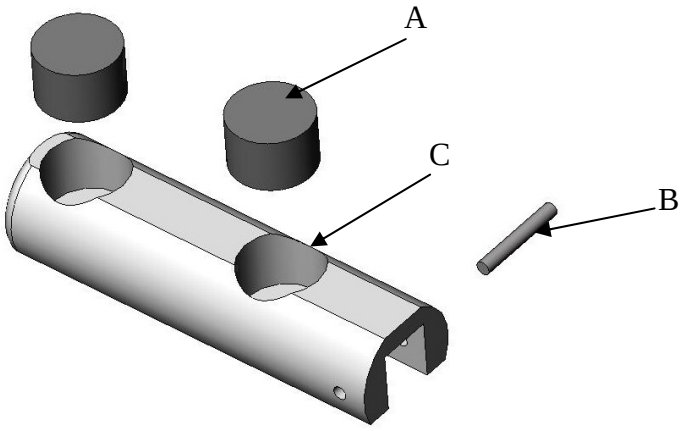

Figure 83. Type 2 internal enclosure, exploded view

- Magnet Sales & Manufacturing

  A. Part number 30DNE2416-NI

     - Two, NdFeB Grade 30, 9.5 millimeter (0.375 inch) diameter by 6.4 millimeter (0.25 inch) thick, nickel plated permanent magnets

- MSC

  B. Part number 60630050

     - 1.6 millimeter (0.063 inch) diameter by 12 millimeter (0.50 inch) long steel dowel pin

- Misc.

  C. One piece of 6061-T6 aluminum approximately 13.7 millimeter (0.54 inch) in diameter by 30 millimeter (1.18) inch long. Later anchors were made of Delrin with the same dimensions.

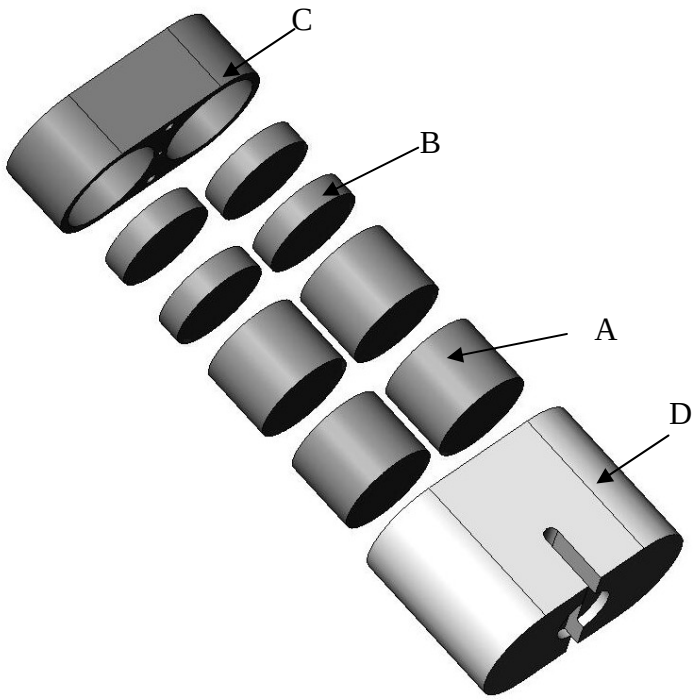

Figure 84. Type 3 external enclosure, exploded view

- Magnet Sales & Manufacturing

  A. Part number 35DNE6448

     - Four, NdFeB Grade 35, 25 millimeter (1 inch) diameter by 19 millimeter (0.75 inch) thick

  B. Part number 35DNE6416-NI

     - Four, NdFeB Grade 35, 25 millimeter (1 inch) diameter by 6.4 millimeter (0.25 inch) thick, nickel plated permanent magnets

- McMaster-Carr

  C. Part number 8920K311

- 38 millimeter (1.50 inch) diameter by 914 millimeter (36 inch) long AISI 1018 carbon steel rod.
    - A piece was machined per the drawing from this material.

- Misc.

D. One piece of delrin approximately 57 by 30 by 40 millimeter (2.25 by 1.20 by1.57 inch)

E. Two 4-40 socket head screws that are 25 millimeter (1.0 inch) in length (not shown)

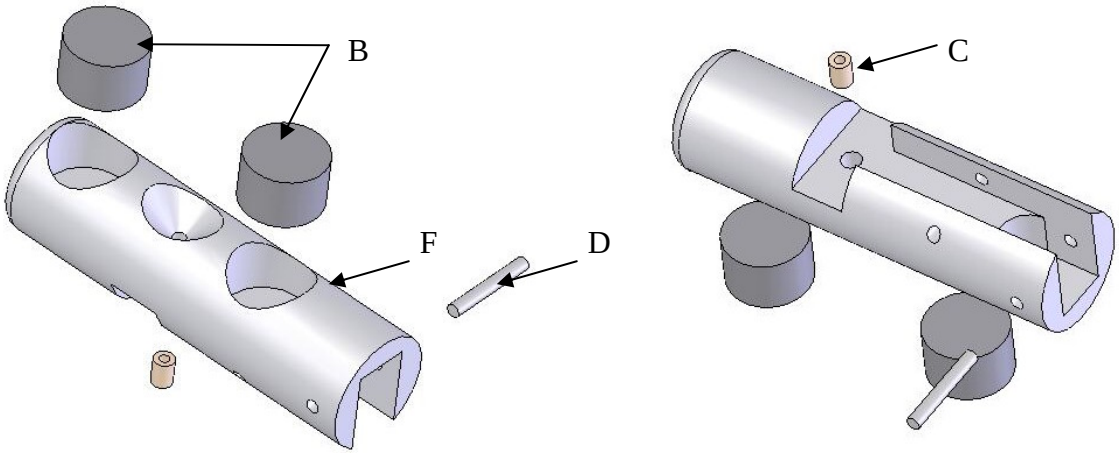

Figure 85. Type 3 internal enclosure, exploded view

- Becton Dickinson

  A. Part number 405184

  - 18 gauge x 89 millimeter (3.5 inch) spinal needles
    - The distal ends were ground flat and threaded with a 0-80 thread for use as the anchoring needles. (not shown)

- Magnet Sales & Manufacturing

  B. Part number 30DNE2416-NI

  - Two, NdFeB Grade 30, 9.5 millimeter (0.375 inch) diameter by 6.4 millimeter (0.25 inch) thick, nickel plated permanent magnets

- McMaster-Carr

  C. Part number 92395A109

  - 0-80 threaded brass insert

- MSC

    D. Part number 60630050

        - 1.6 millimeter (0.063 inch) diameter by 12 millimeter (0.50 inch) long steel dowel pin

- Small Parts

    E. Part number GWX-500-30

        - Stainless Steel Type 304, 1.27 millimeter (0.050 inch) diameter by 762 millimeter (30 inch) long
            - The wire was cut into 165 millimeter (6.50 inch) long sections with one end ground to a point and threaded with 0-80 thread for approximately 6.4 millimeter (0.25 inch). (not shown)

- Misc.

    F. One piece of delrin approximately 13.7 millimeter (0.54 inch) in diameter by 30 millimeter (1.18 inch) long.

APPENDIX E

SLING RETRACTOR

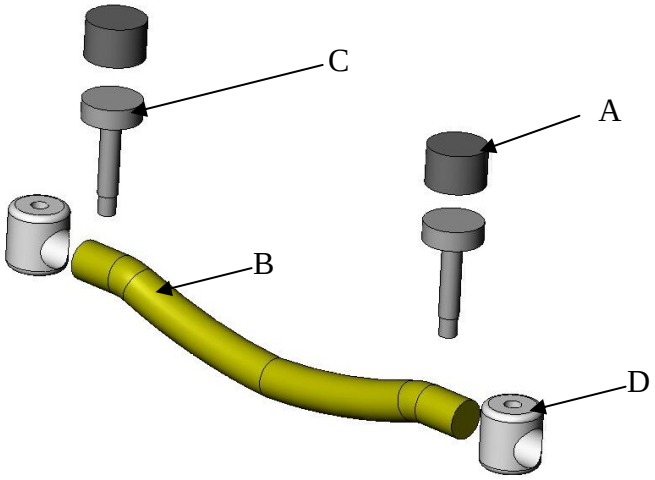

Figure 86. Sling retractor prototype, exploded view

- Magnet Sales & Manufacturing

  A. Part number 30DNE2416-NI

     - Two, NdFeB Grade 30, 9.5 millimeter (0.375 inch) diameter by 6.4 millimeter (0.25 inch) thick, nickel plated permanent magnets

- Primeline Industries

  B. Part number 011RA/RB

     - 15 meter (50 feet) of 3 millimeter (0.13 inch) inner diameter with a wall thickness of 0.8 millimeter (0.03125 inch) natural rubber tubing. The tubing used was amber, but the color does not matter.
       - The tubing was cut to a 76 millimeter (3.0 inch) length.

- Misc.
    C. Two pieces of 6061-T6 aluminum 9.5 millimeter (0.375 inch) in diameter by 19 millimeter (0.75 inch) in length
    D. Two pieces of 6061-T6 aluminum 9.5 millimeter (0.375 inch) in diameter by 10 millimeter (0.40 inch) in length

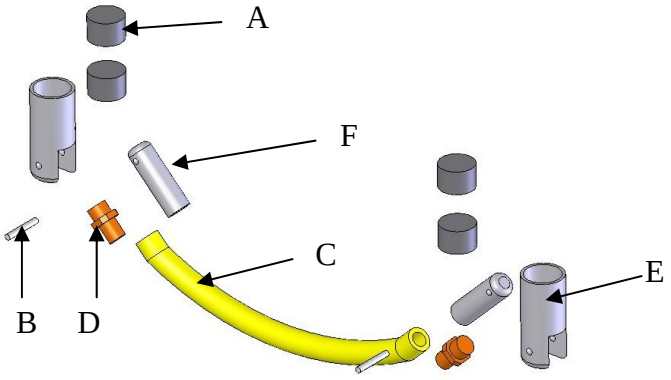

Figure 87. Sling retractor revision r, exploded view

- Magnet Sales & Manufacturing

  A. Part number 30DNE2416-NI

     - Four, NdFeB Grade 30, 9.5 millimeter (0.375 inch) diameter by 6.4 millimeter (0.25 inch) thick, nickel plated permanent magnets

- MSC

  B. Part number 60630050

     - Two, 1.6 millimeter (0.063 inch) in diameter by 12 millimeter (0.50 inch) long dowel pin

- Primeline Industries

  C. Part number 011RA/RB

     - 15 meter (50 feet) of 3.2 millimeter (0.125 inch) inner diameter with a wall thickness of 0.80 millimeter (0.0313 inch) natural rubber tubing. The tubing used was amber, but the color does not matter.

- The tubing was cut to a 76 millimeter (3.0 inch) length.

- Wilson

D. Part number MP2MCB1N

- Two brass barb fittings for 3.2 millimeter (0.125 inch) inner diameter tubing with a 10-32 thread

- Misc.

E. Two pieces of 6061-T6 aluminum 11 millimeter (0.44 inch) in diameter by 24 millimeter (0.95 inch) in length

F. Two pieces of 6061-T6 aluminum 6.4 millimeter (0.25 inch) in diameter by 19 millimeter (0.75 inch) in length

APPENDIX F

PADDLE RETRACTOR

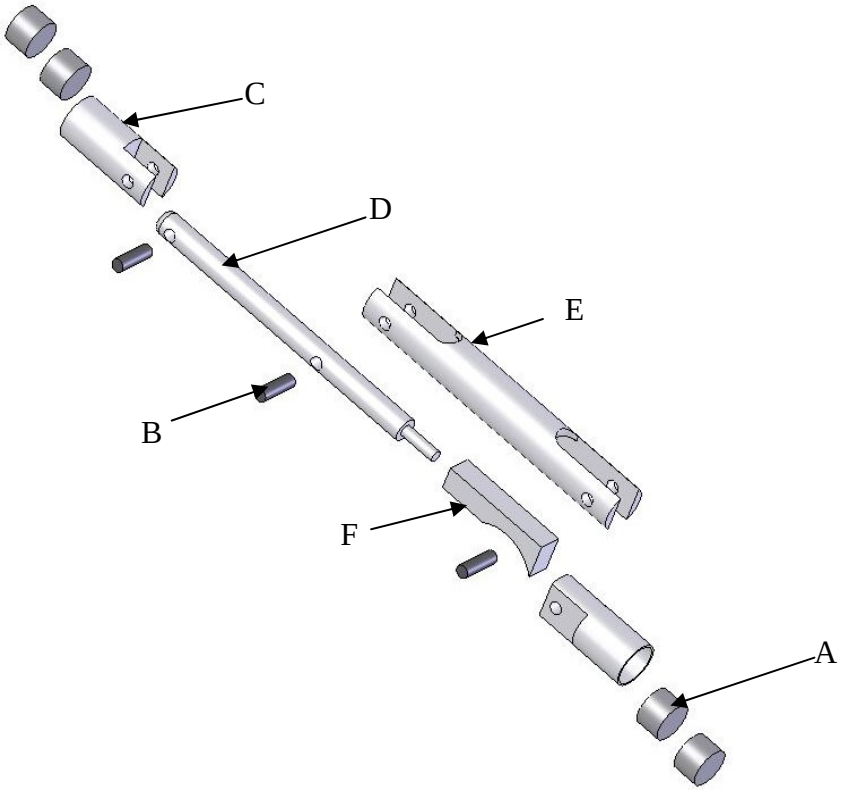

Figure 88. Paddle retractor prototype, exploded view

- Magnet Sales & Manufacturing

  A. Part number 30DNE2416-NI

     - Four, NdFeB Grade 30, 9.5 millimeter (0.375 inch) diameter by 6.4 millimeter (0.25 inch) thick, nickel plated permanent magnets

- MSC

  B. Part number 06022057

     - Three, 3 millimeter (0.125 inch) in diameter by 12 millimeter (0.50 inch) long dowel pins

- Misc.

    C. Two pieces of 6061-T6 aluminum 11 millimeter (0.44 inch) in diameter by 25 millimeter (1.0 inch) in length

    D. One piece of 6061-T6 aluminum 6.4 millimeter (0.25 inch) in diameter by 86 millimeter (3.375 inch) in length

    E. One piece of 6061-T6 aluminum 11 millimeter (0.44 inch) in diameter by 76 millimeter (3.0 inch) in length

    F. One piece of 6061-T6 aluminum 5.8 by 9 by 29 millimeter (0.23 by 0.355 by 1.125 inch)

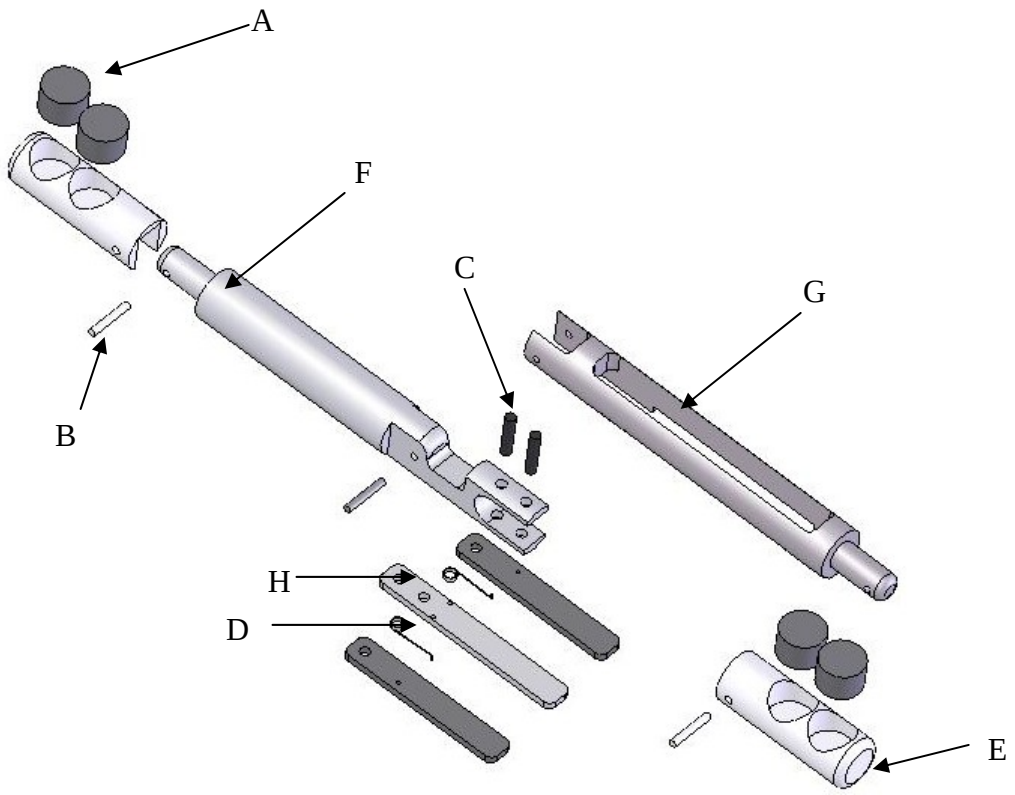

Figure 89. Paddle retractor revision b, exploded view

- Magnet Sales & Manufacturing

  A. Part number 30DNE2416-NI

     - Four, NdFeB Grade 30, 9.5 millimeter (0.375 inch) diameter by 6.4 millimeter (0.25 inch) thick, nickel plated permanent magnets

- MSC

  B. Part number 60630050

     - Three, 1.6 millimeter (0.063 inch) in diameter by 12 millimeter (0.50 inch) long dowel pins

C. Part number 05502059

- Two, socket head cap screw, 2-56 thread, 12 millimeter (0.50 inch) long

- Misc.

D. Two standard 3.5 inch floppy discs. More specifically, the torsion spring that is used to hold the dust shield over the magnetic medium.

E. Two pieces of 6061-T6 aluminum 10 millimeter (0.40 inch) in diameter by 32 millimeter (1.25 inch) in length

F. One piece of 6061-T6 aluminum 11 millimeter (0.44 inch) in diameter by 89 millimeter (3.50 inch) in length

G. One piece of 6061-T6 aluminum 11 millimeter (0.44 inch) in diameter by 95 millimeter (3.75 inch) in length

H. Three pieces of 6061-T6 aluminum 6 by 1.6 by 44 millimeter (0.24 by 0.063 by 1.75 inch)

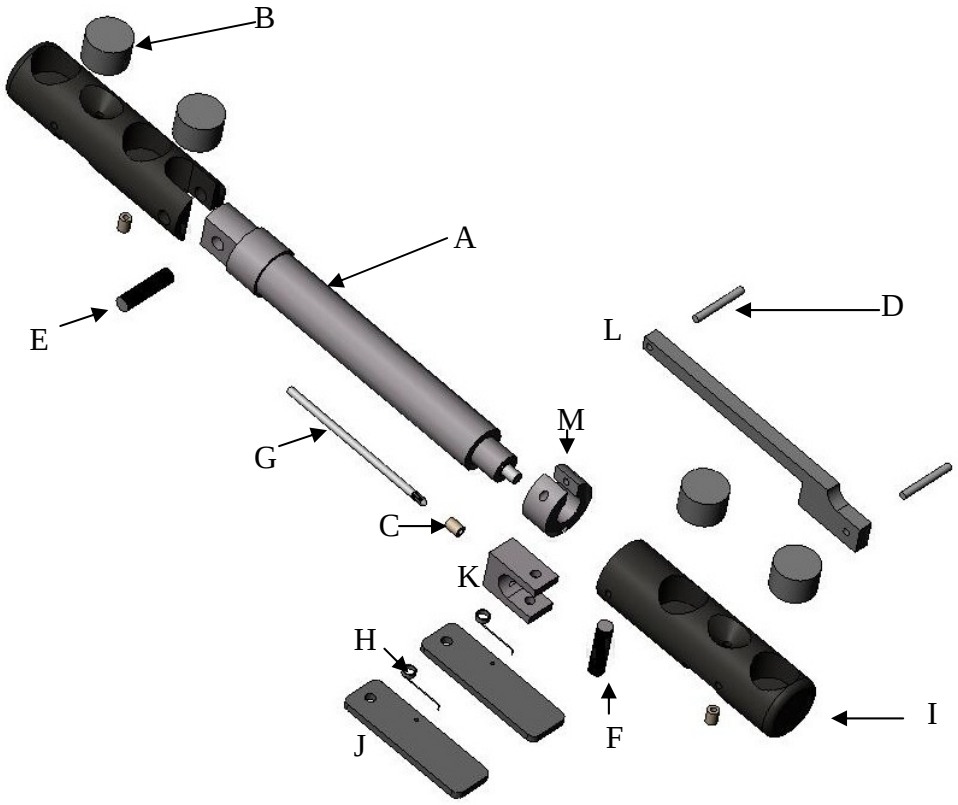

Figure 90. Paddle retractor revision c, exploded view

- Bimba

  A. Part number 0071-XP

     - Single acting, spring return, rear pivot, 5/16 inch bore, 1 inch stroke

- Magnet Sales & Manufacturing

  B. Part number 30DNE2416-NI

     - Four, NdFeB Grade 30, 9.5 millimeter (0.375 inch) diameter by 6.4 millimeter (0.25 inch) thick, nickel plated permanent magnets

- McMaster-Carr
    C. Part number 92395A109
        - Three, 0-80 threaded brass inserts
- MSC
    D. Part number 60630050
        - Two, 1.6 millimeter (0.063 inch) in diameter by 12 millimeter (0.50 inch) long dowel pins
    E. Part number 06022057
        - One, 3 millimeter (0.125 inch) in diameter by 12 millimeter (0.50 inch) long dowel pin
    F. Part number 05502059
        - One, socket head cap screw, 2-56 thread, 12 millimeter (0.50 inch) long
- Small Parts
    G. Part number GWX-500-30
        - Stainless Steel Type 304, 1.3 millimeter (0.050 inch) diameter by 762 millimeter (30 inch) long
            - The wire was cut into a 38 millimeter (1.50 inch) long section and used as a guide pin

- Misc.

H. Two standard 3.5 inch floppy discs. More specifically, the torsion spring that is used to hold the dust shield over the magnetic medium.

I. Two pieces of delrin 13.7 millimeter (0.54 inch) in diameter by 48 millimeter (1.88 inch) in length

J. Two pieces of delrin 9.7 by 1.5 by 32 millimeter (0.38 by 0.06 by 1.25 inch)

K. One piece of delrin 6.4 by 12 by 9.7 millimeter (0.25 by 0.50 by 0.38 inch)

L. One piece of 6061-T6 aluminum 9.5 by 3 by 60 millimeter (0.375 by 0.125 by 2.375 inch)

M. One piece of 6061-T6 aluminum 12 millimeter (0.50 inch) in diameter by 6.4 millimeter (0.25 inch) in length

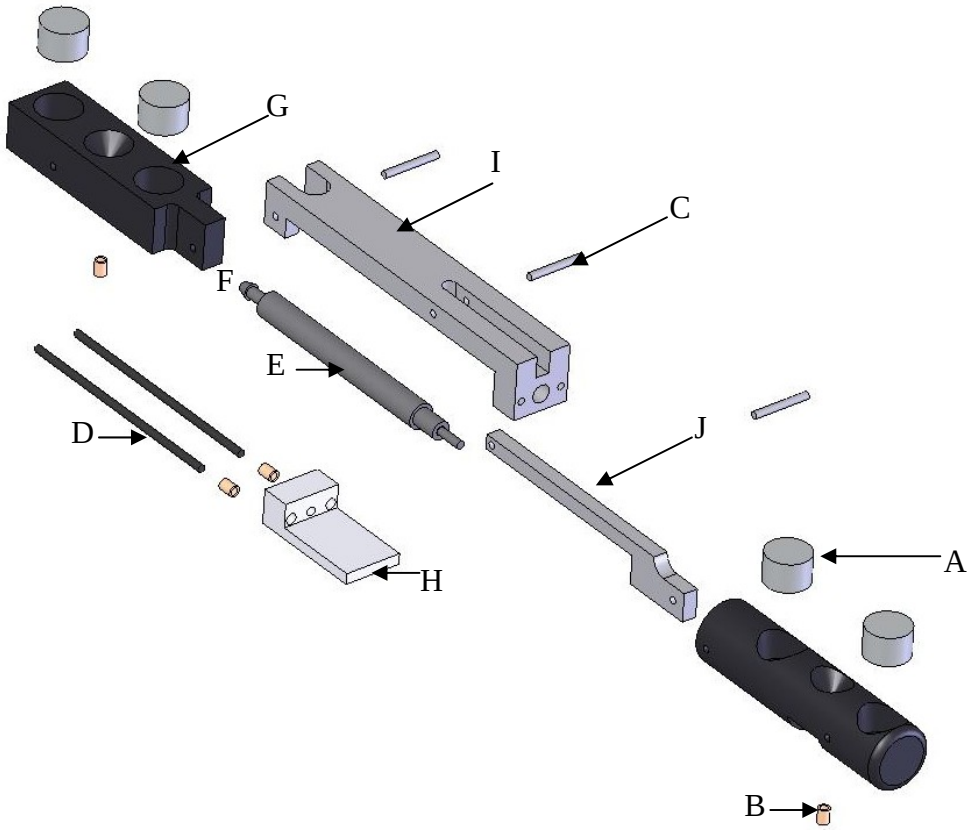

Figure 91. Paddle retractor revision d, exploded view

- Magnet Sales & Manufacturing

  A. Part number 30DNE2416-NI

     - Four, NdFeB Grade 30, 9.5 millimeter (0.375 inch) diameter by 6.4 millimeter (0.25 inch) thick, nickel plated permanent magnets

- McMaster-Carr

  B. Part number 92395A109

     - Four, 0-80 threaded brass inserts

- MSC
    C. Part number 60630050
        - Three, 1.6 millimeter (0.063 inch) in diameter by 12 millimeter (0.50) inch long dowel pins
- Small Parts
    D. Part number GWX-500-30
        - Stainless Steel Type 304, 1.3 millimeter (0.050 inch) diameter by 762 millimeter (30 inch) long
            - The wire was cut into two, 38 millimeter (1.50 inch) long sections and used as a guide pins
- SMC
    E. Part number CJ1B4-20SU4
        - Single acting, spring return, 4 millimeter bore, 20 millimeter stroke
    F. Part number M-3AU-2
        - 2 millimeter fitting
- Misc.
    G. Two pieces of delrin 13.7 millimeter (0.54 inch) in diameter by 54 millimeter (2.13 inch) in length
    H. One piece of delrin 7.6 by 12 by 25 millimeter (0.30 by 0.50 by 1.0 inch)

I. One piece of delrin 12 by 12 by 76 millimeter (0.50 by 0.50 by 3.0 inch)

J. One piece of 6061-T6 aluminum 9.5 by 3 by 60 millimeter (0.375 by 0.125 by 2.375 inch)

APPENDIX G

CAMERA SYSTEM

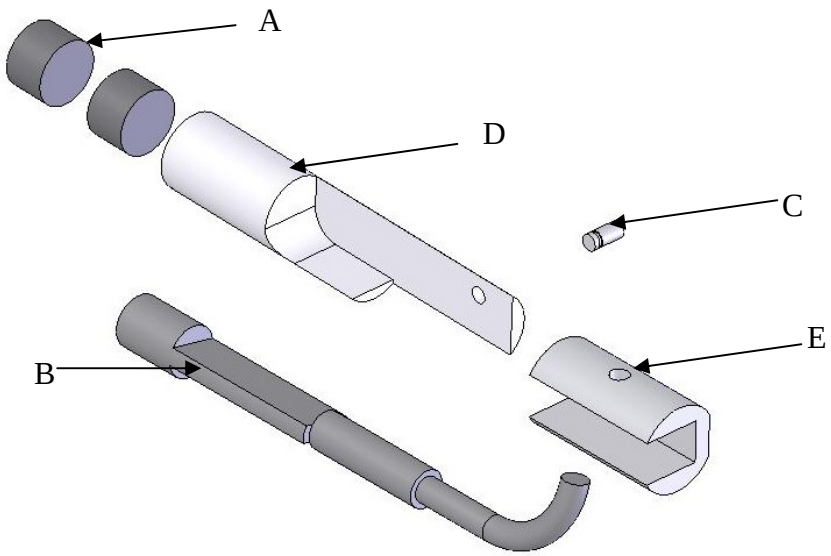

Figure 92. Camera stand prototype, exploded view

- Magnet Sales & Manufacturing

  A. Part number 30DNE2416-NI

     - Two, NdFeB Grade 30, 9.5 millimeter (0.375 inch) diameter by 6.4 millimeter (0.25 inch) thick, nickel plated permanent magnets

- Micro Video Products

  B. Part number MVC-Snake-1

     - 7 millimeter (0.28 inch) in diameter camera head with 305 millimeter (12 inch tether)

- MSC

  C. Part number 06021059

     - One, 2.4 millimeter (0.094 inch) in diameter by 12 millimeter (0.50 inch) long dowel pin

- Misc.

    D. One piece of 6061-T6 aluminum 11 millimeter (0.44 inch) in diameter by 57 millimeter (2.25 inch) long

    E. One piece of 6061-T6 aluminum 12 millimeter (0.50 inch) in diameter by 22 millimeter (0.88 inch) long

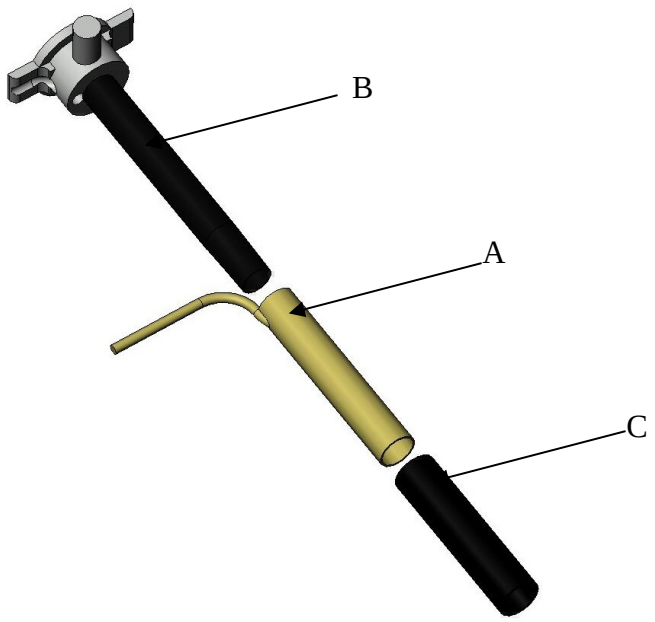

Figure 93. Trocar light, exploded view

- Edmund Optics

  A. Part number NT02-533

     - 0.75 millimeter (0.030 inch) diameter, unjacketed, 9.4 meter (31 feet)
        - The fiber was cut into 61, 152 millimeter (6 inch) long pieces

- United States Surgical

  B. Part number 179071

     - VERSAPORT RPF 5 mm-12 mm Trocar with 100 mm Radiolucent Sleeve

  C. Part number 179078

- VERSAPORT RPF 10 mm-15 mm Trocar with 100 mm Radiolucent Sleeve

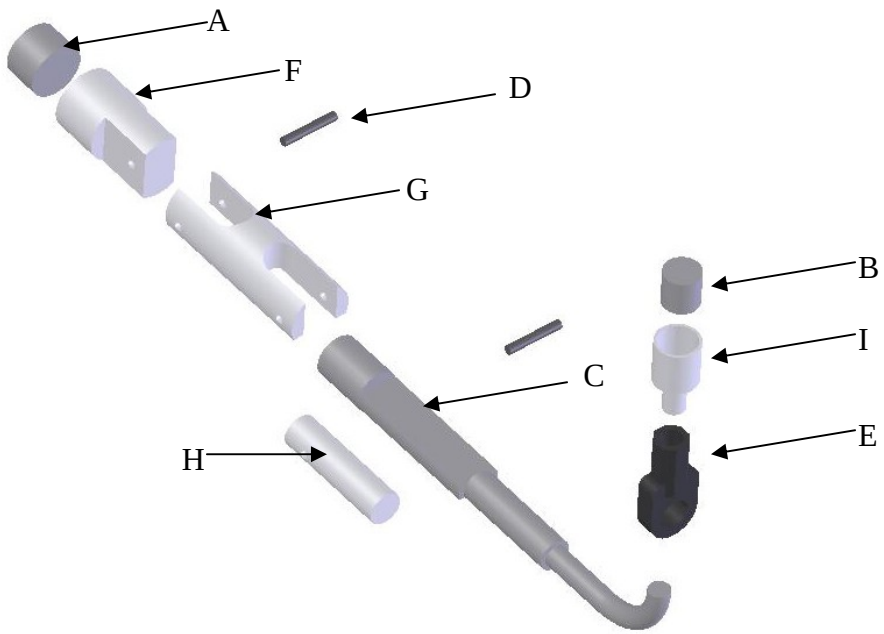

Figure 94. Camera stand revision b, exploded view

- Magnet Sales & Manufacturing
  - A. Part number 30DNE2416-NI
    - One, NdFeB Grade 30, 9.5 millimeter (0.375 inch) diameter by 6.4 millimeter (0.25 inch) thick, nickel plated permanent magnet
  - B. Part number 35DNE1616-NI
    - One, NdFeB Grade 35, 6.4 millimeter (0.25 inch) diameter by 6.4 millimeter (0.25 inch) thick, nickel plated permanent magnet
- Micro Video Products
  - C. Part number MVC-Snake-1

- 7 millimeter (0.28 inch) in diameter camera head with 305 millimeter (12 inch) tether

- MSC

D. Part number 60630050

- Two, 1.6 millimeter (0.063 inch) in diameter by 12 millimeter (0.50 inch) long dowel pins

- Traxxas

E. Part number 2742

- Traxxas rod ends with connectors, LS2
  - One of the nylon rod ends was used with a cut in it to allow for the camera cable to be passed through it

- Misc.

F. One piece of 6061-T6 aluminum 11 millimeter (0.44 inch) in diameter by 19 millimeter (0.75 inch) long

G. One piece of 6061-T6 aluminum 11 millimeter (0.44 inch) in diameter by 32 millimeter (1.25 inch) long

H. One piece of 6061-T6 aluminum 5.8 millimeter (0.23 inch) in diameter by 22 millimeter (0.85 inch) long

I. One piece of 6061-T6 aluminum 7.6 millimeter (0.30 inch) in diameter by 14 millimeter (0.56 inch) long

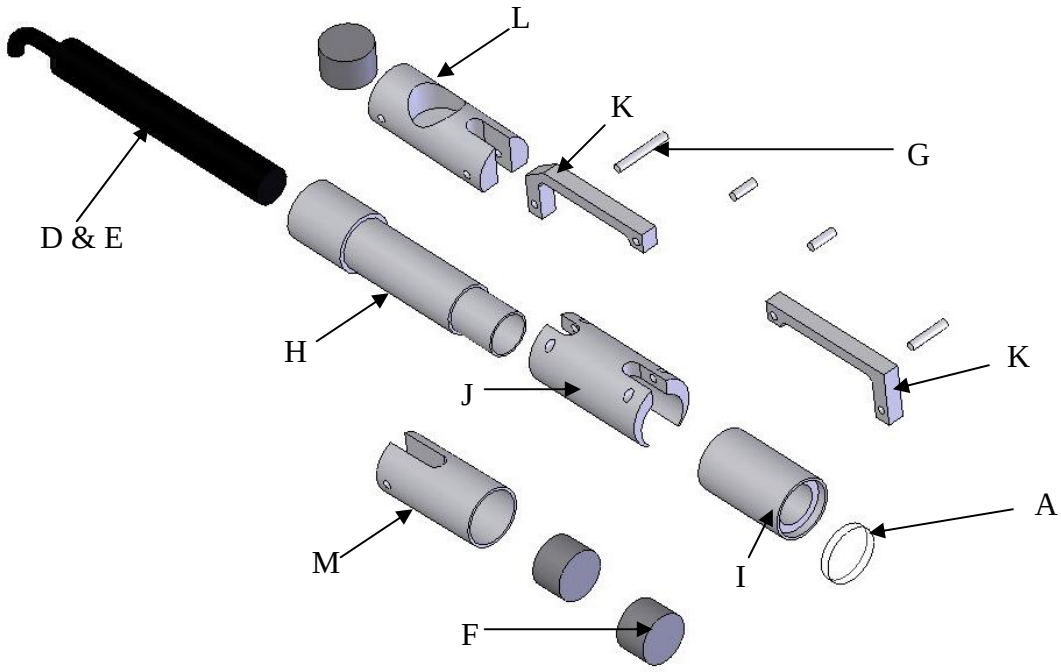

Figure 95. Camera stand revision c, exploded view

- Edmund Optics

  A. Part number NT45-630

     - 10 millimeter (0.39 inch) in diameter by 2 millimeter (0.08 inch) thick window

- Elmo Co., LTD.

  B. Part number 9658

     - CC421E camera controller

  C. Part number 8920-AD1

     - AC-E12A AC adapter for camera controller

  D. Part number 9657

     - QN42H camera head

E. Part number 9813

- Super-micro camera lens, 1:2.8, f = 8 millimeter

- Magnet Sales & Manufacturing

F. Part number 30DNE2416-NI

- Three, NdFeB Grade 30, 9.5 millimeter (0.375 inch) diameter by 6.4 millimeter (0.25 inch) thick, nickel plated permanent magnet

- MSC

G. Part number 60630050

- Four, 1.6 millimeter (0.063 inch) in diameter by 12 millimeter (0.50 inch) long dowel pins

- Misc.

H. One piece of 6061-T6 aluminum 11 millimeter (0.44 inch) in diameter by 48 millimeter (1.9 inch) long

I. One piece of 6061-T6 aluminum 11.7 millimeter (0.46 inch) in diameter by 19 millimeter (0.75 inch) long

J. One piece of 6061-T6 aluminum 12 millimeter (0.50 inch) in diameter by 25 millimeter (1.0 inch) long

K. Two pieces of 6061-T6 aluminum 11 by 29 by 3 millimeter (0.44 by 1.125 by 0.125 inch)

L. One piece of 6061-T6 aluminum 11 millimeter (0.44 inch) in diameter by 27 millimeter (1.063 inch) long

M. One piece of 6061-T6 aluminum 11 millimeter (0.44 inch) in diameter by 22 millimeter (0.88 inch) long

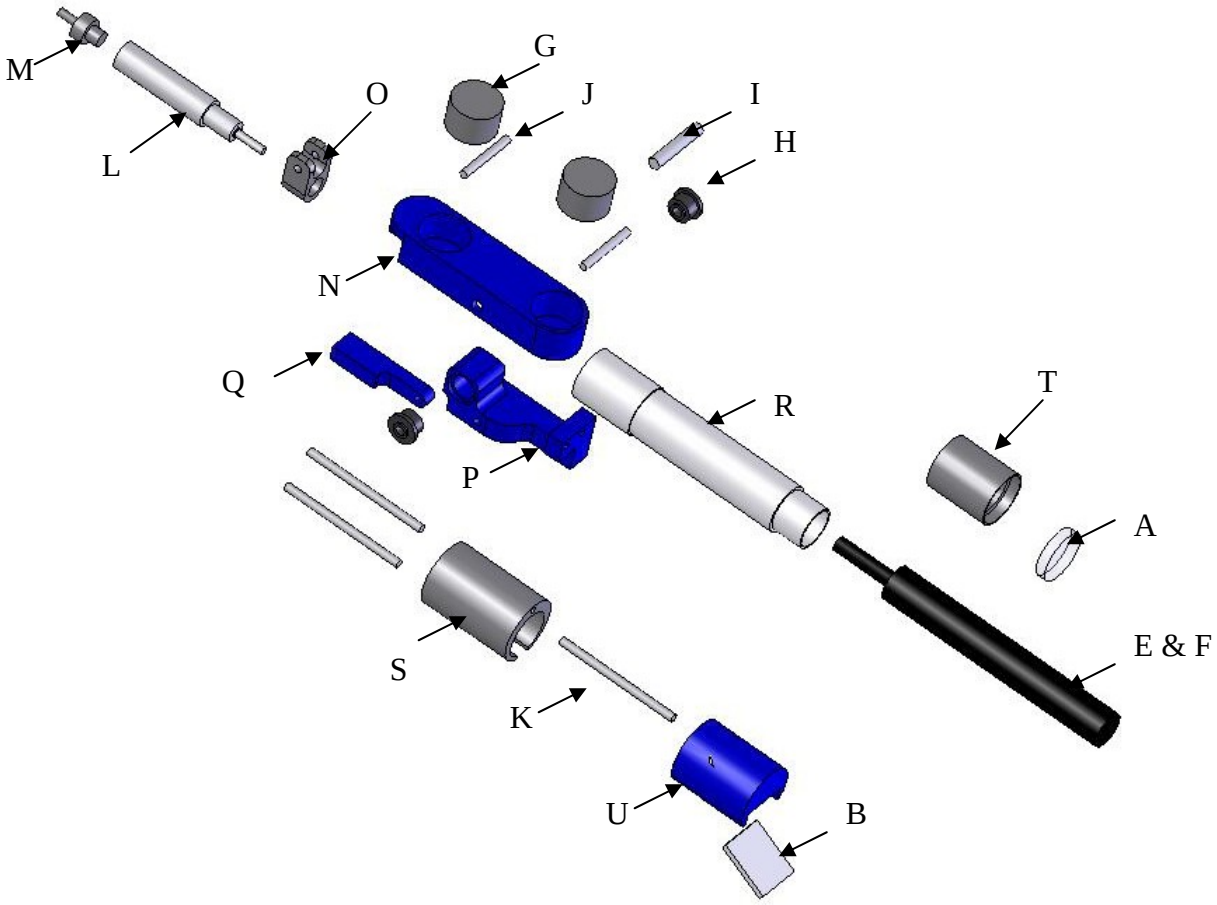

Figure 96. Camera stand revision d, exploded view

- Edmund Optics

  A. Part number NT45-630

     - 10 millimeter (0.39 inch) in diameter by 2 millimeter (0.08 inch) thick window

  B. Part number NT31-418

     - 9.5 millimeter (0.37 inch) by 11.2 millimeter (0.44 inch) rectangular mirror.

- Elmo Co., LTD.
    C. Part number 9658
        - CC421E camera controller
    D. Part number 8920-AD1
        - AC-E12A AC adapter for camera controller
    E. Part number 9657
        - QN42H camera head
    F. Part number 9812
        - Super-micro camera lens, 1:2.5, f = 4 millimeter
- Magnet Sales & Manufacturing
    G. Part number 30DNE2416-NI
        - Two, NdFeB Grade 30, 9.5 millimeter (0.375 inch) diameter by 6.4 millimeter (0.25 inch) thick, nickel plated permanent magnet
- McMaster Carr
    H. Part number 57155K13
        - Miniature precision stainless steel ball bearing, ABEC-5, standard shield, extended inner ring.
            - 2.4 millimeter (0.094 inch) internal diameter, 4.8 millimeter (0.188 inch) outer diameter
            - Two of these bearings were used.

- MSC
    I. Part number 06021059
        - One, 2.4 millimeter (0.094 inch) in diameter by 12 millimeter (0.50 inch) long dowel pins
    J. Part number 60630050
        - Two, 1.6 millimeter (0.063 inch) in diameter by 12 millimeter (0.50 inch) long dowel pins
- Small Parts
    K. Part number GWX-500-30
        - Stainless Steel Type 304, 1.3 millimeter (0.050 inch) diameter by 762 millimeter (30 inch) long
            - The wire was cut into a 44 millimeter (1.75 inch) long section and was threaded with 0-80 for 6.4 millimeter (0.25 inch) on both ends.
            - The wire was cut into two, 22 millimeter (0.88 inch) long sections and was threaded with 0-80 for 6.4 millimeter (0.25 inch) on both ends
- SMC
    L. Part number CJ1B4-10SU4
        - Single acting, spring return, 4 millimeter bore, 10 millimeter stroke
    M. Part number M-3AU-2

        - 2 millimeter fitting

- Misc.

    N. One piece of delrin 7 by 11 by 41 millimeter (0.28 by 0.44 by 1.63 inch)

    O. One piece of 6061-T6 aluminum 5 by 13 by 6.4 millimeter (0.20 by 0.52 by 0.25 inch)

    P. One piece of delrin 10 by 25 by 9.5 millimeter (0.40 by 1.0 by 0.38 inch)

    Q. One piece of delrin 5 by 3 by 21 millimeter (0.20 by 0.13 by 0.83 inch)

    R. One piece of 6061-T6 aluminum 10 millimeter (0.40 inch) in diameter by 50 millimeter (2.0 inch) long

    S. One piece of 6061-T6 aluminum 12 millimeter (0.50 inch) in diameter by 19 millimeter (0.75 inch) long

    T. One piece of 6061-T6 aluminum 11 millimeter (0.42 inch) in diameter by 12 millimeter (0.50 inch) long

    U. One piece of delrin 12 millimeter (0.50 inch) in diameter by 16 millimeter (0.63 inch) long

APPENDIX H

CONTROL BOX

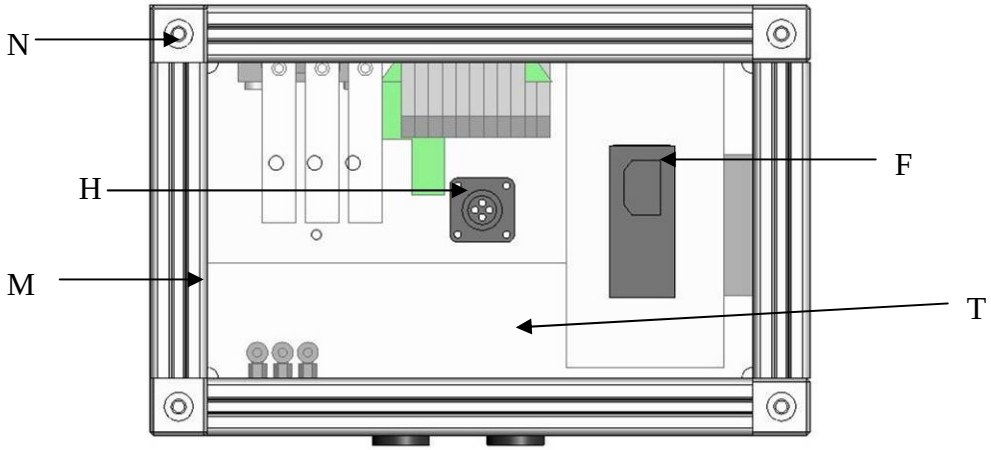

Figure 97. Power entry side

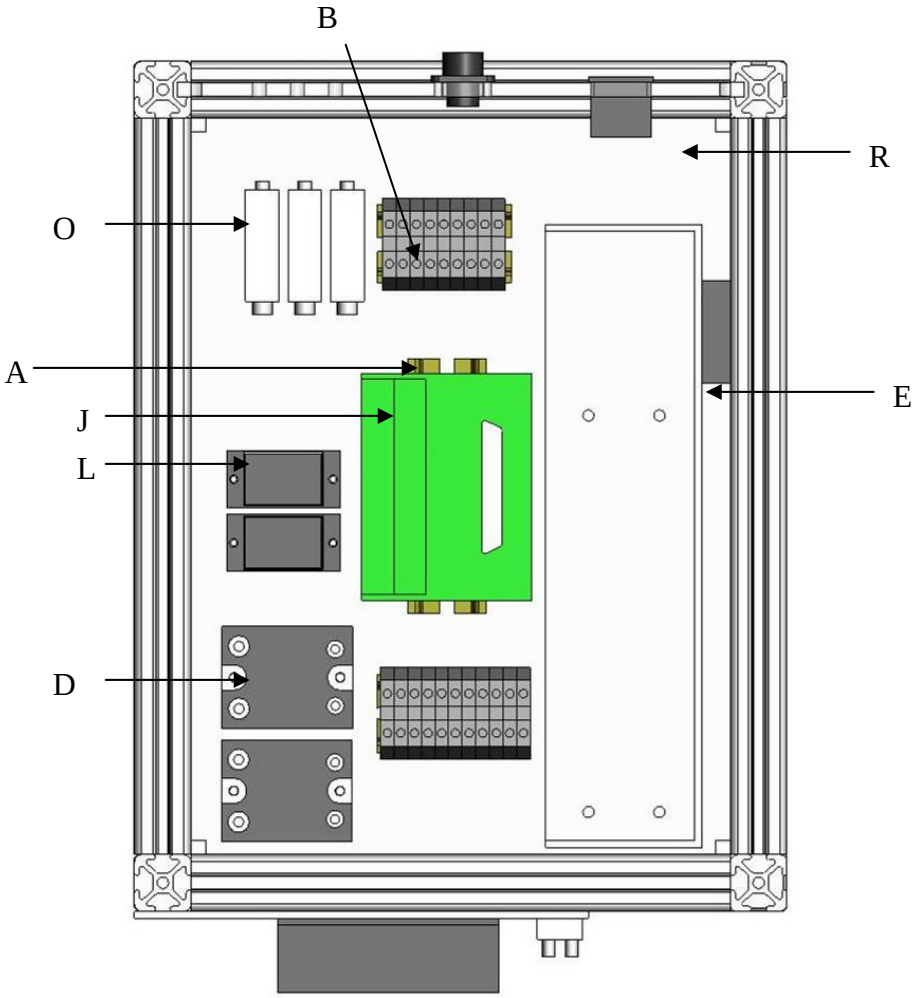

Figure 98. Top view

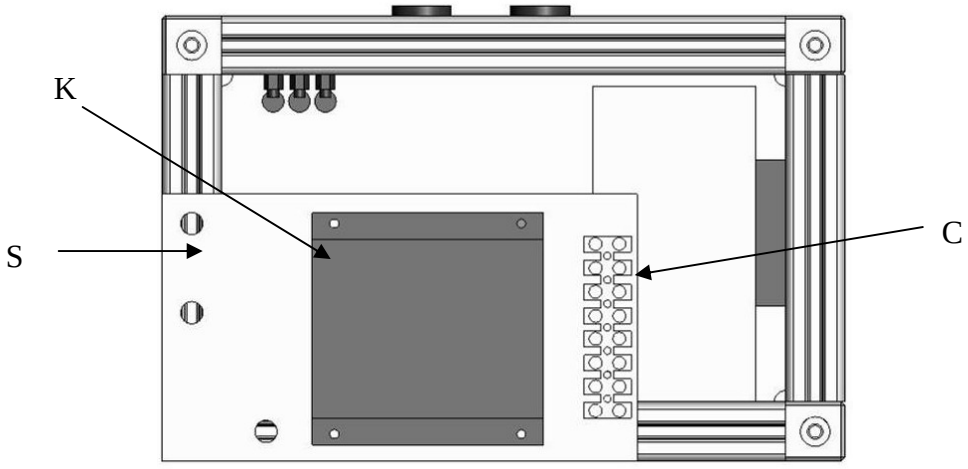

Figure 99. Motor amplifier side

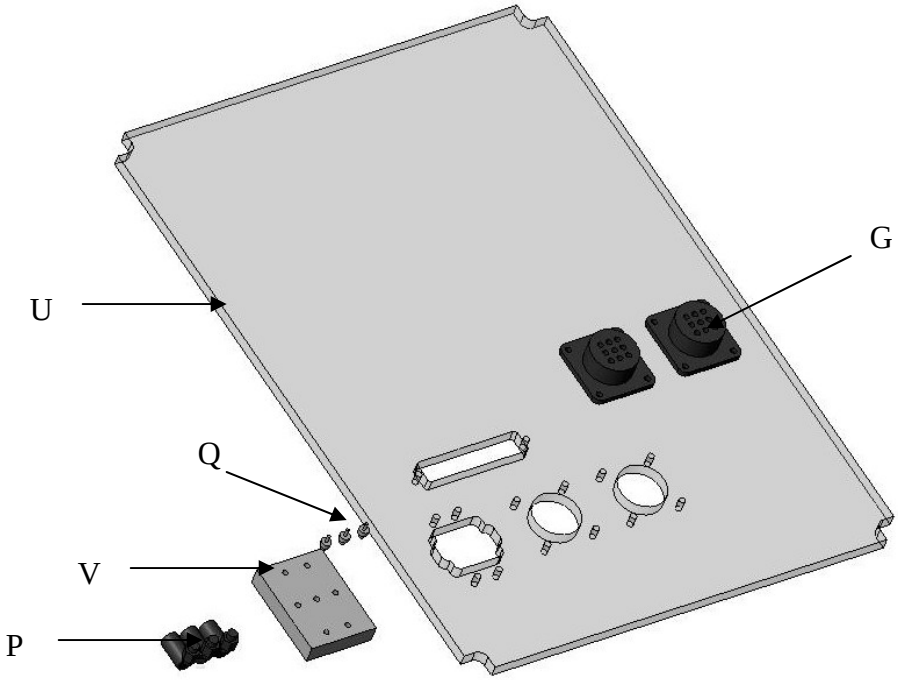

Figure 100. Top cover

- Allied Electronics
    A. Part number 502-0156
        - DIN rail, 3 pieces cut to 69 millimeter (2.7 inch) long, 60 millimeter (2.38 inch) long and 114 millimeter (4.5 inch) long
    B. Part number 502-3742
        - Terminal block, 21 needed
    C. Part number 924-0120
        - Terminal strip, 1 needed
    D. Part number 682-0075
        - Relay, 2 needed
    E. Part number 218-1066
        - 5, 12 and 24 Vdc power supply
    F. Part number 689-5214
        - Power entry block
    G. Part number 512-8872
        - 9-pin AMP connector, 2 needed
    H. Part number 512-1150
        - 4-pin AMP connector, 1 needed
- Cyber Research
    I. Part number PCCDAC 08

- 8 channel D/A PCMCIA card

J. Part number unknown

- D/A card breakout box

- Maxon Motor

K. Part number 4-Q-DC

- Motor amplifier

- Robohand

L. Part number APA-1005

- Trans-conduction amplifier, 2 needed

- Shepherd Controls

M. Part number 8020-1010

- Four, 330 millimeter (13 inch) long
  - All ¼-20 threaded 12 millimeter (0.50 inch) deep on both ends
- Four, 241 millimeter (9.5 inch) long
  - All ¼-20 threaded 12 millimeter (0.50 inch) deep on both ends
- Four, 140 millimeter (5.5 inch) long
  - All ¼-20 threaded 12 millimeter (0.50 inch) deep on both ends

N. Part number 8020-4042

- Corner blocks, 8 needed

- SMC
    O. Part number ITV0030-2S
        - Pressure regulator, 3 are needed
    P. Part number KQ2L04-M5
        - Swivel elbow, 3 are needed
    Q. Part number M-3AU-2
        - 2 millimeter fitting, 3 are needed
- Misc.
    R. One 6061-T6 aluminum plate 343 by 250 by 3 millimeter (13.5 by 10 by 0.125 inch)
    S. One 6061-T6 aluminum plate 114 by 203 by 3 millimeter (4.5 by 8 by 0.125 inch)
    T. One plexiglass plate 152 by 250 by 6.4 millimeter (6.0 by 10 by 0.25 inch)
    U. One plexiglass plate 343 by 250 by 6.4 millimeter (13.5 by 10 by 0.25 inch)
    V. One 6061-T6 aluminum plate 38 by 50 by 6.4 millimeter (1.5 by 2.0 by 0.25 inch)
    W. Logitech Wingman Cordless Joystick, RF 2.4 (not shown)

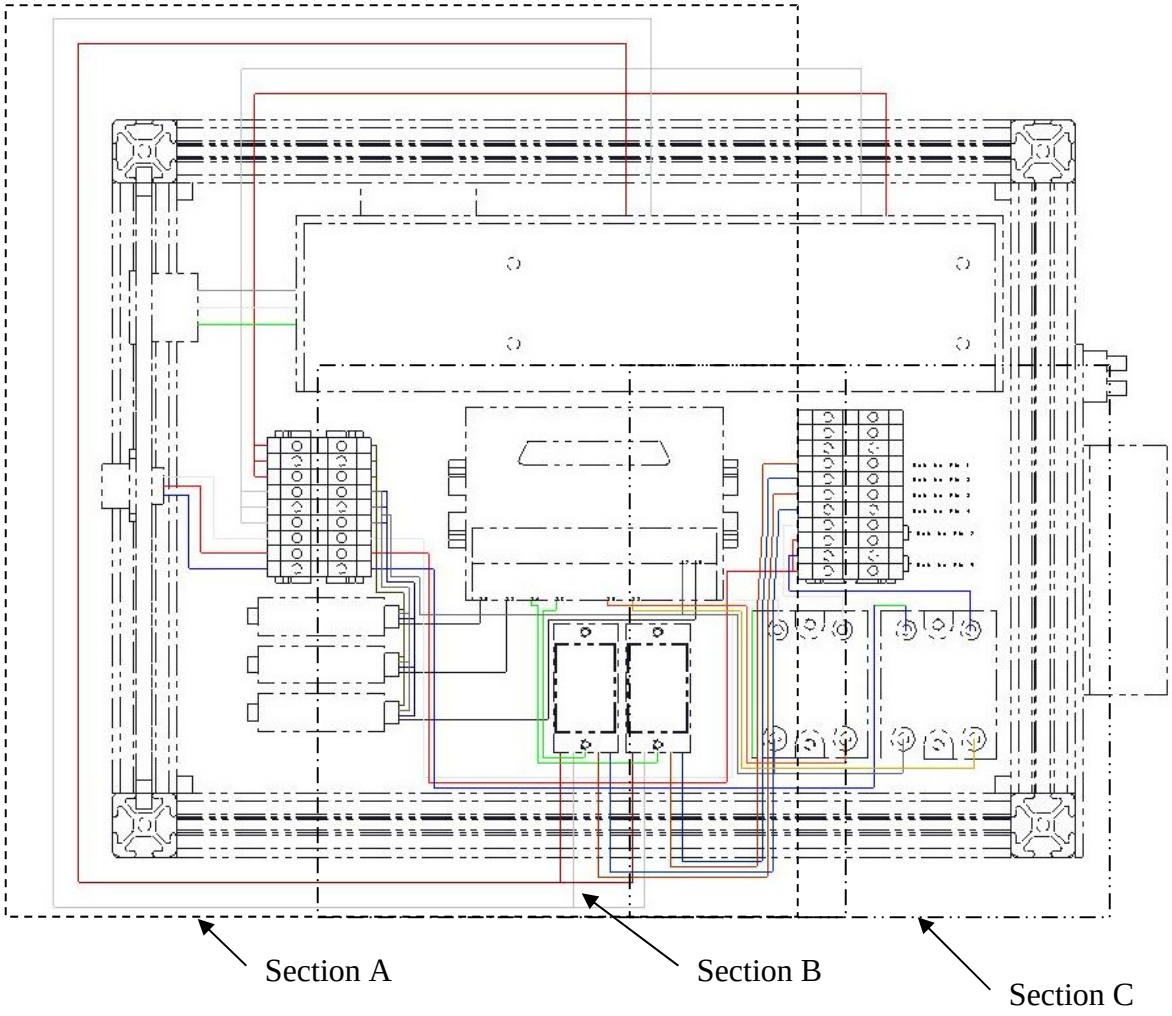

Figure 101. Wiring diagram overview

Table 1. Wiring number and function

Wire Number	Section	Description
1	A	5 or 12 Vdc Negative
2	A	5 or 12 Vdc Positive
3	A	24 Vdc Negative
4	A	24 Vdc Positive
5	A	AC Black
6	A	AC White
7	A	AC Ground. Attaches to base plate as well.
8	A	Cauterizer, white wire
9	A	Cauterizer, red wire
10	A	Cauterizer, blue wire
11	A	Pressure regulator positive power
12	A	Pressure regulator negative power
13	A	Wire used for common ground between power supply and controller
14	B	Command signal for pressure regulator 1
15	B	Command signal for pressure regulator 2
16	B	Command signal for trans-conduction amplifier 1
17	B	Command signal for trans-conduction amplifier 2
18	B	Command signal for relay 1
19	B	Command signal for relay 2
20	B	Common ground for box and controller
21	B	Command signal for pressure regulator 3
22	B	Trans-conduction amplifier 1, positive out
23	B	Trans-conduction amplifier 1, negative out
24	B	Trans-conduction amplifier 2, positive out
25	B	Trans-conduction amplifier 2, negative out
26	C	Output to Pin 1, used for Nitinol wire 1
27	C	Output to Pin 2, used for Nitinol wire 1
28	C	Output to Pin 3, used for Nitinol wire 2
29	C	Output to Pin 4, used for Nitinol wire 2
30	C	Output to Pin 7. Cauterizer's red and white wire are brought together
31	C	Output to Pin 9. Cauterizer's red and blue wire are brought together

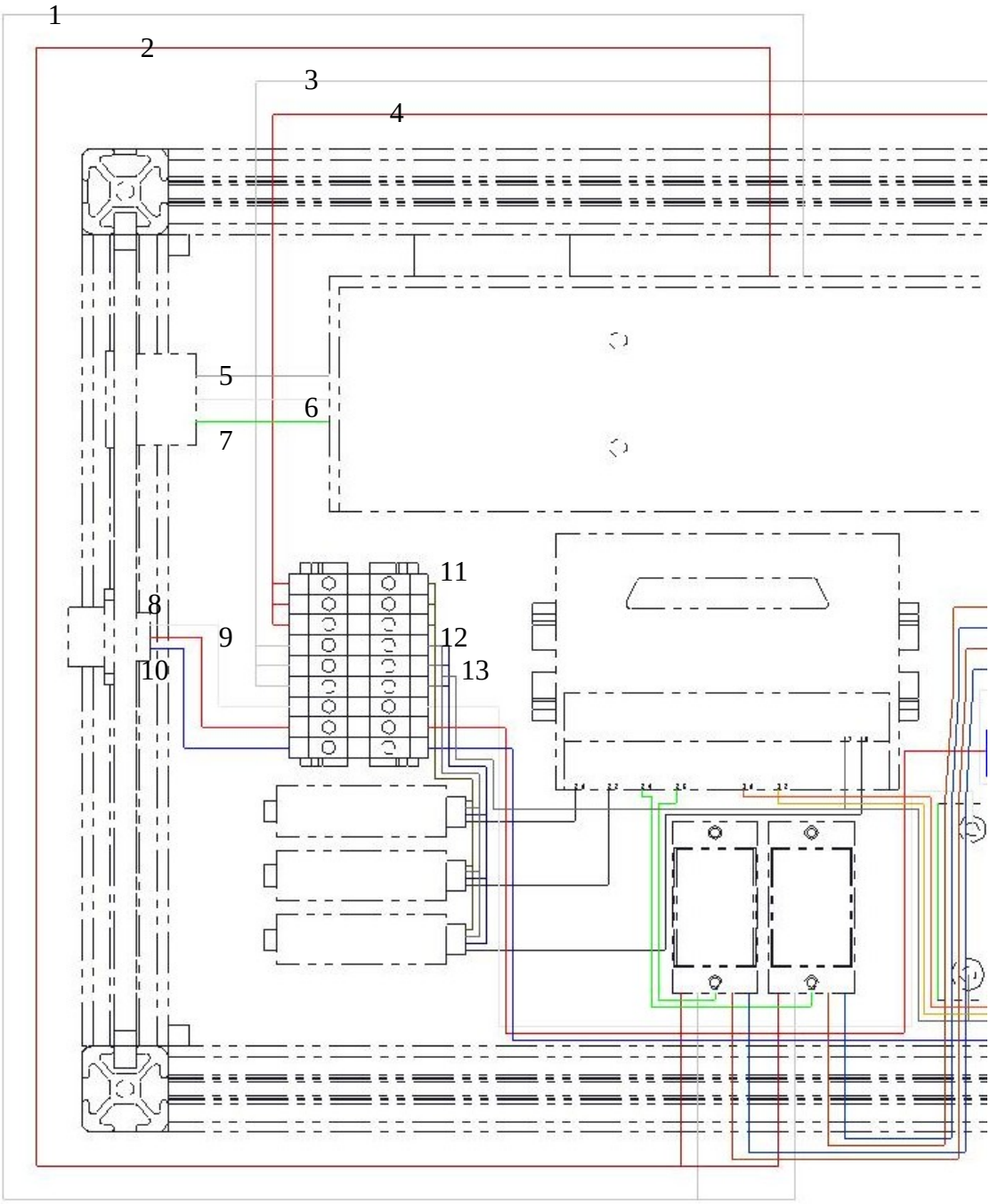

Figure 102. Wiring diagram, section a

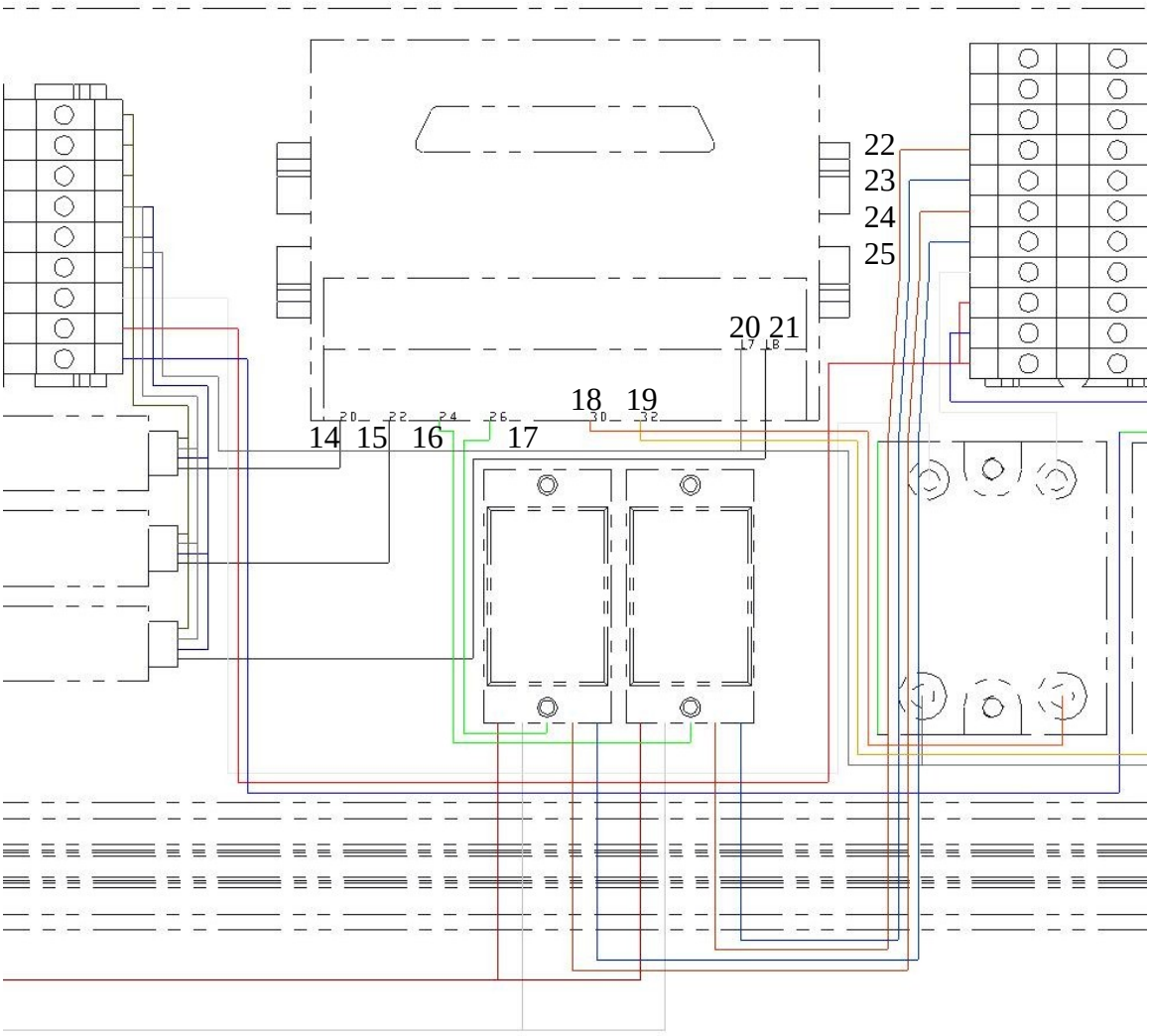

Figure 103. Wiring diagram, section b

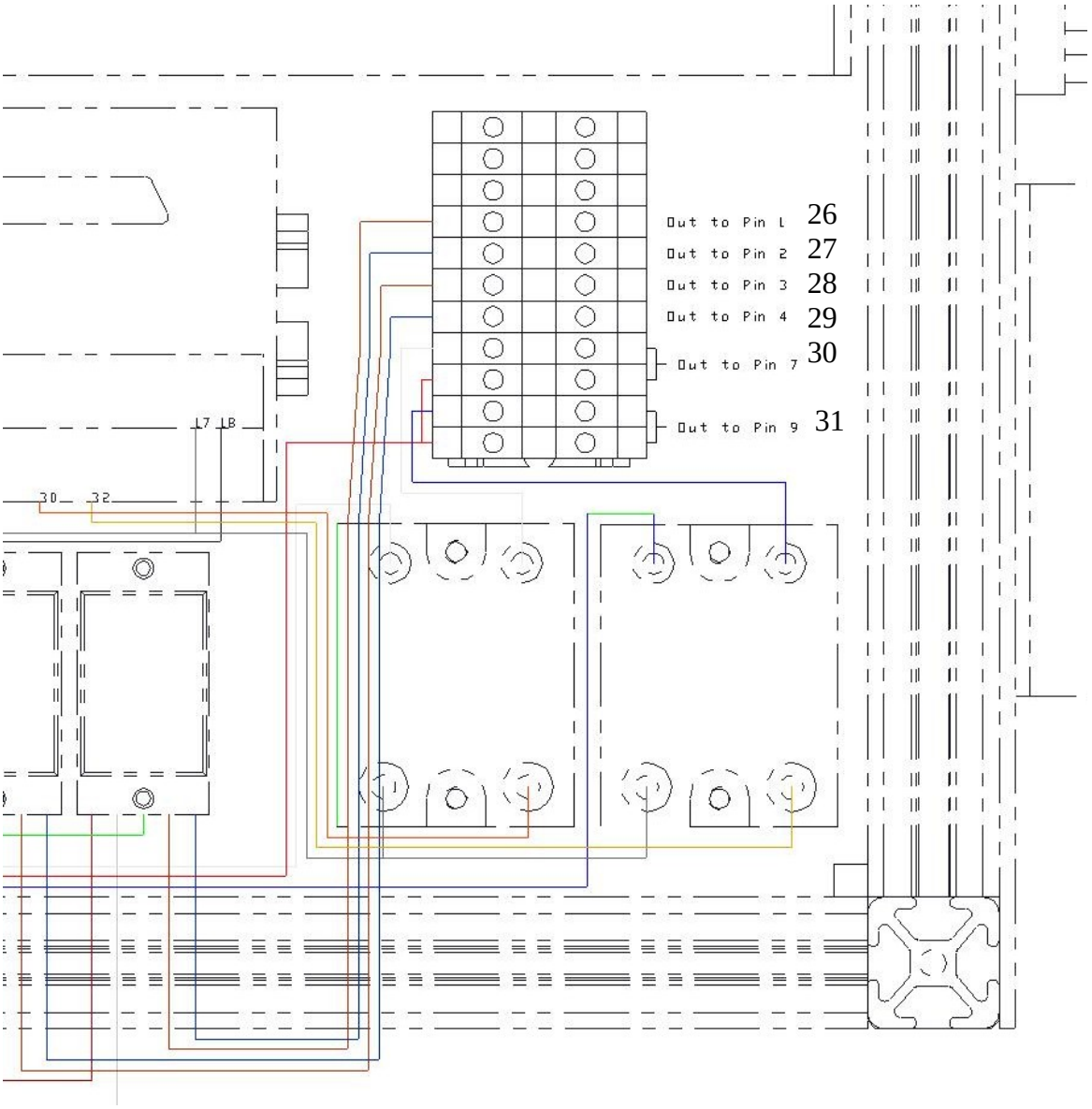

Figure 104. Wiring diagram, section c

```
'============================================================
'   MAS Control Box Program
'   Written:  12/22/03 by R. Bergs
'   Last Update 05/26/04
'
'   Using a USB Joystick, the surgeon can manipulate either the pneumatic
' arm, or the Nitinol arm, and control the cauterizer.  The joystick
' functions are connected with DirectX version 8, or at least the SDK.  The
' SDK MUST be installed for this program to work.  It can be downloaded from
' Mircrosoft.
'
'============================================================
'
' Setup some info for the joystick.  Not sure what they do, but are required
'
        Dim dx As New DirectX8
        Dim di As DirectInput8
        Dim diDev As DirectInputDevice8
        Dim diDevEnum As DirectInputEnumDevices8
        Dim joyCaps As DIDEVCAPS
        Dim js As DIJOYSTATE
        Dim DiProp_Dead As DIPROPLONG
```

```
        Dim DiProp_Range As DIPROPRANGE
        Dim DiProp_Saturation As DIPROPLONG
'
' Setup program specific variables, constants
'
        Private Arm As Integer              ' Choice variable, determines which arm to
                                              activate
        Private JointOneCom As Integer      ' Command from joystick as pressure
        Private JointTwoCom As Integer      ' Command from joystick as pressure
        Private JointThreeCom As Integer    ' Command from joystick as pressure
'
        Const AirSupplyPres = 95            ' Supply pressure value, psi
        Const MinAirPres = 15               ' Min air pressure for 4 mm bore, psi
        Const LowVolt = (MinAirPres / AirSupplyPres) * 5  ' Voltage output from DAQ
                                                            card to generate minimum
                                                            pressure
'
' Because the amplifiers are meant to work from 0-10 Vdc input, and card is only
'capable of 0-5 Vdc, we are using half of the available output.  5 Vdc input
'corresponds to 0 mA output from the amplifier.  The minimum is the voltage at the
'maximum safe output current to the nitinol wire.
'
```

```
        Const VSupplyMax = 5            ' Maximum command voltage to current
                                          amplifiers
        Const VSupplyMin = 4.5 '2.16        ' Minimum command voltage to current
                                              Amplifiers.  4.5 is for 12 Vdc, 2.16 is
                                              for 5 Vdc supply
'
' Mapping of joystick buttons
'
        Const Deadman = 0               ' Trigger
        Const Estop_but = 1             ' Estop button
        Const Cut_but = 2               ' Cauterizer cut
        Const Coag_but = 3              ' Cauterizer coag
        Const Rot_CCW = 4               ' Wrist rotate counter clockwise
        Const Rot_CW = 5                ' Wrist rotate clockwise
'
' Setup DAQ card variables
'
        Const BoardNum% = 0             ' Board number
        Const LowChan% = 0              ' First channel
        Const HiChan% = 7               ' Last channel
        Const NumPoints& = 8            ' Channels + 1
        Const CBCount& = NumPoints&
```

```
        Const Gain% = BIP5VOLTS          ' Ignored if gain is not programmable
        Const CBRate& = 100              ' Rate of data update (ignored if board does
                                           not'support timed analog output)
        Const Options% = 0
        Const OutOn% = 4095              ' Full output, 5 Vdc, digital
        Const OutOff% = 2048             ' No output, 0 Vdc, digital
        Const OutOffTA% = 3028           ' No output, 2.39 Vdc for Trans Amps,
                                           digital
        Const MotorCW% = 3563            ' +4.5, motor spins clockwise, digital
        Const MotorStop% = 2048          ' 0, motor stopped, digital
        Const MotorCCW% = 530            ' -4.5, motor spins counterclockwise, digital
        Dim DAData%(NumPoints&)
        Dim Commands(NumPoints&)
        Dim MemHandle&                   ' define a variable to contain the handle for
                                           memory allocated by Windows through
                                           cbWinBufAlloc%()
        Dim FirstPoint&


Private Sub cmdStart_Click()
'
' Start communications with joystick and get the capabilities of the joystick
'Not sure what individual commands do exactly, but these are the bare minimum
```

```
'to make the joystick work.  No joystick found error control is NOT included.
'The program operates under the assumption that a joystick is ALWAYS present.
'
    Set di = dx.DirectInputCreate
    Set diDevEnum = di.GetDIDevices(DI8DEVCLASS_GAMECTRL,
                        DIEDFL_ATTACHEDONLY)
    Set diDev = di.CreateDevice(diDevEnum.GetItem(1).GetGuidInstance)
    diDev.SetCommonDataFormat DIFORMAT_JOYSTICK
    diDev.GetCapabilities joyCaps
'
    With DiProp_Dead
       .lData = 1000
       .lHow = DIPH_BYOFFSET
       .lObj = DIJOFS_X
          diDev.SetProperty "DIPROP_DEADZONE", DiProp_Dead
       .lObj = DIJOFS_Y
          diDev.SetProperty "DIPROP_DEADZONE", DiProp_Dead
       .lObj = DIJOFS_RZ
          diDev.SetProperty "DIPROP_DEADZONE", DiProp_Dead
    End With
'
    With DiProp_Saturation
```

```
        .lData = 9500
        .lHow = DIPH_BYOFFSET
        .lObj = DIJOFS_X
           diDev.SetProperty "DIPROP_SATURATION", DiProp_Saturation
        .lObj = DIJOFS_Y
           diDev.SetProperty "DIPROP_SATURATION", DiProp_Saturation
        .lObj = DIJOFS_RZ
           diDev.SetProperty "DIPROP_SATURATION", DiProp_Saturation
     End With
'
     With DiProp_Range
        .lHow = DIPH_DEVICE
        .lMin = 0
        .lMax = 10000
     End With
'
     diDev.SetProperty "DIPROP_RANGE", DiProp_Range
     diDev.Acquire
'
' Declare revision level of Universal Library
'
     ULStat% = cbDeclareRevision(CURRENTREVNUM)
```

```
'
' Initiate error handling
'  activating error handling will trap errors like bad channel numbers and non-configured
conditions.
'  Parameters:
'    PRINTALL    :all warnings and errors encountered will be printed
'    DONTSTOP    :if an error is encountered, the program will not stop, errors must be
                  handled locally
'
'
       ULStat% = cbErrHandling(PRINTALL, DONTSTOP)
'
' If cbErrHandling% is set for STOPALL or STOPFATAL during the program
' design stage, Visual Basic will be unloaded when an error is encountered.
' We suggest trapping errors locally until the program is ready for compiling
' to avoid losing unsaved data during program design.  This can be done by
' setting cbErrHandling options as above and checking the value of ULStat%
' after a call to the library. If it is not equal to 0, an error has occurred.
'
' Setup array to hold information for E-Stop condition
'
       MemHandle& = cbWinBufAlloc(NumPoints&)      ' set aside memory to hold data
```

```
        If MemHandle& = 0 Then Stop
'
' If we have made it this far, we have a joystick and are ready to go
'
        tmrProg.Enabled = True
        ESTOP_pressed = False
        lblSystemStatus.Caption = "Joystick Acquired"
'
End Sub


Private Sub tmrProg_Timer()
'
' "Poll" joystick to get locations and button values.  Normally, the joystick would
'be "polled" automatically, but the frequency of the USB port is higher than the
'DAQ card can keep up with.  So, the program is run with a timing of 1 ms.  Whether
'or not this actually happens (due to high-level programming, such as Windows 2000),
'is not known.  However, at this rate, the program responds well and time delays are
'minimal.  Both the joystick and the DAQ card are comfortable at this rate.
'
            diDev.GetDeviceStateJoystick js
'
' Depending upon which arm is being controlled, send appropriate command
```

```
'0 = Pneumatic
'1 = Nitinol
'
' The commands are a function of the returned position of X, Y, and rotation about
'Z.  The "home" position of these variables corresponds to 5000 counts.  Minimum is
'0 counts and maximum is 10000 counts.
'   js.X/5000 for example is the logic for half of the X travel
'   js.X/10000 for example is the logic for full of the X travel

'
If Arm = 0 Then
'
' Take joystick command and generate requested pressure, required output voltage,
'send it and display command and output pressure (both calculated, not measured)
'to screen.
'
      JointOneCom = MinAirPres - (js.y / 10000) * (MinAirPres - AirSupplyPres)
      JointOneVolts! = LowVolt - ((JointOneCom - MinAirPres) / (AirSupplyPres –
                        MinAirPres)) * (LowVolt - 5)
      ULStat% = cbFromEngUnits(BoardNum%, Gain%, JointOneVolts!,
                  Commands(0))
'
```

```
' Output command to user, mainly for diagnostic
'
        lblCylinderPres(0).Caption = JointOneCom
        lblAirComVolt(0).Caption = Format$(JointOneVolts!, "0.0")
'
' Make sure joystick is in rotation about Z direction range.  Motion is limited to
'half of the available rotation.  The arm currently only rotates to the left, so
'right rotation can be and should be ignored
'
        If js.rz > 5000 Then
           js.rz = 5000
        End If
'
' Take joystick command and generate requested pressure, required output voltage,
'send it and display command and output pressure (both calculated, not measured)
'to screen.
'
        JointTwoCom = 0.55 * (AirSupplyPres - (js.rz / 5000) * (AirSupplyPres –
                              MinAirPres))
        JointTwoVolts! = LowVolt - ((JointTwoCom - MinAirPres) / (AirSupplyPres –
                               MinAirPres)) * (LowVolt - 5)
        ULStat% = cbFromEngUnits(BoardNum%, Gain%, JointTwoVolts!,
```

```
                    Commands(1))
'
' Output command to user, mainly for diagnostic
'
    lblCylinderPres(1).Caption = JointTwoCom
    lblAirComVolt(1).Caption = Format$(JointTwoVolts!, "0.0")
'
' Make sure joystick is in the X direction range.  Since the X direction is being used
'to drive the telescoping ability of the arm, having full travel in this direction
'does not make sense, so it is limited
'
    If js.x > 5000 Then
       js.x = 5000
    End If
'
' Take joystick command and generate requested pressure, required output voltage,
'send it and display command and output pressure (both calculated, not measured)
'to screen.
'
    JointThreeCom = 0.65 * (AirSupplyPres - (js.x / 5000) * (AirSupplyPres –
                        MinAirPres))
    JointThreeVolts! = LowVolt - ((JointThreeCom - MinAirPres) / (AirSupplyPres –
```

```
                    MinAirPres)) * (LowVolt - 5)
        ULStat% = cbFromEngUnits(BoardNum%, Gain%, JointThreeVolts!,
                    Commands(2))
'
' Output command to user, mainly for diagnostic
'
        lblCylinderPres(2).Caption = JointThreeCom
        lblAirComVolt(2).Caption = Format$(JointThreeVolts!, "0.0")

'
' Set all nitinol output to zero.  Since they are not being used, there is no need
'for the amplifiers for the nitinol to be doing anything.  Set to zero mainly as
'a safety precaution
'
        Commands(3) = OutOffTA%
        Commands(4) = OutOffTA%
    Else
'
' Make sure joystick is in Y range.  Since by default the arm is full down, it does
'not make sense to have it as a command.  Notice that the limit is reverse that of
'the pneumatic arm.  This is because the command will come from the 5000-10000
range
```

```
'of the joystick motion
'
    If js.y < 5000 Then
       js.y = 5000
    End If
'
' Take joystick command and generate required output voltage, send it and display
'command and output current (both calculated, not measured) to screen. 500 corresponds
'to 500 mA, which is maximum that I can extract from the current power supply to
'safely power both joints.
'
    WireOneVolts! = VSupplyMax - (js.y / 10000) * (VSupplyMax - VSupplyMin)
    WireOneCurrent = 500 - ((WireOneVolts! - VSupplyMin) / (VSupplyMax –
                          VSupplyMin)) * 500
    ULStat% = cbFromEngUnits(BoardNum%, Gain%, WireOneVolts!,
                  Commands(3))

'
' Output command to user, mainly for diagnostic
'
    lblWireVolts(0).Caption = Format$(WireOneVolts!, "0.0")
```

```
        lblWireCurrent(0).Caption = Format$(WireOneCurrent, "0.0")
'
' Make sure joystick is in the rotation about Z direction range.  Since this arm is
'left only as well, a right command should be ignored
'
        If js.rz > 5000 Then
           js.rz = 5000
        End If
'
' Take joystick command and generate required output voltage, send it and display
'command and output current (both calculated, not measured) to screen. 500
‘corresponds to 500 mA, which is maximum that I can extract from the current power
‘supply to safely power both joints.
'
        WireTwoVolts! = VSupplyMin - (js.rz / 5000) * (VSupplyMin - VSupplyMax)
        WireTwoCurrent = 500 - ((WireTwoVolts! - VSupplyMin) / (VSupplyMax –
                                VSupplyMin)) * 500
        ULStat% = cbFromEngUnits(BoardNum%, Gain%, WireTwoVolts!,
                        Commands(4))
'
' Output command to user, mainly for diagnostic
'
```

```
        lblWireVolts(1).Caption = Format$(WireTwoVolts!, "0.0")
        lblWireCurrent(1).Caption = Format$(WireTwoCurrent, "0.0")
'
' Set pressure regulator commands to zero.  Since they are not needed, they should
'not be doing anything.
'
        Commands(0) = OutOff%
        Commands(1) = OutOff%
        Commands(2) = OutOff%
    End If
'
' Wrist control, either +4.5, 0, -4.5 VDC, clockwise, none, counterclockwise,
'respectively.  Proportional control not added yet.  The value of the buttons is 0
'when NOT pressed, and some value when pressed.  Because the value when pressed
‘may not be known, negative logic is used.  The command is limited to EITHER
‘clockwise or counterclockwise command
'
    If Not js.Buttons(Rot_CW) = 0 And js.Buttons(Rot_CCW) = 0 Then
        lblWristStatus.Caption = "Wrist rotating clockwise..."
        lblMotorVolts.Caption = "+4.5"
        Commands(5) = MotorCW%
    ElseIf js.Buttons(Rot_CW) = 0 And Not js.Buttons(Rot_CCW) = 0 Then
```

```
        lblWristStatus.Caption = "Wrist rotating counterclockwise..."
        lblMotorVolts.Caption = "-4.5"
        Commands(5) = MotorCCW%
    Else
        lblWristStatus.Caption = "Wrist Locked."
        lblMotorVolts.Caption = "0.0"
        Commands(5) = MotorStop%
    End If
'
' The cauterizer requires two buttons pressed at the same time to function,
'as a safety precaution.  The trigger [Deadman] and one other button must be
'pressed for cutting or coagulation to occur.  As with the wrist control, negative
'logic is used because the buttons go from 0 (NOT pressed) to some value
'
    If Not js.Buttons(Deadman) = 0 And Not js.Buttons(Cut_but) = 0 And
    js.Buttons(Coag_but) = 0 Then
        lblCauterizerStatus.Caption = "CUT"
        Commands(6) = OutOn%
    ElseIf Not js.Buttons(Deadman) = 0 And Not js.Buttons(Coag_but) = 0 And
    js.Buttons(Cut_but) = 0 Then
        lblCauterizerStatus.Caption = "COAG"
        Commands(7) = OutOn%
```

```
    Else
        lblCauterizerStatus.Caption = "OFF"
        Commands(6) = OutOff%
        Commands(7) = OutOff%
    End If
'
' Since all 8 channels are being used for different functions, the commands are stored
'in memmory then reassembled as an output string for the card.  This output string
'included position commands as well as any and all button presses
'
    For i% = 0 To NumPoints& - 1
        DAData%(i%) = Commands(i%)
    Next i%
    FirstPoint& = 0
    ULStat% = cbWinArrayToBuf(DAData%(0), MemHandle&, FirstPoint&,
                CBCount&)
    ULStat% = cbAOutScan(BoardNum%, LowChan%, HiChan%, CBCount&,
                CBRate&, Gain%, MemHandle&, Options%)
'
' This logic is for the E-Stop mapped to the joystick.  If there is a problem, all
'outputs go to zero.  Program can be restarted by pressing "Start"
'
```

```
    If Not js.Buttons(Estop_but) = 0 Then
        tmrProg.Enabled = False
        ESTOP_pressed = True
        lblSystemStatus.Caption = "Physician EMERGENCY STOP"
        DAData%(0) = OutOff%
        DAData%(1) = OutOff%
        DAData%(2) = OutOff%
        DAData%(3) = OutOffTA%
        DAData%(4) = OutOffTA%
        DAData%(5) = OutOff%
        DAData%(6) = OutOff%
        DAData%(7) = OutOff%
'
        FirstPoint& = 0
        ULStat% = cbWinArrayToBuf(DAData%(0), MemHandle&, FirstPoint&,
                  CBCount&)
        ULStat% = cbAOutScan(BoardNum%, LowChan%, HiChan%, CBCount&,
                  CBRate&, Gain%, MemHandle&, Options%)
        ULStat% = cbWinBufFree(MemHandle&)      ' Free up memory for use by other
                                                  programs
        Beep
    Else
```

```
        lblSystemStatus.Caption = "Running..."
    End If
End Sub

Private Sub optArm_Click(Index As Integer)
' Used to determine which arm is going to be controlled
' 0 = Pneumatic [Default]
' 1 = Nitinol
'
    Arm = Index
End Sub

Private Sub cmdEStop_Click()
' This subroutine controls the (G)raphical (U)ser (I)nterface E-Stop.  It has the
'same function as the joystick E-Stop, in that all outputs are sent to zero.
'
    tmrProg.Enabled = False
    ESTOP_pressed = True
    lblSystemStatus.Caption = "GUI EMERGENCY STOP"
    DAData%(0) = OutOff%
    DAData%(1) = OutOff%
    DAData%(2) = OutOff%
```

```
    DAData%(3) = OutOffTA%
    DAData%(4) = OutOffTA%
    DAData%(5) = OutOff%
    DAData%(6) = OutOff%
    DAData%(7) = OutOff%
'
    FirstPoint& = 0
    ULStat% = cbWinArrayToBuf(DAData%(0), MemHandle&, FirstPoint&,
                  CBCount&)
    ULStat% = cbAOutScan(BoardNum%, LowChan%, HiChan%, CBCount&,
                 CBRate&, Gain%, MemHandle&, Options%)
    ULStat% = cbWinBufFree(MemHandle&)      ' Free up memory for use by other
                                                programs
    Beep
End Sub
```

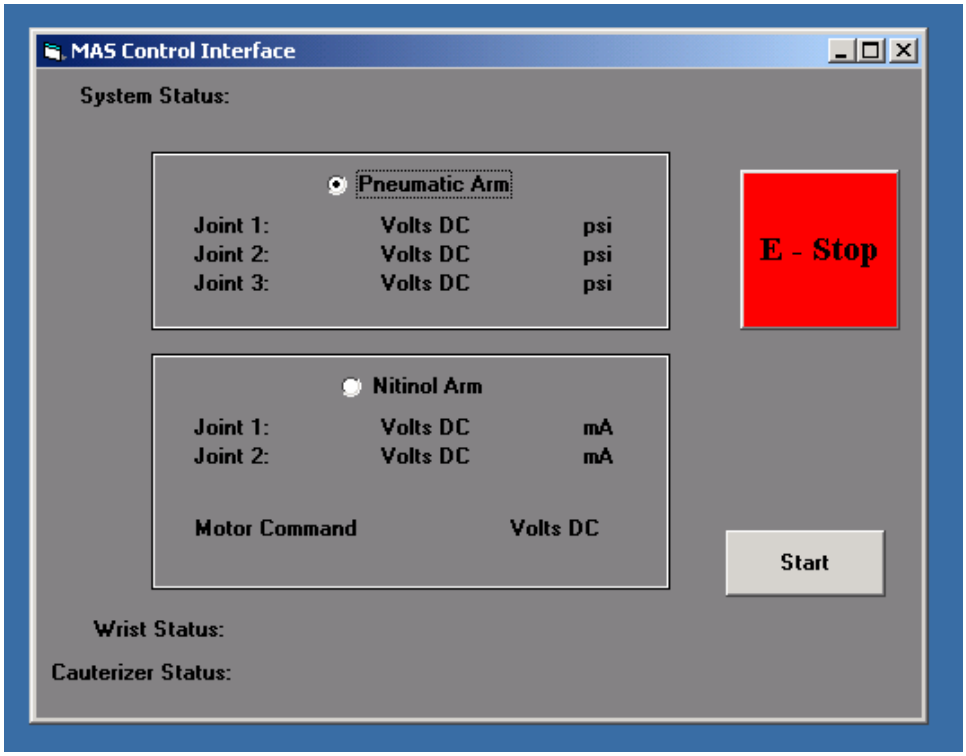

Figure 105. Control program's user interface

APPENDIX I

POWERED TOOLING

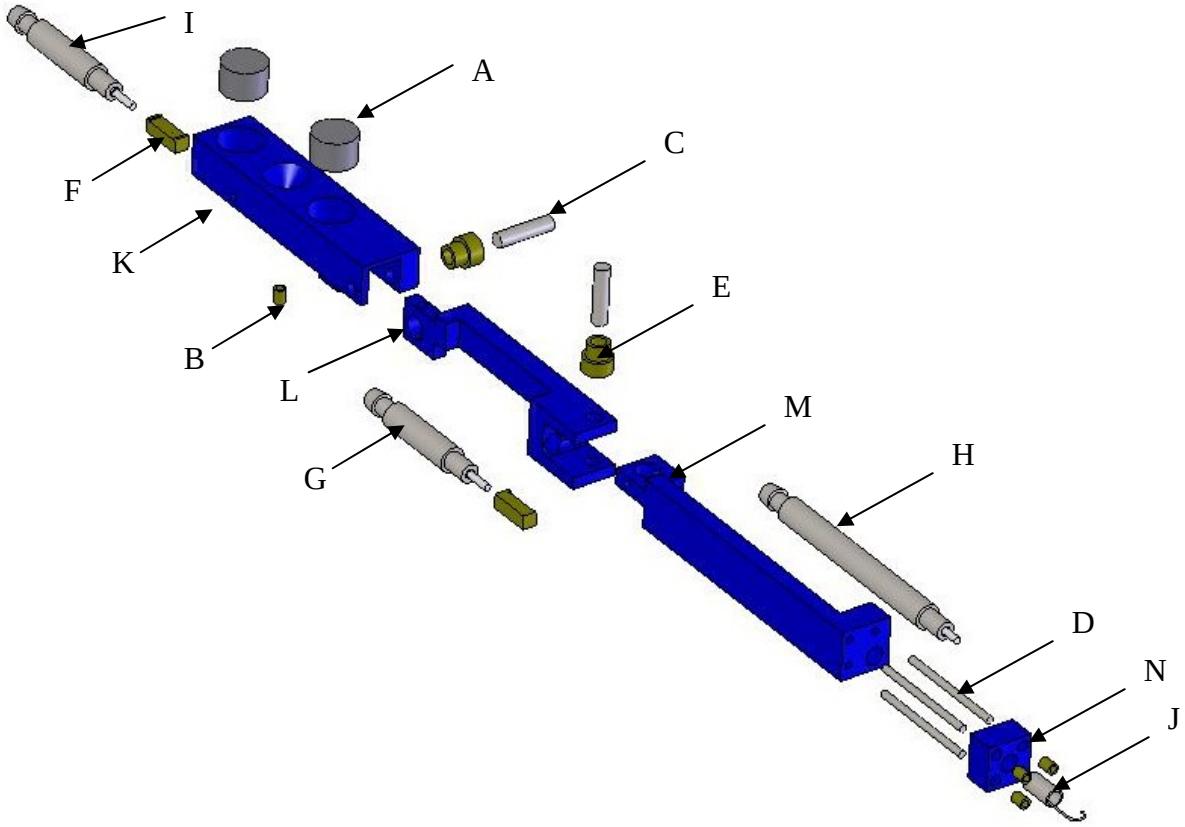

Figure 106. Pneumatically actuated arm prototype, exploded view

- Magnet Sales & Manufacturing

  A. Part number 30DNE2416-NI

     - Two, NdFeB Grade 30, 9.5 millimeter (0.375 inch) diameter by 6.4 millimeter (0.25 inch) thick, nickel plated permanent magnet

- McMaster-Carr

  B. Part number 92395A109

     - Four, 0-80 threaded brass inserts

- Small Parts

C. Part number R-DWX-2-8

- 3 millimeter (0.125 inch) diameter by 12 millimeter (0.50 inch) long, 2 are needed

D. Part number GWX-500-30

- Stainless Steel Type 304, 1.3 millimeter (0.050 inch) diameter by 762 millimeter (30 inch) long
  - The wire was cut into three, 25 millimeter (1.0 inch) long sections and used as a guide pins. One end was thread 0-80 for 6.4 millimeter (0.25 inch)

E. Part number R-PGB-6416

- 64 pitch, 16 tooth brass pinion gear, 2 are needed

F. Part number GRB-64/20-6

- 64 pitch rack, cut to 9.5 millimeter (0.375 inch) in length, 2 of this length are needed

- SMC

G. Part number CJ1B2-5SU4

- Single acting, spring return, 2.5 millimeter bore, 5 millimeter stroke

H. Part number CJ1B2-10SU4

- Single acting, spring return, 2.5 millimeter bore, 10 millimeter stroke

I. Part number CJ1B4-5SU4

- Single acting, spring return, 4 millimeter bore, 5 millimeter stroke

- Misc.

J. Electro-cautery hook, donated by UTSW animal lab

K. One piece of delrin 57 by 14 by 14 millimeter (2.25 by 0.54 by 0.54 inch)

L. One piece of delrin 60 by 12 by 10 millimeter (2.38 by 0.50 by 0.40 inch)

M. One piece of delrin 76 by 11 by 11 millimeter (3.0 by 0.44 by 0.45 inch)

N. One piece of delrin 10 by 10 by 6.4 millimeter (0.40 by 0.40 by 0.25 inch)

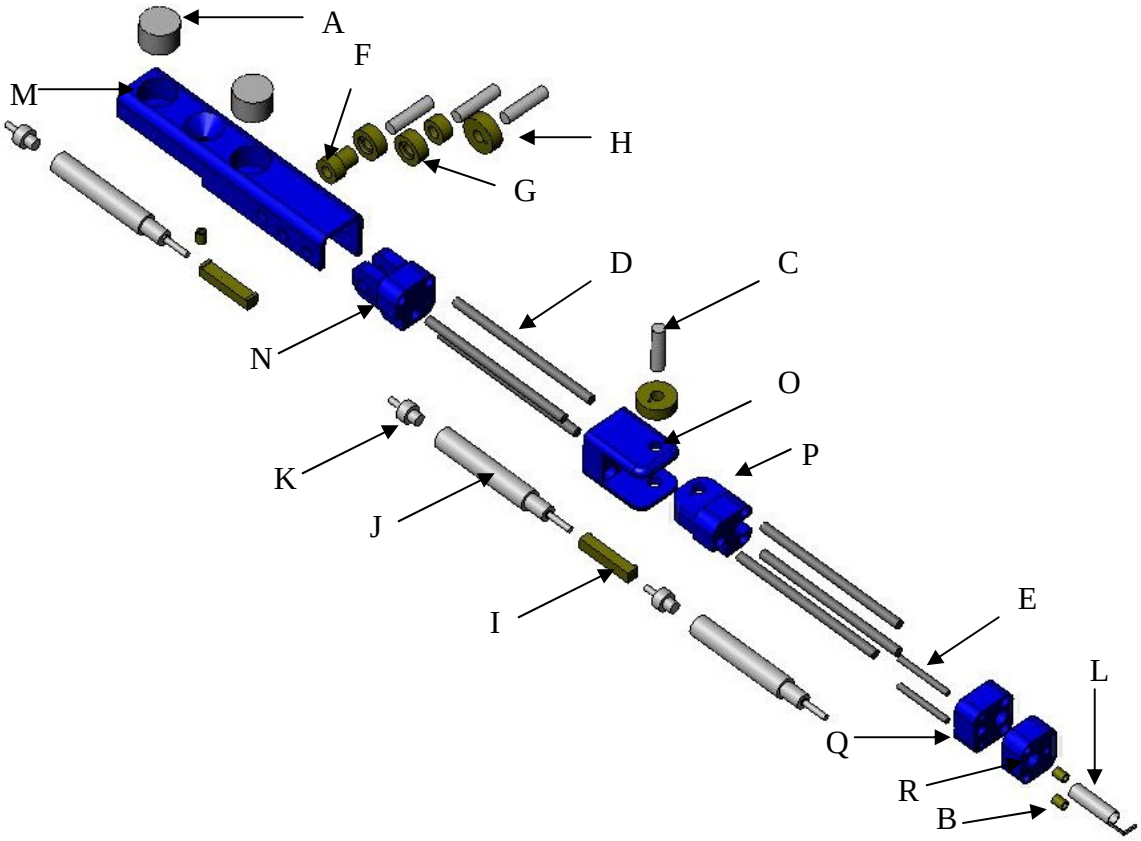

Figure 107. Pneumatically actuated arm revision b, exploded view

- Magnet Sales & Manufacturing

  A. Part number 30DNE2416-NI

     - Two, NdFeB Grade 30, 9.5 millimeter (0.375 inch) diameter by 6.4 millimeter (0.25 inch) thick, nickel plated permanent magnet

- McMaster-Carr

  B. Part number 92395A109

     - Three, 0-80 threaded brass inserts

- Small Parts

C. Part number R-DWX-2-8

- 3 millimeter (0.125 inch) diameter by 12 millimeter (0.50 inch) long, 4 are needed

D. Part number GWX-0800-30

- Stainless Steel Type 304, 2 millimeter (0.080 inch) diameter by 762 millimeter (30 inch) long
    - The wire was cut into six, 44 millimeter (1.75 inch) long sections and threaded for 2-56 for 6.4 millimeter (0.25 inch) on both ends

E. Part number R-DWX-1-16

- 1.6 millimeter (0.063 inch) in diameter by 25 millimeter (1.0 inch) long threaded with 0-80, two are needed
    - Two pins without threads are required to lock the 24 tooth gears with their associated linkage section.

F. Part number PGB-6416

- 64 pitch, 16 tooth brass pinion gear, 2 are needed

G. Part number PGB-6420

- 64 pitch, 20 tooth brass pinion gear, 2 are needed

H. Part number PGB-6424

- 64 pitch, 24 tooth brass pinion gear, 2 needed

I. Part number GRB-64/20-6

- 64 pitch rack, cut to 12 millimeter (0.50 inch) in length, 2 of this length are needed

- SMC

J. Part number CJ1B4-10SU4

- Single acting, spring return, 4 millimeter bore, 10 millimeter stroke, 3 are needed

K. Part number M-3AU-2

- 2 millimeter fitting, 3 are needed

- Misc.

L. Electro-cautery hook, donated by UTSW animal lab

M. One piece of delrin 67 by 14 by 14 millimeter (2.63 by 0.54 by 0.54 inch)

N. One piece of delrin 12 by 12 by 15 millimeter (0.50 by 0.50 by 0.60 inch)

O. One piece of delrin 19 by 14 by 14 millimeter (0.75 by 0.54 by 0.54 inch)

P. One piece of delrin 16 by 12 by 12 millimeter (0.63 by 0.50 by 0.50 inch)

Q. One piece of delrin 12 by 12 by 6.4 millimeter (0.50 by 0.50 by 0.25 inch)

R. One piece of delrin 11.4 by 12 by 6.4 millimeter (0.45 by 0.50 by 0.25 inch)

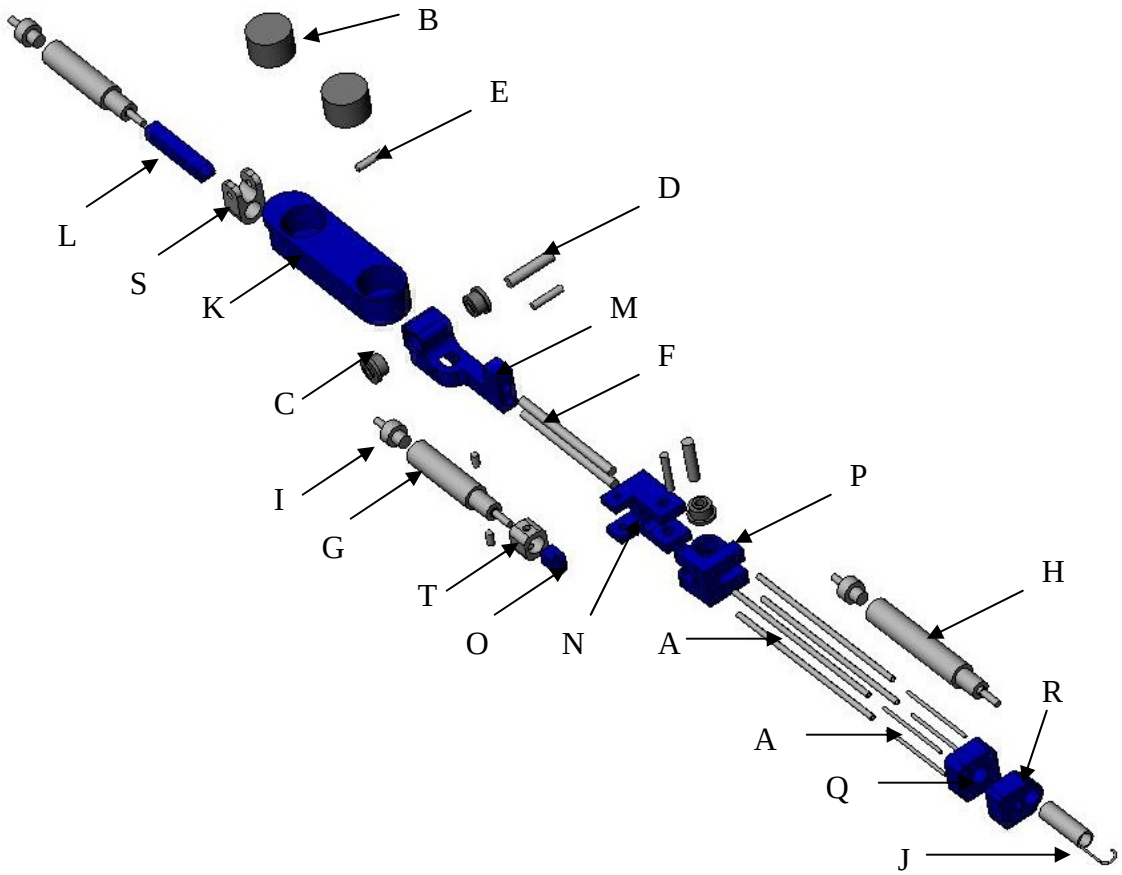

Figure 108. Pneumatically actuated arm revision c, exploded view

- Becton Dickinson

  A. Part number 405184

  - 18 gauge x 89 millimeter (3.5 inch) spinal needles
    - The distal end of the needed was ground flat. The proximal end was cut off resulting in a tube 44.5 millimeter (1.75 inch) long. The needles were then threaded with a 0-80 thread. Four are needed

- Magnet Sales & Manufacturing

    B. Part number 30DNE2416-NI

        - Two, NdFeB Grade 30, 9.5 millimeter (0.375 inch) diameter by 6.4 millimeter (0.25 inch) thick, nickel plated permanent magnet

- McMaster Carr

    C. Part number 57155K13

        - Miniature precision stainless steel ball bearing, ABEC-5, standard shield, extended inner ring.
            - 2.4 millimeter (0.094 inch) internal diameter, 4.8 millimeter (0.188 inch) outer diameter
            - Three of these bearings were used.

- MSC

    D. Part number 06021059

        - Three, 2.4 millimeter (0.094 inch) in diameter by 12 millimeter (0.50 inch) long dowel pins

    E. Part number 60630050

        - Four, 1.6 millimeter (0.063 inch) in diameter by 12 millimeter (0.50 inch long) dowel pins

- Small Parts

    F. Part number GWX-0800-30

- Stainless Steel Type 304, 2 millimeter (0.080 inch) diameter by 762 millimeter (30 inch) long
    - The wire was cut into two, 30 millimeter (1.19 inch) long sections and threaded for 2-56 for 6.4 millimeter (0.25 inch) on both ends

- SMC

G. Part number CJ1B4-5SU4
    - Single acting, spring return, 4 millimeter bore, 5 millimeter stroke, 2 are needed

H. Part number CJ1B4-10SU4
    - Single acting, spring return, 4 millimeter bore, 10 millimeter stroke, 1 needed

I. Part number M-3AU-2
    - 2 millimeter fitting, 3 are needed

- Misc.

J. Electro-cautery hook, donated by UTSW animal lab

K. One piece of delrin 11 by 7 by 41 millimeter (0.44 by 0.28 by 1.63 inch)

L. One piece of delrin 3 by 3 by 19 millimeter (0.125 by 0.125 by 0.76 inch)

M. One piece of delrin 7.6 by 10 by 25 millimeter (0.30 by 0.40 by 1.0 inch)

N. One piece of delrin 11 by 10 by 14 millimeter (0.44 by 0.40 by 0.55 inch)

O. One piece of delrin 3 by 3 by 5 millimeter (0.125 by 0.125 by 0.21 inch)

P. One piece of delrin 10 by 9.7 by 12 millimeter (0.40 by 0.38 by 0.50 inch)

Q. One piece of delrin 9.5 by 9.5 by 5 millimeter (0.38 by 0.38 by 0.20 inch)

R. One piece of delrin 12 by 8.4 by 5 millimeter (0.50 by 0.33 by 0.20 inch)

S. One piece of 6061-T6 aluminum 5 by 5.6 by 6.4 millimeter (0.20 by 0.22 by 0.25 inch)

T. One piece of 6061-T6 aluminum 6.4 by 5 by 10.4 millimeter (0.25 by 0.20 by 0.41 inch)

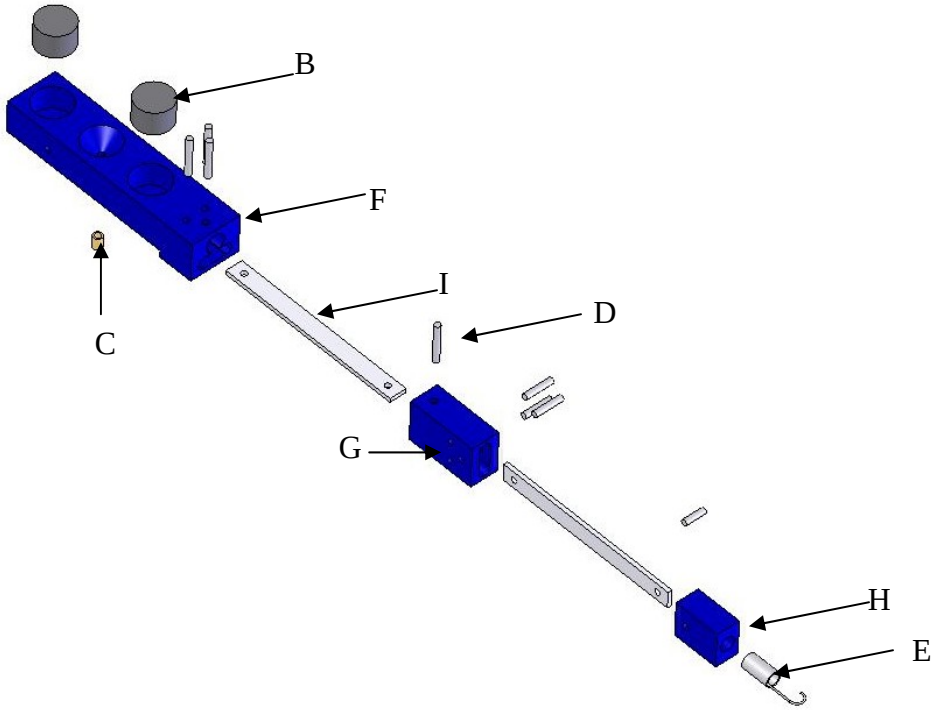

Figure 109. Nitinol actuated arm prototype, exploded view

- Dynalloy

    A. Part number n/a The wire was ordered as follows (not shown)

        - Quantity = 2
        - Crimp Style = Ring Terminal
        - Measurement Method = B
        - Length = 5 inch
        - Flexinol diameter = 0.008 inch
        - Transition temperature = 90 degree Celsius
        - Lead wires = Yes
        - Length of lead wires = 6 inch

- Magnet Sales & Manufacturing

    B. Part number 30DNE2416-NI

        - Two, NdFeB Grade 30, 9.5 millimeter (0.375 inch) diameter by 6.4 millimeter (0.25 inch) thick, nickel plated permanent magnet

- McMaster Carr

    C. Part number 92395A109

        - One, 0-80 threaded brass inserts

- MSC

    D. Part number 60630050

        - Six, 1.6 millimeter (0.063 inch) in diameter by 12 millimeter (0.50 inch) long dowel pins

- Misc.

    E. Electro-cautery hook, donated by UTSW animal lab

    F. One piece of delrin 13.7 by 11 by 57 millimeter (0.54 by 0.42 by 2.25 inch)

    G. One piece of delrin 7.6 by 11 by 19 millimeter (0.30 by 0.44 by 0.75 inch)

    H. One piece of delrin 12 by 6.4 by 12 millimeter (0.50 by 0.25 by 50 inch)

    I. Two zip ties cut to the approximate dimensions to be operated by the wire

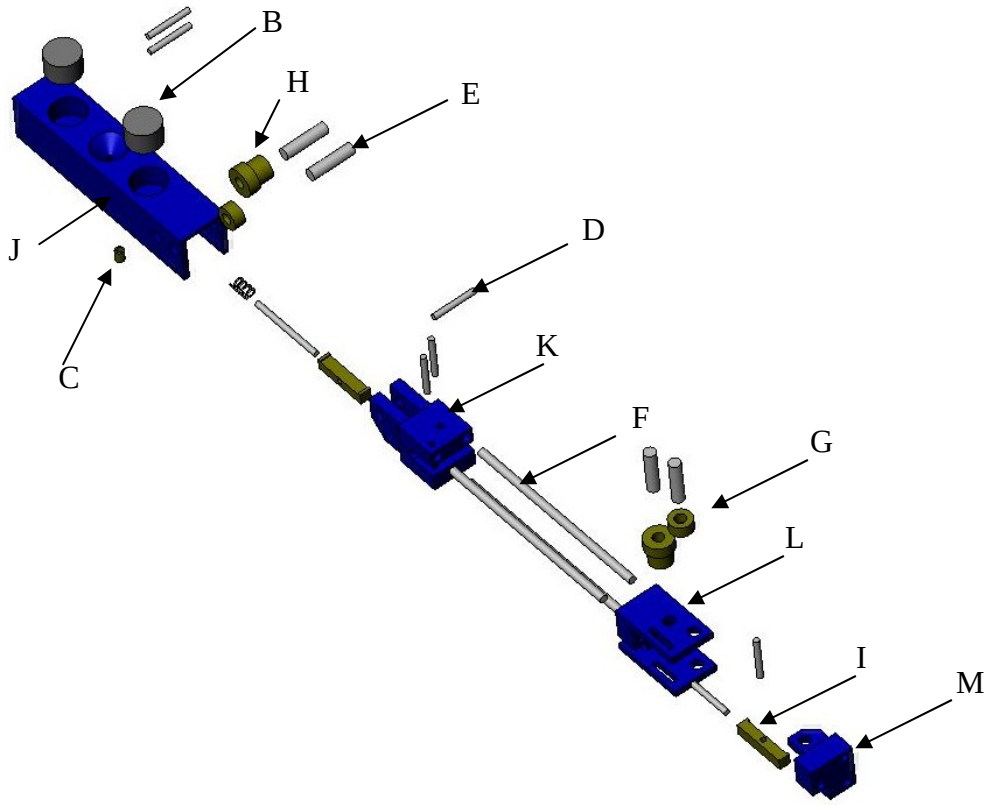

Figure 110. Nitinol actuated arm revision b, exploded view

- Dynalloy
  - Part number n/a The wire was ordered as follows (not shown)
    - Quantity = 3
    - Crimp Style = Ring Terminal
    - Measurement Method = B
    - Length = 5 inch
    - Flexinol diameter = 0.008 inch
    - Transition temperature = 90 degree Celsius
    - Lead wires = Yes

        - Length of lead wires = 6 inch
- Magnet Sales & Manufacturing
    - Part number 30DNE2416-NI
        - Two, NdFeB Grade 30, 9.5 millimeter (0.375 inch) diameter by 6.4 millimeter (0.25 inch) thick, nickel plated permanent magnet
- McMaster Carr
    - Part number 92395A109
        - One, 0-80 threaded brass inserts
- MSC
    - Part number 60630050
        - Eight, 1.6 millimeter (0.063 inch) in diameter by 12 millimeter (0.50 inch) long dowel pins
- Small Parts
    - Part number R-DWX-2-8
        - 3 millimeter (0.125 inch) diameter by 12 millimeter (0.50 inch) long, 4 are needed
    - Part number GWX-0800-30
        - Stainless Steel Type 304, 2 millimeter (0.080 inch) diameter by 762 millimeter (30 inch) long

        - The wire was cut into three, 44.5 millimeter (1.75 inch) long sections and threaded for 2-56 for 6.4 millimeter (0.25 inch) on both ends
    - Part number PGB-6416
        - 64 pitch, 16 tooth brass pinion gear, 2 are needed
    - Part number PGB-6420
        - 64 pitch, 20 tooth brass pinion gear, 2 are needed
    - Part number GRB-64/20-6
        - 64 pitch rack, cut to 12 millimeter (0.50 inch) in length, 2 of this length are needed
- Misc.
    - One piece of delrin 13.7 by 13.7 by 64 millimeter (0.54 by 0.54 by 2.50 inch)
    - One piece of delrin 25 by 12 by 12 millimeter (1.0 by 0.50 by 0.50 inch)
    - One piece of delrin 13.7 by 12 by 21 millimeter (0.54 by 0.50 by 0.84 inch)
    - One piece of delrin 12 by 12 by 16 millimeter (0.50 by 0.50 by 0.63 inch)

APPENDIX J

ELECTROMAGNET MATHEMATICAL MODEL

Knowing that the electromagnet must stay under 100 mm in diameter, the maximum power input was 60 watts, and the assembly needed to stay as close to the abdominal wall as possible, a mathematical model was written in Microsoft Excel.

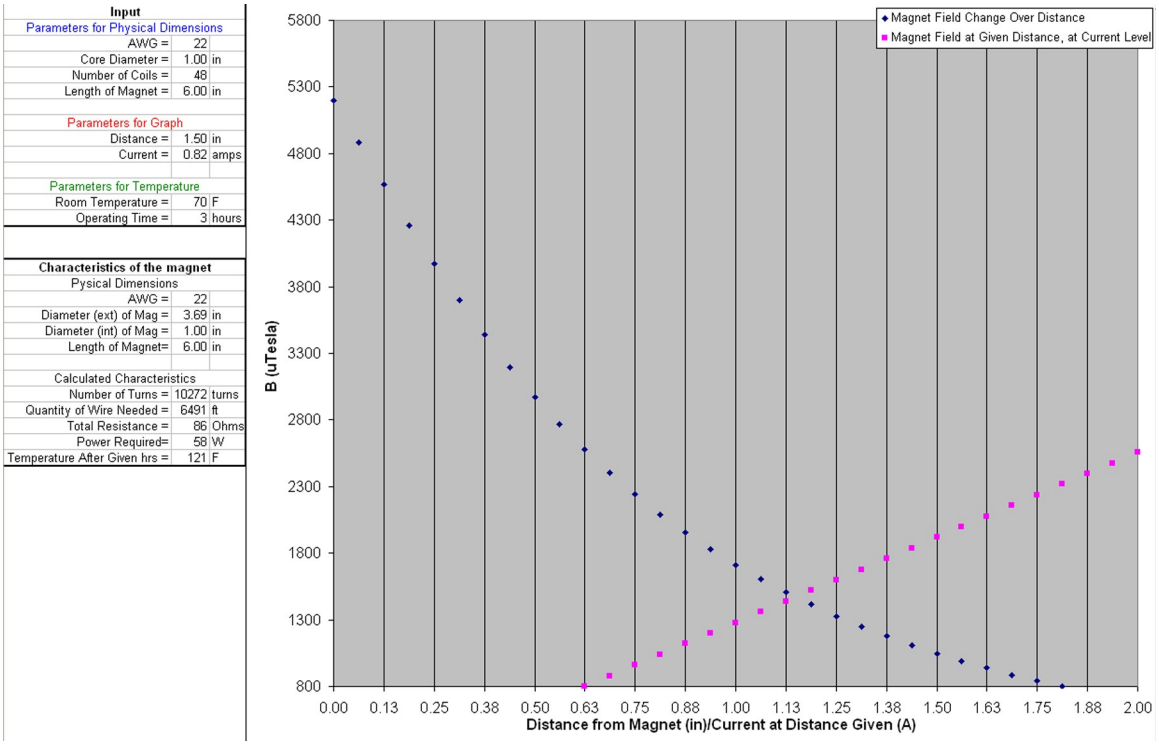

Input		
Parameters for Physical Dimensions		
AWG =	22	
Core Diameter =	1.00	in
Number of Coils =	48	
Length of Magnet =	6.00	in
Parameters for Graph		
Distance =	1.50	in
Current =	0.82	amps
Parameters for Temperature		
Room Temperature =	70	F
Operating Time =	3	hours

Characteristics of the magnet		
Pysical Dimensions		
AWG =	22	
Diameter (ext) of Mag =	3.69	in
Diameter (int) of Mag =	1.00	in
Length of Magnet=	6.00	in
Calculated Characteristics		
Number of Turns =	10272	turns
Quantity of Wire Needed =	6491	ft
Total Resistance =	86	Ohms
Power Required=	58	W
Temperature After Given hrs =	121	F

Figure 111. Electromagnet model

The input parameters were as follows:

- The gauge of the wire to be used. The value could range from AWG 20 to 26. The smaller the gauge of wire, the more compact the electromagnet could be since more turns of wire could be in the same volume, but more heat would be generated due to the increase in resistance.

- The diameter of the core. The core diameter originally was to help determine the amount of wire required to build the electromagnet, but it was found that by making the electromagnet's core larger, the magnetic field would be stronger within a certain range without increasing input power, wire, etc. This is because the ferromagnetic material cans only accommodate a certain amount of magnetic field. The ferromagnetic material is less resistant than air, and if it were saturated, the magnetic field would be reduced since more would have to travel through the air. However, the larger the core material, the lower the number of turns the magnet could be made of due to size constraints.
- Number of coils. What is meant by this parameter is the number of hollow cylinders made by the wire. The mathematics assumes that the wire is wrapped around the core circumference in rings that are the core diameter plus two times the diameter of the wire. For the rings that are not in direct contact with the core material, the total diameter, core and rings before this one, are used. A coil is a collection of these rings along the length of the core. This value is required to be an even number because the leads for the electromagnet are desired to be on the same end of the magnet
- Length of the magnet. The length of the magnet has somewhat flexible size constraints because height was deemed to not be as big a problem as the diameter, or footprint of the magnet. Knowing the length of the magnet, the

model calculates the best way to package the requested number of coils and gauge of wire.

- Distance. This is the distance from the magnetic surface of the core to the target. This value is displayed on the graph as the pink curve. This curve represents the magnetic field at the given distance as a function of varying the current induced in the electromagnet. This information was used to find the effect of powering the magnet with a more powerful power supply (higher current capacity).
- Current. This is the current induced in the magnet. Truthfully, this should be voltage and the current should be calculated, but since current is what is used in the calculations, it is input directly. The blue curve shows the magnetic field at the different distances at this current level.
- Room Temperature. This is the operating room temperature, which is used for the electromagnet temperature calculations. The electromagnet generates heat due to power loss caused by the resistance in the wire. The temperature of the electromagnet is important for two reasons: if the resistance of the wire and the current are not matched properly, the electromagnet could generate enough heat to burn the enamel off the wire, causing it to short, and if the temperature was too great, it could cause tissue damage.
- Operating time. This is used for the temperature calculations of the model. Since the heat generation would be a function of time as well, this value was needed as well.

The modeling equations used were developed for metric measurements, so all input values were converted to metric. The model outputs the following information:

- Wire gauge to be used. This is specified in the input and is presented just for reference. The input value is used to determine the physical characteristics of the magnet.
- Diameter (ext) of the magnet. This is an estimate of the assembled magnet diameter. This value is based on the size of the core, the wire gauge used, and the number of coils to be made. The diameter is the core plus the diameter of the wire times the number of coils. The calculation is generally within roughly 1 millimeter of actual size. The equation is as follows:

$$Dia_{ext} = Dia_{core} + (2 * Dia_{wire} * Coils)$$

- Diameter (int) of magnet. Like the wire gauge, this is just restating the core diameter.
- Length of magnet. As with the internal diameter, and the wire gauge, this too is just restating an input value.
- Number of turns. Using the number of turns per coil, and the number of coils, the number of turns can be easily calculated. The integer value of the turns per coil is used because it can only be and integer value in reality.

$$Turns_{coil} = \frac{Length_{magnet}}{Dia_{wire}}$$

$$Turns_{magnet} = Turns_{coil} * Coils$$

- Quantity of wire needed. This value is a little complicated. The value is based on the number of coils requested, then a table that was generated in the spreadsheet is used to determine the wire needed. The circumference of the core is determined to calculate the wire required for one turn around that core. The number found is then taken and multiplied by the number of turns in the magnet. This information combined with the diameter of the wire, diameter of the core, and the number of coils is used to determine the length. The value found when carrying out the mathematics is then divided by 12 to convert from inches to feet, for ordering purposes.

$$Qty_{wire} = \frac{Dia_{core} Turns_{coil} \pi (1 + 0.5) + \sum_{i=0}^{Coils} 2\pi Turns_{coil} \left(Dia_{wire} * i + \frac{Dia_{core}}{2} \right)}{12}$$

- Total Resistance. This value is based on the quantity of wire needed, which gives the total length, the material properties of the wire, the diameter of the wire, which is given by the gauge. This value is used to calculate the required power, which also gives the heat generation.

$$Resistance = \frac{Resistivity * Qty_{wire}}{\frac{\pi}{4} Dia_{wire}^{\ 2}}$$

- Power Required. The power required is very simply calculated by using the current and the resistance. Since the power supply available was only capable of 60 watts of power, calculating that 100 watts of power was needed for acceptable performance would be an unrealistic result. This value had to stay under 60 watts to be sure that the magnet could run for

extended amounts of time. This value is also important for keeping track of the temperature change in the magnet itself, to make sure that the magnet did not create tissue damage, nor overheat.

$$Power = Current^2 * Resistance$$

- Temperature after given hours. The magnet was thermally modeled as a long wire carrying a given current in an ambient environment for a set amount of time. The material properties of the wire can effect this result as well as the heat transfer coefficient. The heat transfer coefficient was used at the lowest possible value to simulate worse case conditions, i.e., pure conduction heat transfer because there is no fluid movement past the wire. This was done to test for worst case conditions, so if the magnet would overheat during this condition the design would need to be changed, but also accounted for some of the effect of the wire being coiled around a core and itself. The wire in direct contact with the core can transfer its heat to the core, while the outermost windings can transfer heat to the environment. However, most of the wire used in the magnet would be between these two extremes, and would not have fluid movement. While a more exhaustive study could have been implemented, the goal of this part of the model was to get an approximate value to be certain the magnet would be safe to use. Testing was done to validate the model and was found to be within +/-10 ° Fahrenheit. More importantly however, is the heat generated would need to be dissipated because the temperature would reach into the 120 °F range.

The magnet would be fine at this temperature, but mild burning of the tissue could result.

APPENDIX K

MAGNETIC TERMS

The magnetic permeability of a material represents the ratio of the magnetic induction or flux density to the inducing magnetic force, i.e., it represents the ease of which the magnetic field can pass through material. Magnetic susceptibility is the intensity of magnetization of a body placed in a uniform magnetic field of unit strength, i.e., it represents the amount of material that becomes magnetized when a magnetic field is introduced. The permeability and susceptibility of a material results in its classification of either being a diamagnetic, paramagnetic or ferromagnetic material.

Diamagnetism is weak and only exists while an external field is present. This is induced by change in the orbital motion of electrons due to the magnetic field. The magnetic moment caused by this is also very weak and is opposite the applied field. This results in the magnetic permeability of the material to be less than unity, and the magnetic susceptibility is negative, meaning the magnitude of the magnetic field is less than what it would be in a vacuum. Diamagnetic materials are attracted to areas of a magnet where the field is weakest. This type of magnetism is usually ignored because its effects are so small that they are only observed when all other types of magnetism are absent.

In some materials, each atom possesses a permanent magnet dipole moment because of cancellation effects present in other materials. When absent of a magnetic field. The orientation of these moments are random and the material possesses no net magnetization. Since these dipoles are free to rotate, paramagnetism results when they are preferentially aligned with an external magnetic field. Since the magnetic dipoles

align with the field, they enhance the magnetic field, resulting in a magnetic permeability of greater than unity, and a relatively small, but positive magnetic susceptibility.

Certain metallic materials possess permanent magnetic moments in the absence of an external field and give very large and permanent magnetization. This ability, referred to as ferromagnetism, is displayed in transition metals iron, cobalt, nickel and some of the rare earth metals such as gadolinium. Magnetic susceptibilities are orders of magnitude higher than in either diamagnetic or paramagnetic materials, e.g., 10^{6} vs. 10^{-5}. Because of the electron structure, the electron spins go uncancelled, allowing for permanent magnet moments. In a ferromagnetic material, coupling interactions cause net spin magnetic moments of adjacent atoms to align, even without an external field. The saturation magnetization of a ferromagnetic material represents the magnetization when all magnetic dipoles are aligned with an external field. This saturation is equal to the product of the net magnetic moment for each atom and the number of atoms present.

Permanent magnets are made by using ferromagnetic materials and applying a large magnetic field. The flux density (B) and the field intensity (H) are the two characteristics that permanent magnets are grouped by.

When a material undergoes magnetization, the magnet dipoles are random. As the field intensity is increased, the magnetic flux increases slowly at first, then finally levels off and becomes independent of the field intensity, which results in the saturation point. When the field intensity is reduced, a hystersis effect is developed in which the flux density lags behind the field intensity. When the field intensity is zero, the residual

flux will exist and is called the remanence, or remanent flux density. The residual flux can be removed by applying a field in the opposite direction, and is usually referred to as the coercive force.

The area within the hysterisis loop represents the magnetic energy loss per unit volume of material, per magnetization-demagnetization cycle. This gives rise to another set of classification; soft and hard magnetic materials. Soft magnetic materials are used in devices where they are subjected to alternating magnetic fields and in which the energy losses must be low, such as a transformer core. The hysterisis loop for this material is much smaller, the permeability is initially much higher, and the coercitivity is low. Hard magnetic materials are highly resistant to demagnetization and are characterized by having high remanence, coercivity and saturation flux density, as well as low initial permeability losses and high hysterisis energy losses.

The permanent magnet material that has been employed in MAS are neodymium-iron-boron (NdFeB) rare earth magnets. Currently, they are the strongest rare earth permanent magnets available in terms of magnetic flux. Mechanically, they are very brittle and most of the magnets, especially ones exposed to biological tissue, are chromium plated to protect the tissue, as well as the magnet.

APPENDIX L

POWER MODALITIES

When the decision was made to start the development of powered tooling, three modalities were found that offered equipment in the size that was required: electric motors, shape memory alloys, and pneumatic actuators.

Electric motors were the first modality looked into for their ease of power deliver, availability and ease of control. The anchoring needle concept was tested and was proven capable of delivering voltages that were high enough to drive one of these motors without endangering the patient, so the tools could be wireless, which was a great advantage for this modality. The torque developed by the electric motors is a function of the magnetic field developed and the radius of the armature and windings, meaning that the larger magnetic field and bigger diameter gives more torque and power, ideally. Since the diameter of the motor is so small, torque and power output are hampered. Again, due to their size, the magnetic field developed is hampered because there is only so many winds of wire that can fit on the armature, and that wire can only handle a small amount of current, both of which hamper the magnetic field. Conventional size motors can sometimes be used without a gear head, but the motors in this scale require a gear head to be useful.

The gear heads available are commonly in the 1,000:1 range, which results in a gear head that is actually larger than the motor driving it. Also, every gear reduction comes at a cost of efficiency, which again, hampers performance. The complication from this project was in two parts: we needed an actuator in the 6-8 mm diameter range, and something that could be coupled relatively easily to a drive shaft or link of a

tool directly. The are multiple motors available in this diameter range, but due to the gear heads, they are fairly long. Where this becomes a problem is that the output shaft of the motor needs to couple to an axis that is perpendicular to it. Conventional wisdom would lead one to use a miter gear set, but unfortunately I was unable to find a set small enough to fit the size constraints presented by the trocar port. The concept of having the motor possibly swivel into position to align itself with the axis of the link was looked into as well, but there was a problem of getting the motor back to its start position when the tool was removed because without returning to a position where it was aligned with the tool, it could not be removed.

There are possible uses for an electric motor in the tooling in the future and present. One possibility would be to drive a reel on the sling retractor anchors to wind and unwind the medium used, but the tool could not be adjust while loaded due to power limitations and a possible locking mechanism may be needed to keep the reel from unwinding under load.

Shape memory alloys, in this case Nitinol wire, was looked into as an actuator as well. The wire used has the trade name Flexinol, and is a slight variation to the standard Nitinol, it is specifically designed for repeated actuation. As with all three of the modalities, the shape memory wire has some issues that limit its effectiveness in this project, which are actuation time, proportional control and motion generated.

The wire contracts when heat causes its temperature to reach a transition temperature, and relaxes as it cools. Two transition temperatures are available to choose from, 70 and 90 degree C. The 90 degree C wire was chosen because although

its actuation temperature is higher, the temperature difference is greater between it and the environment that it would be used in, which causes the wire to relax slightly quicker. The cycle time of the wire is dependent upon the time it takes to heat and cool the wire, and through testing the 90 degree C wire is quicker in relaxation, which is where most of the actuation time is spent (contraction takes 1 second, relaxation takes around 10 seconds). While relatively slow compared to the other two modalities, the force per area of actuator of this modality cannot be ignored. A wire 0.381 mm in diameter can pull with a force of 2 kg. By contrast, an electric motor 6 mm in diameter has a torque output of 0.012 kg-mm, and a pneumatic cylinder 5 mm in diameter with 550 kPa applied can generate 0.332 kg. While the force capability of this wire would allow for very strong powered tooling, the time delays in activation limit its usefulness in a heavily active tool, but may work quite well for something like a retractor where the added force output would be needed and actuation time is not as great a concern.

As stated earlier, the wire reacts to a temperature difference. This difference can occur due to environmental temperatures, an example would be a water bath, or electrical heating due to resistance in the wire. While controlling the environment around the wire was never attempted due to complexity, this may hold the key to making the wire perform in a more useful way. The response to electrical stimulus to cause the temperature needed results in a very non-linear response, which makes proportional control very difficult. I was unable to find work that was able to successfully control the wire without great investment in electrical engineering to build very special electronics to control the voltage sent to the wire, and even then the wire

was not very reliable in holding positions. This required electronics was beyond my abilities, but would be a good place to put future efforts because if the actuation of the wire can be made comparable to other modalities, its force per area would be of great use.

The smallest problem with this modality is the stroke length of the Nitinol. Normal contraction of the wire is only about 5% of its total length, with a recoverable maximum of about 10%. In uses for fluidic valving, which is one of Flexinol's biggest markets, this is not such an issue because the valve can be made to account for this small motion. In other applications a lever ratio, or just using a long section of wire must be employed to generate the required motion. In this application, a large enough lever ratio to generate the ultimate goal of 90 degree motion per joint would be extremely difficult to package. One method that was tested and seemed to work well was to couple the wire to a gear rack, which was connected to a set of gears. The gears were chosen to amplify the motion of the rack, which resulted in the approximate 3 mm of wire contraction to 70 degrees of joint travel. While this result was within an acceptable range, because of the gearing the joints require more wires to regain the strength lost in over-gearing the joints. Because of their size, this is a viable solution, but I was unable to add more wires due to power supply capabilities. This concept seems to work, but would require more development time to work out some of the problems.

Fluid power was considered for multiple reasons; ease of control, relative ease of powering, availability, and the motion generated was of usable amount. Fluid power

can be of two forms; pneumatic and hydraulic, both with strengths and weaknesses. Pneumatic power was incorporated for the following reasons:

- Supply of gas can be from an air compressor, a bottle or from the wall in the operating room.
- A blessing and a curse is the compressibility of the gas. If there was an erroneous command to the arm, the compressibility of the fluid would cause the arm to stall, not puncture the tissue. A problem associated with this is that the cylinders do not perform well when trying to lift a heavy object.
- If a supply line leaked, the gas can be removed by the insuflator, or just leak out of the body. If the hydraulic lines leaked, which a saline solution may be a possible fluid to used, it may need to be either sucked up or taken up by the body.
- Supply lines for gas are usually much more flexible than hydraulic lines. The flexibility of the cabling or supply lines important because any additional loading from supply lines limits the amount of coupling force or position control available.
- The pneumatic actuators are readily available at this scale, as well as the required equipment to operate them. Hydraulic actuators tend to not be as small as needed for this project due to the seals that are required to deal with the higher pressures.

Pneumatic cylinders come in two varieties, single acting and double acting, the difference being how the cylinder is actuated. A single acting cylinder is driven by gas

and returned by a spring to a neutral position, which can either be with the piston fully retracted, called normally retracted, or with the piston fully extended, called normally extended. A double acting cylinder is driven by gas to both extend and retract.

A very simple position control can be accomplished with a single acting cylinder by controlling the pressure that enters the cylinder. Since the force of the cylinder is a function of the area of the piston and the pressure of the fluid, one can balance the force of the return spring with the correct pressure. In doing so, it is possible to make the cylinder act proportionally. While this is not ideal control, it does allow for decent control of the actuator. A possible improvement would be to use a double acting cylinder, but controlling the cylinder would be more complex because the pressure on both sides of the piston would have to be unbalanced, then balanced again. This control is how most hydraulic position servos are operated, and there is no reason that pneumatic control could not be accomplished this same way. The downside to this approach is that another supply line must be ran to each actuation joint.

Unlike the nitinol wire, a pneumatic cylinder is ordered with a specified stroke. As long as the cylinder can generate enough force, it will extend to this stroke. This brings up another key feature and issue: stalling. Stalling an electric motor causes it to overheat and fail. Stalling the nitinol wire can cause it to overstress, and fail. Fluid power actuators can be stalled without any damage to the actuator and powering system. If a stroke of 8 mm is required, one can use a 10 mm stroke cylinder without fear of damaging the actuator.

REFERENCES

Callister, William D. "Magnetic Properties." Materials Science and Engineering an Introduction, Fourth Edition. New York: John Wiley & Sons Inc., 1997. 659-688.

DJ, Ostlie. "Single cannula technique and robotic telescopic assistance in infants and children who require laparoscopic Nissen fundoplication." Journal of Pediatric Surgery. Jan. 2003: 111-115.

.Eves, H. Mathematical Circles Adieu, Boston: Prindle, Weber and Schmidt, 1977.

GM, Roy. "Safe technique for laparoscopic entry into the abdominal cavity." Journal of the American Association of Gynecologic Laparoscopists. Nov 2001: 519-528.

Intuitive Surgical Home Page. Intuitive Surgical Inc. 3 Sept. 2005. <http://www.intuitivesurgical.com>

MIPInfo.com – Information on Minimally Invasive Procedures (MIP). Ethicon Endo-Surgery. 3 Sept. 2005. < http://www.mipinfo.com/dtcf/>

MP, Milad. "The spinal needle test effectively measures abdominal wall thickness before cannula placement at laparoscopy." Journal of the American Association of Gynecologic Laparoscopists. Nov 2002: 514-518.

R, Pasic. "Laparoscopy in morbidly obese patients." Journal of the American Association of Gynecologic Laparoscopists. Aug 1999: 307-312.

United States Patent and Trademark Office Homepage. 05 Nov. 2005. United States Patent and Trademark Office. 3 Sept. 2005. <http://patft.uspto.gov/netahtml/srchnum.htm> Patent number 5352219.

BIOGRAPHICAL INFORMATION

The author received his Master of Science in Biomedical Engineering from The University of Texas at Arlington in May 2006.

Richard Antone Bergs, a native of Ortonville, Michigan, born in Wausau, Wisconsin, received a Bachelor of Science in Mechanical Engineering in May 2001.

Mr. Bergs is a member of the American Society of Mechanical Engineers (ASME), as well as the Society of Manufacturing Engineers (SME), and was the Joint Council of Engineering Organizations (JCEO) representative for both.

Upon receiving his degree, he would like to continue in the research and development field applying the knowledge and understanding that has come from years of working at the Automation & Robotics Research Institute.